ERCOFTAC
European Research Community
On Flow, Turbulence And Combustion

15th ERCOFTAC SIG 33 Workshop

Progress in Flow Instability, Transition and Control

Alghero, Italy, June 28-30, 2023

List of participants

Name		Affiliation	Email
Andrey	**Aleksyuk**	Department of Mathematics, University of Manchester	andrey.aleksyuk@manchester.ac.uk
Franco	**Auteri**	Politecnico di Milano	franco.auteri@polimi.it
Elliot	**Badcock**	Imperial College London	ejb321@ic.ac.uk
Marina	**Barahona**	TU Delft	m.barahonalopez@tudelft.nl
Daniel	**Bodony**	University of Illinois at Urbana-Champaign	bodony@illinois.edu
Pietro Carlo	**Boldini**	TU Delft	p.c.boldini@tudelft.nl
Alessandro	**Bongarzone**	EPFL	alessandro.bongarzone@epfl.ch
Edouard	**Boujo**	EPFL	edouard.boujo@epfl.ch
Quentin	**Chevalier**	LadHyX	quentin.chevalier@ladhyx.polytechnique.fr
Alessandro	**Chiarini**	Okinawa Institute of Science and Technology	alessandro.chiarini@polimi.it
Nicola	**Ciola**	Politecnico di Bari	n.ciola@phd.poliba.it
Thales	**Coelho Leite Fava**	KTH	fava@kth.se
Simon	**Demange**	TU Berlin	s.demange@tu-berlin.de
Yves-Marie	**Ducimetière**	EPFL	yves-marie.ducimetiere@epfl.ch
David	**Fabre**	IMFT	david.fabre@toulouse-inp.fr
Hermann	**Fasel**	University of Arizona	faselh@email.arizona.edu
Alessandro	**Franchini**	Ecole National des Arts et Metier (Dynfluid lab)	alessandro.franchini@ensam.eu
Juan Alberto	**Franco**	DLR	juan.franco@dlr.de
Tomas	**Fullana**	EPFL	tomas.fullana@epfl.ch
François	**Gallaire**	EPFL	francois.gallaire@epfl.ch
Flavio	**Giannetti**	Università degli Studi di Salerno	fgiannetti@unisa.it
Ardeshir	**Hanifi**	KTH Royal Institute of Technology	hanifi@kth.se
Jonathan	**Healey**	Keele University	j.j.healey@keele.ac.uk
Stefan	**Hein**	DLR	stefan.hein@dlr.de
Peter	**Jordan**	Université de Poitiers	peter.jordan@univ-poitiers.fr
Antoine	**Jouin**	ENSAM	antoine.jouin@ensam.eu
Thomas Ludwig	**Kaiser**	TU Berlin	t.kaiser@tu-berlin.de
Ugur	**Karban**	Middle East Technical University	ukarban@metu.edu.tr
Kentaro	**Kato**	Shinshu University	kentaro_kato@shinshu-u.ac.jp
Markus	**Kloker**	University of Stuttgart, IAG	markus.kloker@iag.uni-stuttgart.de
Marios	**Kotsonis**	TU Delft	m.kotsonis@tudelft.nl
Colin	**Leclercq**	ONERA	colin.leclercq@onera.fr
Pier Giuseppe	**Ledda**	DICAAR, Università degli Studi di Cagliari	pier.ledda@epfl.ch
Lutz	**Lesshafft**	LadHyX, CNRS/École Polytechnique	lesshafft@ladhyx.polytechnique.fr
Paolo	**Luchini**	Università di Salerno, DIIN	luchini@unisa.it
Valerio	**Lupi**	KTH	lupi@mech.kth.se
Ganlin	**Lyu**	Imperial College London	g.lyu19@imperial.ac.uk
Alice	**Marcotte**	EPFL	alice.marcotte@epfl.ch
Olivier	**Marquet**	ONERA/DAAA, Université Paris-Saclay	Olivier.Marquet@onera.fr
Eduardo	**Martini**	ISAE-ENSMA, Institute Pprime	eduardo.martini@ensma.fr
Marcello	**Medeiros**	University of Sao Paulo	marcello@sc.usp.br
Théo	**Mouyen**	Università degli Studi di Salerno	tmouyen@unisa.it
Gabriele	**Nastro**	ISAE-SUPAERO	Gabriele.NASTRO@isae-supaero.fr
Harrison	**Nobis**	KTH	nobis@kth.se
Kilian	**Oberleithner**	TU Berlin	oberleithner@tu-berlin.de
Bernardo	**P. P. de Vasconcellos**	Saint-Gobain Recherche Paris / CNRS-Institut Pprime	bernardo.vasconcellos@univ-poitiers.fr
Georgios	**Rigas**	Imperial College London	g.rigas@imperial.ac.uk
Ulrich	**Rist**	Stuttgart University	ulrich.rist@iag.uni-stuttgart.de
Alberto Felipe	**Rius-Vidales**	TU Delft	a.f.riusvidales@tudelft.nl
Jean-Christophe	**Robinet**	Arts et Métiers Institute of Technology	Jean-Christophe.Robinet@ensam.eu
Daniel	**Rodriguez**	Universidad Politecnica de Madrid	daniel.rodriguez@upm.es
Tristan M.	**Römer**	University of Stuttgart	roemer@iag.uni-stuttgart.de
Julien	**Sablon**	ISAE-SUPAERO	julien.sablon@isae-supaero.fr
Timothée	**Salamon**	EPFL	timothee.salamon@epfl.ch
Taraneh	**Sayadi**	Sorbonne University	taraneh.sayadi@sorbonne-universite.fr
Peter	**Schmid**	KAUST	peter.schmid@kaust.edu.sa
Oliver T.	**Schmidt**	University of California San Diego	oschmidt@ucsd.edu
Javier	**Sierra-Ausin**	Università degli Studi di Salerno / IMFT	javier.sierra@imft.fr
András	**Szabó**	Budapest University of Technology and Economics	aszabo@hds.bme.hu
Christoph	**Wenzel**	University of Stuttgart, IAG	wenzel@iag.uni-stuttgart.de
Sven	**Westerbeek**	TU Delft	S.H.J.Westerbeek@tudelft.nl
Kevin	**Wittkowski**	EPFL	kevin.wittkowski@epfl.ch
Asahi	**Yoshida**	Shinshu University	22w4077d@shinshu-u.ac.jp

15th ERCOFTAC SIG 33 Workshop

Progress in Flow Instability, Transition and Control

Alghero, Italy, June 28-30, 2023

Organisers:

Franco Auteri (Politecnico di Milano),
David Fabre (IMFT),
Flavio Giannetti (Univ. Di Salerno),
Ardeshir Hanifi (KTH)

POLITECNICO MILANO 1863

INSTITUT DE MECANIQUE DES FLUIDES DE TOULOUSE

UNIVERSITÀ DEGLI STUDI DI SALERNO

KTH VETENSKAP OCH KONST

FLOW

15TH ERCOFATC SIG33 WORKSHOP

Progress in Flow Instability, Transition and Control

June 28-30, 2023

Alghero, Sardinia, Italy

Wednesday, June 28				
8:30		Registration		
8:45		Welcome		
9:00	Peter	Jordan	Linear mean-flow modelling of turbulent shear flow	Chair: P. Luchini
09:45	Oliver T.	Schmidt	Modal analysis of nonlinear turbulent jet dynamics	
10:05	Bernardo	P. P. de Vasconcellos	Characterizing absolute instability in annular swirling jets	
10:25	Alessandro	Franchini	Global stability analysis of screeching jets via automatic differentiation	
10:45	Coffee			
11:15	Javier	Sierra-Ausín	The identification of the instability core of instabilities underpinned by an acoustic-hydrodynamic feedback	Chair: T. Sayadi
11:35	Eduardo	Martini	Decomposing Long-range-resonant Instability Using Forced One-way Navier-stokes (OWNS)	
11:55	Thomas Ludwig	Kaiser	Using a linear mean flow analysis with an active flame approach to model the response of a turbulent jet flame to acoustic excitation	
12:15	Yves-Marie	Ducimetière	Noise-induced transitions after a steady symmetry-breaking bifurcation: the case of the sudden expansion.	
12:35	Alessandro	Chiarini	Linear global and asymptotic stability analysis of rectangular cylinders in ground effect	
12:55	Lunch			
14:25	Olivier	Marquet	Data-assimilation and linear analysis of turbulent mean flows around airfoils close to stall	Chair: G. Rigas
15:10	Nicola	Ciola	Nonlinear optimal perturbations engendering extreme events in the turbulent channel flow	
15:30	Lutz	Lesshafft	Instability from non-local feedback in a laminar V-shaped flame	
15:50	Coffee			
16:20	Quentin	Chevalier	Resolvent analysis of a round swirling turbulent jet	Chair: P. Jordan
16:40	Colin	Leclercq	Mean resolvent operator of a statistically steady flow	
17:00	Ugur	Karban	Resolvent optimisation via nonlinear variable transformation	
17:20	Reception			
Thursday, June 29				
8:30	Taraneh	Sayadi	Towards Efficient and Robust Optimisation of Unsteady Complex Flows	Chair: H. Fasel
9:15	Julien	Sablon	Energy growth in variable-density trailing vortices	
9:35	Pier Giuseppe	Ledda	Linear path instability of buoyancy-driven permeable disks	
9:55	Andrey	Aleksyuk	Mechanisms for three-dimensional instabilities in the wake behind a cylinder	
10:15	Antoine	Jouin	Quasi-periodic optimal perturbations in a streaky boundary layer	
10:35	Coffee			
11:05	Théo	Mouyen	Stability prediction of multiple freely-oscillating bodies	Chair: D. Fabre
11:25	Alessandro	Bongarzone	A revised gap-averaged model for Faraday waves in Hele-Shaw cells	
11:45	Daniel	Bodony	Adjoint-based sensitivity of shock-laden flows	
12:05	Gabriele	Nastro	Nonlinear dynamics, stability and sensitivity of a simplified dragonfly wing in gliding flight	

12:25	András	Szabó	Stability analysis of a streaky boundary layer induced by miniature vortex generators	
12:45	Valerio	Lupi	Error-driven global stability analysis of 180°-bend pipe transitional flow	
13:05	Lunch			
14:30	François	Gallaire	Weak nonlinearity for strong nonnormality	Chair: J. Healey
15:15	Georgios	Rigas	Nonlinear transition mechanisms of separation bubbles	
15:35	Daniel	Rodriguez	The impact of periodic inflow fluctuations on the size and dynamics of the separated flow over a bump	
15:55	Thales	Coelho Leite Fava	Spanwise modulation and secondary instability of Kelvin- Helmholtz rolls by crossflow modes on a rotating airfoil	
16:15	Hermann	Fasel	Delay of separation and transition for a laminar airfoil using active flow control	
16:35	Alberto Felipe	Rius-Vidales	Passive control of crossflow instability and transition delay using a smooth surface protuberance	
16:55	Social event			
Friday, June 30				
9:00	Asahi	Yoshida	Establishment of extraction method using linear response to artificial disturbance for boundary layer transition process induced by free stream turbulence	Chair: J.-C. Robinet
9:20	Pietro Carlo	Boldini	Transient growth in flat-plate boundary layers with a highly non-ideal fluid	
9:40	Simon	Demange	Effect of eddy viscosity on the resolvent analysis of coherent structures in the near-field of a NACA0012 airfoil	
10:00	Marina	Barahona	Stability and transition of swept boundary layers in cooled wall conditions: commissioning of experiments and initial results	
10:20	Markus	Kloker	Effects of a highly-non-ideal fluid for the instability of a three-dimensional boundary-layer flow	
10:40	Coffee			
11:10	Elliot	Badcock	Three-Dimensional Instabilities	Chair: S. Hein
11:30	Jonathan	Healey	Global instability produced by infinitesimal roughness	
11:50	Harrison	Nobis	Topology optimization of roughness elements to delay modal transition in boundary layers	
12:10	Juan Alberto	Franco	Influence of surface imperfections with slightly rounded corners on the expected laminar-turbulence transition location	
12:30	Tristan M.	Römer	Delay of laminar–turbulent transition by rotating cylindrical roughness elements in a laminar water channel	
12:50	Marcello	Medeiros	Numerical and experimental study of the gap-induced boundary layer transition	
13:10	Ganlin	Lyu	Transonic boundary layer natural transition analysis over a gapped wing section	
13:30	Lunch			
	End of the conference			

LINEAR MEAN-FLOW MODELLING OF TURBULENT SHEAR FLOW

Peter Jordan
Institut Pprime, UPR 3346, CNRS · Université de Poitiers · ISAE-ENSMA

Organised motion in turbulent shear flow, first observed in the 1960s [1], motivates the search for an underlying dynamic law simpler than that expressed by the Navier-Stokes system. The first such models date from the 1970s and are based on a linearisation about the turbulent mean [2]. They have since been found to describe many characteristics of coherent structures in high-Reynolds-number turbulent jets [3], and they have been used to clarify the mechanisms by which turbulent jets generate sound [4].

Linear mean-flow modelling has recently been revisited, but with the non-linear flow equations split into a linear operator and an endogeneous forcing term associated with non-linear scale interactions. Such a reorganisation of the Navier-Stokes system was first proposed by Lighthill for the problem of jet noise [5]. Extensions of Lighthill's formulation, where the linear operator is based on a shear flow, have been proposed by Lilley [6], and later by Goldstein [7]. Similar *ansätze* have been proposed for the study of wall-bounded turbulence by Landahl [8]. More recently, Sharma & McKeon [9] and Hwang & Cossu [10] have shown how singular-value decomposition of the resolvent operator can enhance analysis and modelling, and in particular for flows underpinned by a low-rank dynamics. Resolvent analysis has since been used for the study of compressible turbulent jets by Towne *et al.* [11], Lesshafft *et al.* [12], Cavalieri *et al.* [15], Nogueira *et al.* [13] and Pickering *et al.* [14].

The talk will overview a number of recent numerical and experimental studies where linear mean-flow models have been used: (1) for the exploration of self-similarity in wall-bounded flows [16]; (2) for the modelling of sound-generation mechanisms in turbulent jets [17]; for the estimation and control of free and wall-bounded turbulent shear flows [18, 19, 20]. Our objective will be to highlight the surprising versatility of linear mean-flow models, but also to discuss their limitations.

References

[1] E. Mollo-Christensen, (1963) *easurements of near field pressure of subsonic jets.* Tech. Rep., Advis. Group Aeronaut. Res. Dev., Paris.
[2] S. Crow and F. Champagne, (1971) *Orderly structure in jet turbulence.* . Journal of Fluid Mechanics, Vol. 48.
[3] A. V. J. Cavalieri, D. Rodriguez, P. Jordan, T. Colonius and Y. Gervais, (1971) *Wavepackets in the velocity field of turbulent jets.* Journal of Fluid Mechanics, Vol. 730.
[4] P Jordan, and T. Colonius, (2013) *Wave packets and turbulent jet noise.* Ann. Rev. Fluid Mech., Vol 45.
[5] M. J. Lighthill, (1952) *On sound generated aerodynamically I. General theory.* Proc. Royal Soc. A. Vol. 211.
[6] G. M. Lilley (1974) *On the noise from jets.* AGARD Conf. Proc., Vol. 131.
[7] M. E. Goldstein (2003) *A generalized acoustic analogy.* Journal of Fluid Mechanics, Vol. 488.
[8] M. T. Landahl (1967) *A wave-guide model for turbulent shear flow.* Journal of Fluid Mechanics, Vol. 29.
[9] A. S. Sharma, and B. J. McKeon (2010) *A critical-layer framework for turbulent pipe flow.* Journal of Fluid Mechanics, Vol. 658
[10] Y. Hwang, and C. Cossu (2010) *Linear non-normal energy amplification of harmonic and stochastic forcing in the turbulent channel flow.* Journal of Fluid Mechanics, Vol. 664.
[11] O. T. Schmidt, A. Towne, G. Rigas, T. Colonius, and G. Brès (2018) Spectral analysis of jet turbulence Journal of Fluid Mechanics, Vol. 855.
[12] L. Lesshafft, O. Semeraro, V. Jaunet, A. V. J. Cavalieri, and P. Jordan (2019) *Resolvent-based modeling of coherent wave packets in a turbulent jet.* Physical Review Fluids, Vol. 4.
[13] P. A. S Nogueira, A. V. J. Cavalieri, P. Jordan and V. Jaunet, (2019) *Large-scale streaky structures in turbulent jets.* Journal of Fluid Mechanics, Vol. 873.
[14] E. Pickering, G. Rigas, P. A. S Nogueira, A. V. J. Cavalieri, O. Schmidt and T. Colonius, (2019) *Lift-up, Kelvin–Helmholtz and Orr mechanisms in turbulent jets.* Journal of Fluid Mechanics, Vol. 896.
[15] A. V. J. Cavalieri, P. Jordan and L. Lesshafft (2019) *Wave-packet models for jet dynamics and sound radiation.* App. Mech. Rev., Vol. 71.
[16] U. Karban, E. Martini, A. V. J. Cavalieri, L. Lesshafft and P. Jordan (2022) *Self-similar mechanisms in wall turbulence studied using resolvent analysis.* Journal of Fluid Mechanics, Vol. 939.
[17] U. Karban, B. Bugeat, A. Towne, L. Lesshafft, A. Agarwal and P. Jordan (2023) *An empirical model of noise sources in subsonic jets.* Journal of Fluid Mechanics, In press.
[18] K. Sasaki, S. Piantanida, A. V. J. Cavalieri and P. Jordan (2017) *Real-time modelling of wavepackets in turbulent jets.* Journal of Fluid Mechanics, Vol. 821.
[19] E. Martini, J. Jung, A. V. J. Cavalieri, P. Jordan and A. Towne (2022) *Resolvent-based tools for optimal estimation and control via the Wiener–Hopf formalism.* Journal of Fluid Mechanics, Vol. 937.
[20] I. A. Maia, P. Jordan, A. V. J. Cavalieri, E. Martini, K. Sasaki and F. Silvestre (2021) *Real-time reactive control of stochastic disturbances in forced turbulent jets.* Physical Review Fluids, Vol. 6.

MODAL ANALYSIS OF NONLINEAR TURBULENT JET DYNAMICS

Oliver T. Schmidt[1], Akhil Nekkanti[1]
[1] *Dept. of Mechanical and Aerospace Eng., University of California San Diego, La Jolla, CA, USA*

The quadratic nonlinearity of the convective term in the Navier-Stokes equations gives rise to triadic interactions that redistribute energy between frequency components. Bispectral mode decomposition (BMD,[1]) is a processing technique for spatiotemporal flow data that extracts flow structures associated with triadic interactions by detecting quadratic phase coupling between frequency components related by the zero-sum (or resonance) condition, $f_1 \pm f_2 \pm f_3 = 0$. The two main outcomes of BMD are the mode bispectrum which indicates which interactions are active, and the bispectral modes which represent the flow structures generated by the nonlinear interactions. BMD is conceptually closely related to spectral proper orthogonal decomposition (SPOD, [2]) and can be understood as an extension of the latter to third-order statistics. In this work, we use BMD and SPOD to investigate the nonlinear dynamics of unforced initially laminar, and forced turbulent jets [3, 4] computed using large-eddy simulation [5]. Figure 1 shows BMD modes for a Reynolds number $Re = 5 \times 10^4$, Mach number $M_j = 0.4$ turbulent jet. The boundary layer inside the nozzle is not tripped any remains laminar. This leads to an initially

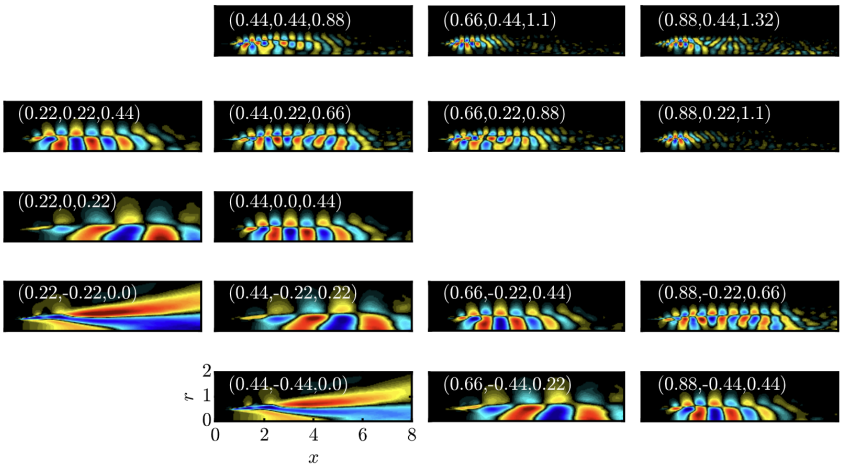

FIGURE 1. *Bispectral mode decomposition identifies a triadic nonlinear interaction cascade. Sum interactions (top two rows) generate harmonics at integer multiples of the fundament frequency, $f_0 = 0.22$, up to the sixth harmonic. Difference interactions give rise to the mean flow deformation and scatter energy back into the fundamental. The real part of the streamwise velocity is shown.*

laminar shear layer that quickly transitions to fully-developed turbulence. The short instability of the initial shear layer prior to the transition point imprints rich nonlinear dynamics onto the entire flow field. This can be seen in figure 1, which maps out a cascade of triadic interactions involving the fundamental frequency, f_0, and its multiples. We will address specific phenomena like vortex pairing and backscatter through the lens of BMD and demonstrate energy flow analysis based on the spectral turbulent kinetic energy equation in conjunction with SPOD and BMD. The combination of these tools provides remarkable physical insight and paves the way for reduced-order models that incorporate and faithfully reproduce the nonlinear dynamics of turbulent flows.

References

[1] Schmidt, O. T. Bispectral mode decomposition of nonlinear flows. *Nonlinear Dynamics*, 102 (4), 2479–2501.
[2] Towne, A., Schmidt, O. T. and Colonius, T. Spectral proper orthogonal decomposition and its relationship to dynamic mode decomposition and resolvent analysis. *Journal of Fluid Mechanics*, 847, pp.821-867, 2018.
[3] Nekkanti, A. and Maia, I. and Jordan, P. and Heidt, L. and Colonius, T. and Schmidt, O. T., Triadic nonlinear interactions and acoustics of forced versus unforced turbulent jets. *12th International Symposium on Turbulence and Shear Flow Phenomena*, 2020.
[4] Maia, I., Jordan, P., Heidt, L., Colonius, T., Nekkanti, A., and Schmidt, O. T. Nonlinear dynamics of forced wavepackets in turbulent jets. *AIAA Paper 2021-2277*, 2021.
[5] Brès G. A. and Lele S. K. Modeling of jet noise: a perspective from large-eddy simulations. *Philosophical Transactions of the Royal Society A*, 377(2159):20190081, 2019

CHARACTERIZING ABSOLUTE INSTABILITY IN ANNULAR SWIRLING JETS

Bernardo P. P. de Vasconcellos[1], Eduardo Martini[2], Eric Foucault[3], Peter Jordan[3]
[1] *PhD candidate, Institut Pprime-CNRS-Université de Poitiers, Saint Gobain Recherche Paris F-93303 Aubervillers, France, bernardo.vasconcellos@univ-poitiers.fr*
[2] *Maître de conférence,* [3] *Professor, Institut Pprime-CNRS-Université de Poitiers*

Annular swirling jets are known for having rich dynamics, exhibiting different and complex behaviors as a function of swirl intensity and geometry. It has been shown that this type of flow can be locally absolutely instable if certain conditions are met [2]. These conditions are the presence of black-flow, due to the wake behind the jet's center body, or swirl. Those results align with results from round-jet stability analysis [1]. Though a description of the annular jet geometry effect on transition from absolute to convective instability is still lacking.
The present work aims to adress the impact of the blockage ratio, here described as an aspect ratio, swirl, and back-flow intensity on the annular swirling jet absolute instability (AI). We use a simplyfied model that explores the limiting case $R_{in} >> R_{out} - R_{in}$ (very small aspect ratio), where the jet lips can be approximated by two straight strips instead of an annular lip as show in Figure 1. The base flow velocity is supposed to be constant inside each one of the zones delimited by the strips, which results in a combination of four vortex-sheets.

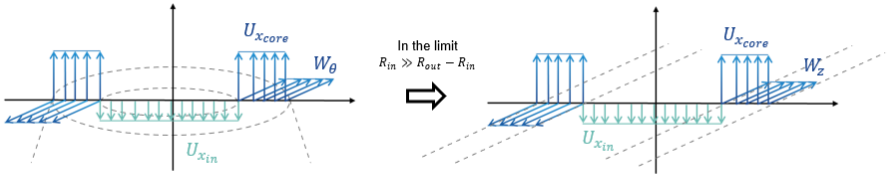

FIGURE 1. *Quad vortex-sheet model approximation from the annular cylindrical coordinates.*

Under the hypothesis that the flow is inviscid, incompressible and homogeneous in the span and streamwise directions, it is possible to derive an analytical dispersion relation for the model. Using the Briggs-Bers criterion [3], absolutely unstable saddles can be mapped for different flow parameters. This results in the map shown in Figure 2, where we identify at least three different kinds of absolute instability. For small aspect ratio and high back-flow intensity the AI has Strouhal number (St) equals to 1.2 and a symmetric shape (with respect to y direction). In the region of intermediary aspect ration the AI is 'slower' at St equals to 0.6 and it has an anti-symmetric shape. Finally, in the region where the jet is thick, the AI is significantly 'faster' at St equals to 5.0 and it is symmetric again.

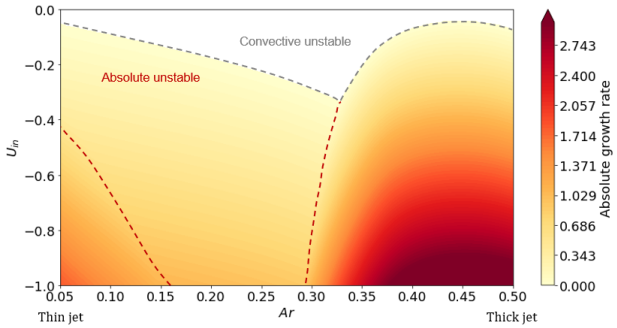

FIGURE 2. *Absolute instability growth rate map as a function of the back-flow (U_{in}) and aspect ratio ($Ar = (R_{out} - R_{in})/R_{out}$).*

References

[1] Ivan Delbende, Jean-Marc Chomaz, and Patrick Huerre. Absolute/convective instabilities in the Batchelor vortex: a numerical study of the linear impulse response. *Journal of Fluid Mechanics*, 355:229–254, January 1998. Publisher: Cambridge University Press.
[2] A. Michalke. Absolute inviscid instability of a ring jet with back-flow and swirl. *European Journal of Mechanics - B/Fluids*, 18(1):3–12, January 1999.
[3] Richard J. Briggs. *Electron-Stream Interaction with Plasmas*. The M.I.T. Press, Cambridge, Massachusetts, December 1964.

GLOBAL STABILITY ANALYSIS OF SCREECHING JETS VIA AUTOMATIC DIFFERENTIATION

Alessandro Franchini[1], Nicolas Alferez[2], Jean Christophe Robinet[1]
[1]*DynFluid Laboratory, Arts et Métiers, 151, boulevard de l'hôpital, 75013 Paris*
alessandro.franchini@ensam.eu, jean-christophe.robinet@ensam.eu
[2]*DynFluid Laboratory, CNAM, Arts et Métiers, 151, boulevard de l'hôpital, 75013 Paris*
nicolas.alferez@lecnam.net

In certain conditions, imperfectly expanded jets can produce a sound of discrete pitch referred as screech. This phenomenon has been extensively studied since its discovery by Powell in the early 1950s [1]. The understanding of screech is of great importance in the design of civil and advanced aircraft, since it may cause sonic fatigue failure of aircraft structures. Powell explanation for screech was that a disturbance originating at the nozzle lips grows and propagates downstream, it interacts with the shock-cells and produces sounds. These sound waves propagates upstream and interacts with the nozzle lip by generating a disturbance and closing the resonant loop. Our goal is to explore this phenomenon within the framework of linear global stability analysis. Beneddine *et al.* [2] showed that a laminar underexpanded supersonic cold jet can exhibit globally unstable modes. The structure of the modes found presents good agreement with the existing empirical formulas for the prediction of screech frequency. Our work aims at exploring a linear global stability analysis of 2D and 3D underexpanded screeching jets, coupled with non linear simulations to improve the understanding of the phenomenon.

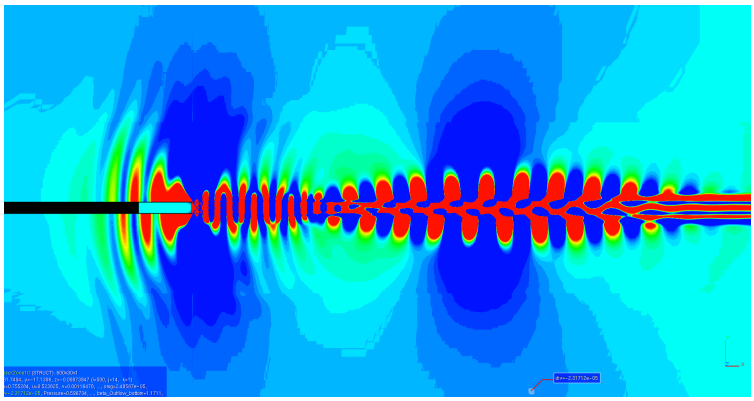

FIGURE 1. *Divergence of the velocity vector in a 2D non linear simulation, which is the material derivative of density. JPR = 1.15 , h = 0.063, respectively the jet pressure ratio and nozzle lip thickness.*

Figure 1 refers to a preliminary non linear simulation in which we are capturing an upstream propagating acoustic wave. This study is achieved with the use of two fundamental tools: a framework for solving arbitrary systems of balance laws (`dNami`) [4], coupled with an algorithmic differentiation (AD) software (`TAPENADE`) [3]. The two software combined create a high performance program able to march the linearized compressible Navier-Stokes equation in time. Then a time-stepper method, based on snapshots from the linearized simulation will be used to compute the spectrum of the 3D operator. The fixed point and eigenvalue problems will be solved using the HPC linear algebra environments provided by PETSc [5] and SLEPc [6].
The stability analysis of the screeching jet will be analyzed at different JPRs (Jet Pressure Ratios, i.e. the ratio between the jet and environment pressure) and different nozzle lips thicknesses.

References

[1] Powell Alan. *On the noise emanating from a two-dimensional jet above the critical pressure*. Aeronautical Quarterly, 4, 2, 103–122, 1953, Cambridge University Press.
[2] S. Beneddine, C. Mettot, D. Sipp. *Global stability analysis of underexpanded screeching jets*. European Journal of Mechanics-B/Fluids, 49, 392–399, 2015, Elsevier.
[3] L. Hascoet and V. Pascual. *The Tapenade automatic differentiation tool: Principles, model, and specification*. ACM Trans. Math. Softw. 39:3, 2013.
[4] N. Alferez, E. Touber, S. Winn, Y. Ali. *dNami: a framework for solving systems of balance laws using explicit numerical schemes on structured meshes*. https://doi.org/10.5281/zenodo.6720593, 2022, Zenodo.
[5] Satish Balay et al., *PETSc Web page*. https://petsc.org/, 2022.
[6] V. Hernandez, J. E. Roman, V. Vidal *SLEPc: A scalable and flexible toolkit for the solution of eigenvalue problems*. ACM Trans. Math. Software, 31,3, 351–362, 2005.

THE IDENTIFICATION OF THE INSTABILITY CORE OF INSTABILITIES UNDERPINNED BY AN ACOUSTIC-HYDRODYNAMIC FEEDBACK.

Javier Sierra-Ausin[1,2], Flavio Giannetti[2], David Fabre[1], Paolo Luchini[2]
[1] *Institut de Mécanique des fluides de Toulouse (IMFT), Toulouse 31400, France*
[2] *Dipartimento di Ingegneria (DIIN),Universitá degli Studi di Salerno,Fisciano 84084, Italy*

Acoustic-hydrodynamic feedbacks are a common theme in jet noise. Strong sound emissions are supported by fluid instabilities, whose core is not necessarily localized in space. A common example is the feedback-loop instability of cavity flows, impinging jets or the flow past airfoils. The feedback-loop is composed of a convective instability, which is usually an instability of the shear layer, and an acoustic pressure wave or a hydrodynamic non-local effect. Despite the fact that such a mechanism is widely accepted, a precise identification of the most sensitive spatial regions underpinning the instability is missing. Herein, we propose a non-local decomposition of the *structural sensitivity* [1] and the *endogeneity* [2] concepts. These notions allow us to precisely identify the most sensitive regions of the flow responsible for the closure of the feedback-loop. The systematic use of these techniques could be applied in the design of passive flow control devices.
First, we decompose the direct global mode, respectively the adjoint; the velocity field follows the Helmholtz-Hodge decomposition,

$$\hat{\mathbf{u}} = \hat{\mathbf{u}}_{ac} + \hat{\mathbf{u}}_{hyd} = \nabla\phi_c + \nabla\times\boldsymbol{\Psi}, \qquad \hat{\mathbf{u}}^\dagger = \hat{\mathbf{u}}^\dagger_{hyd} + \hat{\mathbf{u}}^\dagger_{ac} = \nabla\phi^\dagger_c + \nabla\times\boldsymbol{\Psi}^\dagger. \tag{1}$$

In a second step, we analyse the effect of a localised harmonic forcing $\mathbf{H}(\hat{\mathbf{q}}) \equiv \delta(\mathbf{x}-\mathbf{x}_0)\mathbf{P_H}\mathbf{C}_0\mathbf{P}_{\hat{\mathbf{q}}}\hat{\mathbf{q}}$ on

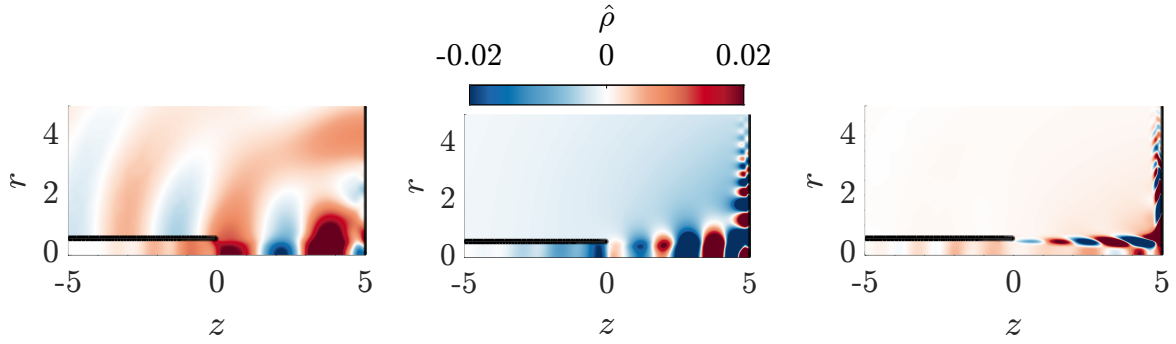

Figure 1: Decomposed density field of a mode ($Re = 900$, $M_J \approx 0.9$). (left) $\hat{\rho}_{ac}$, (centre) $\hat{\rho}_{hyd}$, (right) $\hat{\rho}_s$.

the linearised dynamics $\Big(-\mathrm{i}\omega\mathbf{B}|_{\mathbf{q}_0} + \mathbf{DF}|_{\mathbf{q}_0}\Big)\hat{\mathbf{q}} = \mathbf{H}(\hat{\mathbf{q}})$ by means of a *decomposed* structural sensitivity

$$\begin{aligned} \mathrm{i}\delta\omega_j^k = \langle\hat{\mathbf{u}}_k^\dagger, \delta(\mathbf{x}-\mathbf{x}_0)\mathbf{C}_0\hat{\mathbf{u}}_j\rangle &\leq ||\mathbf{C}_0||||\hat{\mathbf{u}}_k^\dagger(\mathbf{x}_0)||||\hat{\mathbf{u}}_j(\mathbf{x}_0)|| = ||\mathbf{C}_0||\mathbf{S}^{(j,k)}_{\mathbf{u},s}(\mathbf{x}_0), \\ \mathbf{S}^{(j,k)}_{\mathbf{u},s}(\mathbf{x}_0) &= ||\hat{\mathbf{u}}_k^\dagger(\mathbf{x}_0)||||\hat{\mathbf{u}}_j(\mathbf{x}_0)|| \text{ with } j,k = \mathrm{ac},\mathrm{hyd},\mathrm{s}. \end{aligned} \tag{2}$$

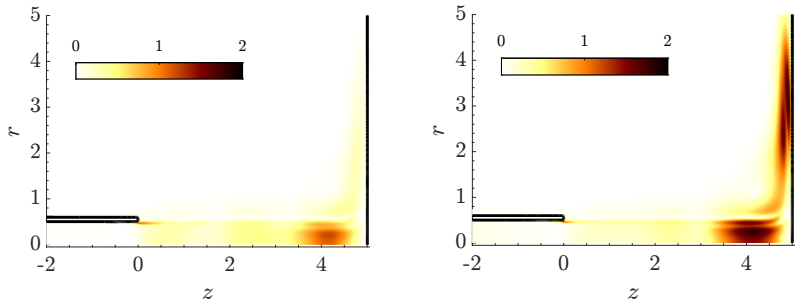

Figure 2: (left) $\mathbf{S}^{(hyd,ac)}_{\mathbf{u},s}$, (right) $\mathbf{S}^{(ac,hyd)}_{\mathbf{u},s}$ for the same global mode as Fig. 1.

References

[1] Giannetti, Flavio, and P. Luchini (2007). *Structural sensitivity of the first instability of the cylinder wake.* Journal of Fluid Mechanics, 581, 167-197.
[2] Marquet, Olivier, and L. Lesshafft. *Identifying the active flow regions that drive linear and nonlinear instabilities* arXiv preprint arXiv:1508.07620 (2015).

DECOMPOSING LONG-RANGE-RESONANT INSTABILITY USING FORCED ONE-WAY NAVIER-STOKES (OWNS).

Eduardo Martini[1], Peter Jordan[1], Daniel Rodríguez[2], Aaron Towne[3], Tim Colonius[4]
[1] *Institut Pprime, CNRS, Université de Poitiers, ISAE-ENSMA*
[2] *ETSIAE-UPM (School of Aeronautics) – Universidad Politécnica de Madrid, Spain*
[3] *Department of Mechanical Engineering, University of Michigan, Ann Arbor, MI 48109, USA*
[4] *Division of Engineering and Applied Science, California Institute of Technology, Pasadena, CA 91125, USA*

Global flow instabilities can be broadly classified into two categories: those underpinned by short-range and long-range resonances. Short-ranged resonant instability originates locally in a specific flow region, sometimes referred to as the wavemaker. Hot jets and cold wakes are underpinned by such a mechanism. Long-range-resonant instability arises due to feedback downstream- and upstream-traveling waves, which are reflected into each other at different flow positions. When these waves are neutrally stable, they can lead to weak forced resonance, as in the acoustic resonances in subsonic jets [1]. When one of the modes is convectively unstable, they may lead to global instability. While global stability analysis captures these phenomena, extracting the underlying physical mechanisms from global modes is not straightforward.

To model long-ranged interactions, two ingredients are needed; the upstream-/downstream-travelling modes, and the reflection mechanisms. While in some cases the reflection mechanism is clear, often when they are given by geometric discontinuities, such as in jet-edge resonances [2], in others the identification of a reflection point and the associated mechanism is not straightforward.

One such example is the screech of supersonic jets. This has been linked to a resonance between a trapped upstream-traveling mode and a KH wave [3], but the details of the reflection mechanism are still elusive. While there is agreement that the upstream reflection point is the jet nozzle, the downstream point is less clear. While the shocks play an important role in the reflection mechanism, where reflection occurs and which is the reflection coefficient are still open questions. A method capable of quantitatively predicting a long-ranged instability, while providing insights into the physical mechanisms, is thus desired.

We thus propose to use the forced One-Way Navier-Stokes (OWNS)[4] approach to break down and study these modes and mechanisms. Starting from the jet nozzle, OWNS tracks the evolution of a KH wave while filtering any reflected waves. The novelty of our approach is to compute the residue of the linearized equations and use it as a source term in an upstream-marching run. We will show that this yields the first reflection of the KH wave. Secondary (and higher-order) reflections can be computed by iterating the proposed procedure. These iterations, each carrying a specific physical mechanism, can be composed to provide a global solution to the linearized problem, which can now be physically interpreted.

Figure 1 illustrates the approach applied to a tensioned string with density variation. It illustrates the contribution of both density changes to the reflected waves, and a secondary reflection, which contributes to the total transmission. When applied to a supersonic jet, the method will make clear the reflection mechanisms present, and their relative contribution to screech.

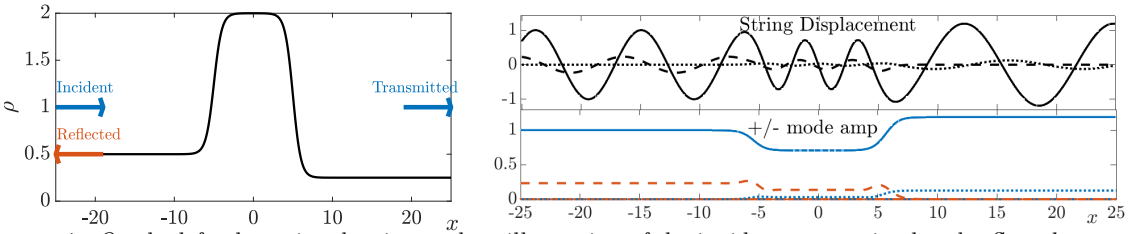

FIGURE 1. *On the left, the string density, and an illustration of the incident, transmitted and reflected waves. The right pane shows the incident wave (solid lines) and the primary and secondary reflections (dashed and dotted) waves. The top and bottom panels show the string displacement and its decomposition into up and downstream traveling waves. Up/downstream traveling waves are depicted in blue/red.*

References

[1] A. Towne et al., Acoustic resonance in the potential core of subsonic jets, Journal of Fluid Mechanics, vol. 825, pp. 1113–1152, Aug. 2017, doi: 10.1017/jfm.2017.346.
[2] P. Jordan et al., Jet–flap interaction tones , Journal of Fluid Mechanics, vol. 853, pp. 333–358, Oct. 2018, doi: 10.1017/jfm.2018.566.
[3] D. Edgington-Mitchell et al., A unifying theory of jet screech, Journal of Fluid Mechanics, vol. 945, p. A8, Aug. 2022, doi: 10.1017/jfm.2022.549.
[4] A. Towne et. al., Efficient global resolvent analysis via the one-way Navier–Stokes equations, Journal of Fluid Mechanics, vol. 948, p. A9, Oct. 2022, doi: 10.1017/jfm.2022.647.

USING A LINEAR MEAN FLOW ANALYSIS WITH AN ACTIVE FLAME APPROACH TO MODEL THE RESPONSE OF A TURBULENT JET FLAME TO ACOUSTIC EXCITATION

Thomas Ludwig Kaiser[1], Gregoire Varillon[2], Wolfgang Polifke[2], Feichi Zhang[3], Thorsten Zirwes[3], Henning Bockhorn[3], Kilian Oberleithner[1]
[1] *Technical University Berlin*
[2] *Technical University Munich*
[3] *Karlsruhe Institute of Technology*

Flow instabilities in turbulent reacting flows are of critical importance in combustion chambers of stationary gas turbines, flight engines, and rockets. One consequence of flow instabilities in reacting flows is a fluctuation in heat release rate, resulting in flame noise, which adds to the overall noise emission of the engine. Furthermore, in an even worse scenario, the heat release oscillations can lock in with an acoustic mode of the combustion chamber, giving rise to a thermoacoustic instability, a phenomenon with potentially catastrophic consequences. To control these phenomena, comprehending the underlying physics is of critical importance. Linear mean flow analysis has elucidated the origin of various types of flow dynamics, among others in turbulent flows. The missing key-link to its application to turbulent reacting flows is the question how a turbulent flame can be modeled in the linearized framework. In our talk, we shed light on this open question.

We model the response of a turbulent reacting methane-air jet to upstream acoustic actuation using linearized methods. The reference solution is obtained by the means of LESs. Based on first principles, we argue that in order for a flame model to be suitable for linearization (and therefore to model the response to the acoustic actuation), it must be able to reproduce the temporal average of the reaction rate when the temporal means of the state variables are used as input to the model. Typically this is the case for RANS reaction models while in general LES and DNS flame models fail to fulfill this mean flow consistency criterion. We substantiate this hypothesis by analyzing three different flame models: an Arrhenius model, widely used in LES and DNS, as well as a turbulent flame speed closure (TFC) and an eddy-break-up (EBU) model, both frequently used in RANS simulations. It is shown that the Arrhenius model does not fulfill the mean flow consistency criterion, the TFC model performs adequate, while the EBU model reproduces the temporal mean reaction rate at high accuracy. If the hypothesis related to the mean flow consistency criterion stated above is correct, the linearized Arrhenius model is supposed to perform worst while the linearized EBU model is expected to perform best among the three investigated models. An a priori analysis illustrated in Fig. 1 confirms our hypothesis. On the left it shows the real part of the reaction rate Fourier mode at the acoustic forcing frequency, $\widehat{\dot{\Omega}}_\mathrm{r}$, based on the LES, which serves as the reference solution. Furthermore, the figure illustrates the reaction rates obtained from the three linearized flame models, when they are fed with the fluctuations of the state variables obtained by the LES (a priori analysis). As predicted, by far best agreement with the LES is obtained by the linearized EBU model. We furthermore discuss the results of an a posteriori analysis using the EBU model, that means we solve the full set of linearized governing equations for upstream acoustic actuation. Finally, the far-reaching consequences of the flame models' necessity to fulfill the mean flow consistency criterion in order to be applicable in the linear framework are discussed in a broader context.

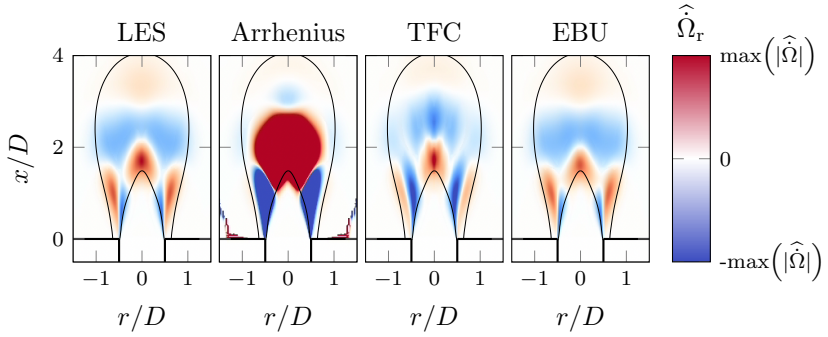

FIGURE 1. *Response of a turbulent reacting jet flow in terms of reaction rate fluctuations to acoustic actuation from upstream direction; left: LES (reference solution); center/left to right: reaction rates based on an a priori analysis of three different linearized flame models*

NOISE-INDUCED TRANSITIONS AFTER A STEADY SYMMETRY-BREAKING BIFURCATION: THE CASE OF THE SUDDEN EXPANSION

Yves-Marie Ducimetière[1], Edouard Boujo[1], François Gallaire[1]
[1]*Laboratory of Fluid Mechanics and Instabilities, École Polytechnique Fédérale de Lausanne, Lausanne CH-1015, Switzerland*

Some nonlinear dynamical systems are metastable: subject to a weak noise, they randomly switch back and forth between two configurations, after long and unpredictable times. This is for instance occurring in the barotropic quasi-geostrophic equations, used to model quasi-stationary turbulent zonal jets, e.g. over Jupiter. Subject to a weak noise, these equations exhibit robust bimodality with abrupt transition, where new jets spontaneously nucleate from westward jets [1]. A similar behavior was also observed in transitional localized turbulence in shear flows, which either decay to an absorbing laminar state, or proliferate via splitting: the average passage time between these two states depends super-exponentially on the Reynolds number, and might thus be enormously long. [2].

However, precisely because the mean transition time to change from one attractor state to the other is extremely large, this situation will usually not be easily detected by simply running the numerical models. Instead, rare event algorithms based on the large-deviation theory are generally used [1, 2].

Alternatively, to compute the flow statistics at a cheaper numerical cost, we propose to generalize the multiple-scale weakly nonlinear expansion technique deployed in [3] for the response of the Duffing oscillator, to the Navier-Stokes equations. Specifically, the Navier-Stokes equations are forced by a weak, narrow-band noise, which therefore acts on the same slow time scale as the amplitude of the dominant mode shortly after a bifurcation point. Thereby, in the case of a steady symmetry-breaking bifurcation, we rigorously derive a stochastically forced Stuart-Landau equation for the dominant symmetry-breaking mode (WNL). The probability density function of the solution is then easily determined by solving the Fokker-Planck equation.

The validity of this reduced order model is tested on the flow past a sudden expansion after the symmetry-breaking bifurcation $Re > Re_c$ (see [4] for the deterministic study), and for different noise amplitudes (see figure 1). At a very low numerical cost, the statistics obtained by solving the Fokker-Planck equation accurately reproduce those of a long-time DNS.

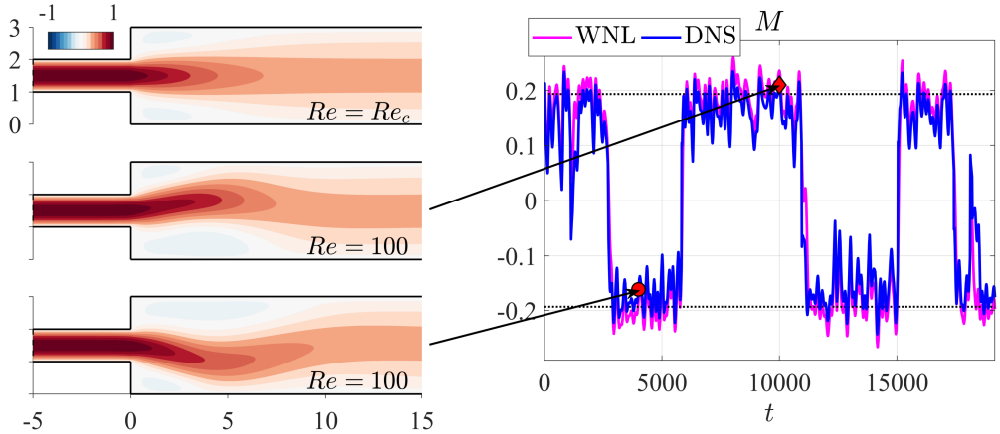

FIGURE 1. *The flow past a sudden expansion at $Re = 100 > Re_c$, beyond the symmetry-breaking bifurcation, and subject to a stochastic forcing. The flow switches from one attractor state to the other at random, extremely long times.*

References

[1] E. Simonnet, J. Rolland, and F. Bouchet. Multistability and rare spontaneous transitions in barotropic β-plane turbulence. *J. Atmos. Sci.*, 78(6):1889–1911, 2021.
[2] S. Gomé, L. Tuckerman, and D. Barkley. Extreme events in transitional turbulence. *Phil. Trans. R. Soc. A.*, 380:20210036, 2022.
[3] H. Rong, W. Xu, and T. Fang. Principal response of Duffing oscillator to combined deterministic and narrow-band random parametric excitation. *Journal of Sound and Vibration*, 210(4):483–515, 1998.
[4] S. Camarri, and G. Mengali. Stability properties of the mean flow after a steady symmetry-breaking bifurcation and prediction of the nonlinear saturation. *Acta Mechanica*, 230:3127—3141, 2019.

LINEAR GLOBAL AND ASYMPTOTIC STABILITY ANALYSIS OF RECTANGULAR CYLINDERS IN GROUND EFFECT

Alessandro Chiarini[1], Franco Auteri[2]
[1] *Complex Fluids and Flows Unit, Okinawa Institute of Science and Technology Graduate University, 1919-1 Tancha, Onna-son, Okinawa 904-0495, Japan*
[2] *Dipartimento di Scienze e Tecnologie Aerospaziali, Politecnico di Milano, via La Masa 34, 20156, Milano (Italy)*

The present work studies the primary instability of the steady two-dimensional flow past rectangular cylinders moving along a solid wall in a two-dimensional parameter space: the cylinder length-to-thickness aspect ratio $\mathcal{AR} = L/D$ and the dimensionless distance from the wall $g = G/D$. The aspect ratio of the cylinder and the gap height are varied between $0.5 \leq \mathcal{AR} \leq 7$ and $0.125 \leq g \leq 10$, to consider short and elongated cylinders, and small and large gap heights. Independently of $\mathcal{AR}$, the primary instability consists of a Hopf bifurcation towards a two-dimensional unsteady state for $g \geq 0.5$, or a regular bifurcation towards a three-dimensional steady state for smaller $g \leq 0.5$, like for the circular-cylinder case [1]. For short cylinders, the critical Reynolds number of the Hopf bifurcation $Re_{c,2D}$ monotonically increases when the gap height decreases. For elongated cylinders, instead, $Re_{c,2D}$ does not have a monotonic dependence on the gap height; a decrease of g destabilises the flow for large gap heights, while the opposite occurs for the smallest gap heights. This is because the ground proximity affects the base flow velocity in the gap in a way that depends on the aspect ratio of the cylinder. For elongated bodies the critical Reynolds number of the regular bifurcation $Re_{c,3D}$ monotonically increases with g towards the free-stream value. For short bodies, instead, it increases for $g \leq 1$ and slightly decreases for larger gap heights.

The structural sensitivity [2] suggests that the main triggering mechanism of the regular bifurcation changes for large and small gap heights. For large g, the wavemaker is localised in the wake recirculating region, and the perturbation fields resemble that of the Crow instability [3] of a counter-rotating vortex pair. For small g, the triggering mechanism is embedded in the large recirculating region over the side of the cylinder opposite to the wall. The hyperbolic/elliptic/centrifugal character of the bifurcation is discussed. For small gap heights, the local WKBJ analysis [4] in the inviscid and short-wave limit has been used. It shows that it is possible to identify close streamlines along which the integrated growth rate is positive. Three branches of unstable orbits are found, two are stationary and one is unsteady. For elongated cylinders, the critical orbit with maximum growth rate (blue line in figure 1 left) is associated with the steady branch of orbits, and crosses the regions where the structural sensitivity is maximum. Once the corrections for finite Reynolds number and spanwise length scales are applied, the asymptotic results compare very well with the results of the global stability analysis (figure 1 right).

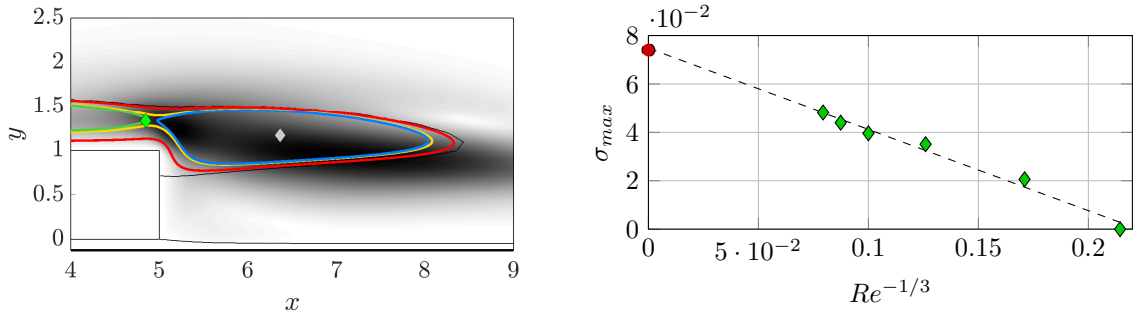

FIGURE 1. *Left: Orbits associated with the three unstable branches detected with the WKBJ analysis superimposed on the structural sensitivity map for $\mathcal{AR} = 5$, $g = 0.125$. Right: Global and local stability analysis results for $\mathcal{AR} = 5$ and $g = 0.125$; the green diamonds are the results for the maximum growth rate from the global stability analysis and the red circle from the local analysis.*

References

[1] A. Rao, M.C. Thompson, T. Leweke, K. Hourigan. *The Flow Past a Circular Cylinder Translating at Different Heights above a Wall J. Fluids Struct.*, 41:9–21, 2013.
[2] F. Giannetti, P. Luchini. *Structural Sensitivity of the First Instability of the Cylinder Wake J. Fluid Mech.*, 581:167–197, 2007.
[3] S.C. Crow. *Stability Theory for a Pair of Trailing Vortices AIAA J.*, 8(12):2172–2179, 1970.
[4] B.J. Bayly. *Three-dimensional Centrifugal-type Instabilities in Inviscid Two-dimensional Flows Phys. Fluids*, 31(1):56–64, 1988.

DATA-ASSIMILATION AND LINEAR ANALYSIS OF TURBULENT MEAN FLOWS AROUND AIRFOILS CLOSE TO STALL

Olivier Marquet
ONERA/DAAA, Université Paris-Saclay

The prediction of turbulent mean flows around airfoil near stalling conditions is still nowadays a challenge for numerical simulation based on Reynolds Averaged Navier Stokes equations. Transition and linear-eddy viscosity turbulence models classicaly used in the aeronautical industry do not properly capture the separation and reattachment of laminar/turbulent boundary layers that occur when increasing the angle of attack. This lack of accuracy prevents such turbulence models from properly predicting not only the mean flow but also the onset of low–frequency oscillations [1] or transverse cellular patterns [2] that are observed experimentally close to the stall angle. In this talk, we will show recent results of our group to improve (i) the turbulence mean flow estimation thanks to adjoint-based data-assimilation techniques [3] and (ii) the prediction of low-frequency oscillations and stall cells using global stability analysis of assimilated mean flows. Firstly, we will consider the onset of stall cells around a NACA4412 airfoil at Reynolds number $Re = 3.5\,10^5$. A transition/turbulence model is corrected using a full-state mean flow velocity field obtained from Direct Numerical Simulation. The stability analysis of the assimilated mean flow, based on the linearization of the RANS and turbulence models, reveals the existence of a three-dimensional steady global mode that gets unstable for angle of attack and transverse wavenumber in agreement with the experimental results. Those results will be discussed and compared to those obtained with methods recently proposed in the litterature and based on frozen eddy-viscosity approaches and eddy-viscosity fields estimated from DNS mean-flow [4]. Secondly, we will consider the low-frequency flow-oscillations around a NACA0012 airfoil at angles of attack 10° and various Reynolds numbers in the range $3.10^4 \leq Re \leq 6.10^4$. In that case, velocity fields measured with Particle Image Velocimetry (PIV) are used to calibrate the turbulence model. The stability analysis of those assimilated mean flows predicts the existence of an unstable low-frequency global mode that may explain bursting events observed in the mean flow. We will conclude this talk by discussing the limit of our approach and the remaining challenges.

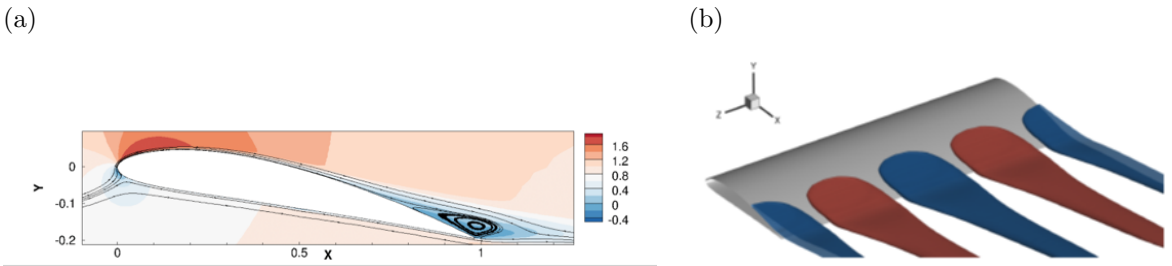

FIGURE 1. *Streamwise velocity of (a) the mean-flow around a NACA4412 airfoil and (b) the least stable three--dimensional global mode at spanwise wavelength* $\lambda = 1.25$ *explaining the onset of stall cells at Reynolds number* $Re = 3.5\,10^5$ *and angle of attack* $\alpha = 12°$.

References

[1] D. Busquet, O. Marquet, F. Richez, M. Juniper & D. Sipp. Bifurcation scenario for a two-dimensional static airfoil exhibiting trailing edge stall, *Journal of Fluid Mechanics*, 928:A3, 2021.
[2] F. Plante, J. Dandois, S. Beneddine, E. Laurendeau, & D. Sipp. Link between subsonic stall and transonic buffet on swept and unswept wings: from global stability analysis to nonlinear dynamics, *Journal of Fluid Mechanics*, 908:A16, 2021.
[3] L. Franceschini, D. Sipp & O. Marquet. Mean-flow data assimilation based on minimal correction of turbulence models: Application to turbulent high Reynolds number backward-facing step, *Physical Review Fluids*, 5(9):094603, 2020.
[4] E. Pickering, G. Rigas,O. T. Schmidt, D. Sipp & T. Colonius. Optimal eddy viscosity for resolvent-based models of coherent structures in turbulent jets, *Journal of Fluid Mechanics*, 917:A29, 2021.

NONLINEAR OPTIMAL PERTURBATIONS ENGENDERING EXTREME EVENTS IN THE TURBULENT CHANNEL FLOW

N. Ciola[1,2], S. Cherubini[1], P. De Palma[1], J.-C. Robinet[2]
[1] *DMMM, Politecnico di Bari, Via Re David 200, 70125 Bari, Italy*
[2] *DynFluid, Arts et Métiers Paris /CNAM, 151 Bd de l'Hôpital, 75013 Paris, France*

In this work, we search optimal perturbations leading to extreme dissipative events in the turbulent channel flow at $Re_\tau = 180$. Motivated by the recent work in [1], we try to establish a link between streak instability and extreme events generation. To this aim, the procedure presented in [2] is extended to compute an optimal perturbation with respect to a generic three-dimensional turbulent snapshot instead of the one-dimensional mean profile. The optimization problem is formulated using the turbulent dissipation as objective function and imposing a short target time, typical of extreme events. The resulting optimal is localized in the near-wall region and displays the upstream tilting characteristic of the Orr's mechanism. Interestingly, it is found that the perturbation is positioned along the pre-existing structures of the turbulent snapshot with respect to which it was computed. In particular, as shown in Figure 1, it is placed at the interface between a positive and a negative sign streamwise velocity streak, i.e. in the zones of highest shear, where inflection points may exist. Indeed, when the evolution of the perturbed flow is compared to the unperturbed one, we observe that the perturbation leads to: (i) a sudden breakdown of the pre-existing structures (Figure 2); (ii) a strong peak in the global turbulent dissipation; (iii) a heavier tail in the dissipation PDF (probability density function) distribution, meaning a higher number of extreme events. The robustness and statistical relevance of this behaviour is assessed repeating the numerical experiment using different initial snapshots (realizations). The POD analysis presented in [1] is performed to show that the local structure of the events is actually the same in the perturbed and in the unperturbed flow, i.e. that the optimal perturbation captures physically relevant mechanisms.

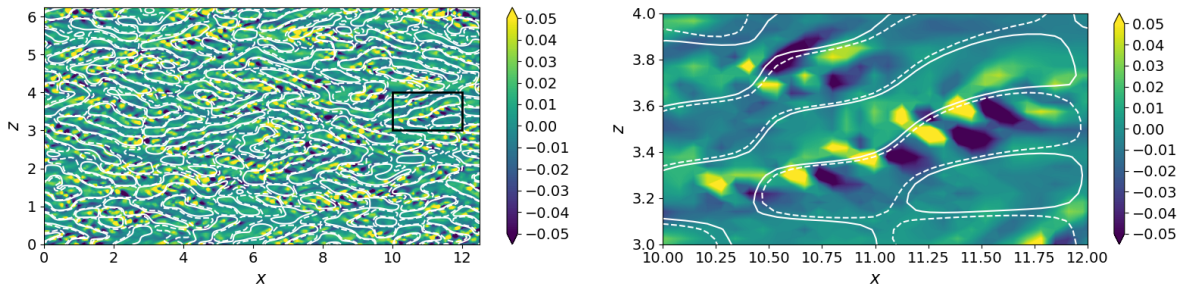

Figure 1: Distribution of the streamwise perturbation (shaded contours) with respect to the streaks of the unperturbed flow at t_0 (white lines, solid for positive and dashed for negative) in the $y^+ = 10$ plane.

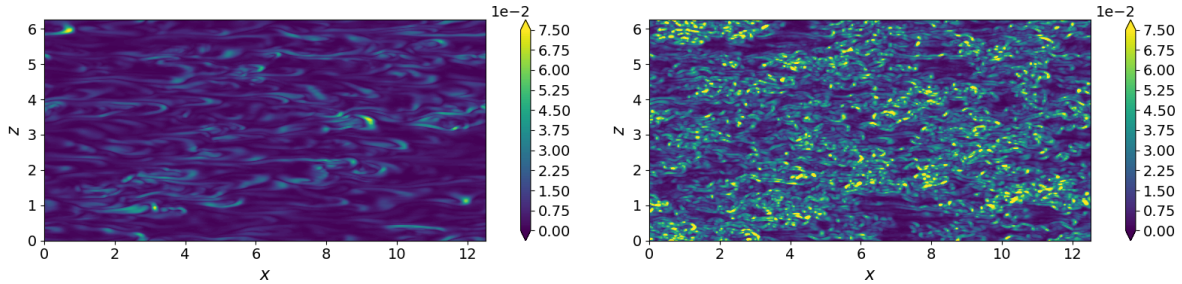

Figure 2: Contours of the dissipation at $t = t_0 + T = 302$ on the $y^+ = 10$ plane. Left: unperturbed flow. Right: optimally perturbed flow.

References

[1] M. J. P. Hack, and O. T. Schmidt. Extreme events in wall turbulence. *J. Fluid Mech.*, 907(A9), 2021.
[2] M. Farano, and S. Cherubini, J.-C. Robinet, P. De Palma. Optimal bursts in turbulent channel flow. *J. Fluid Mech.*, 817, 35-60, 2017.

INSTABILITY FROM NON-LOCAL FEEDBACK IN A LAMINAR V-SHAPED FLAME

Chuhan Wang[1,2], Lutz Lesshafft[2], Grégoire Varillon[3], Wolfgang Polifke[3], Xu Chunxiao[1]
[1] *AML, Department of Engineering Mechanics, Tsinghua University, 100084 Beijing, PR China*
[2] *LadHyX, CNRS, Ecole polytechnique, Institut Polytechnique de Paris, 91120 Palaiseau, France*
[3] *TUM School of Engineering and Design, Department of Engineering Physics and Computation, Technical University of Munich, 85747 Garching, Germany*

Unsteadiness in flames is a fascinating field of application for linear instability analysis and flow control, both because of their technical relevance and because of the rich dynamics that can result from the interplay of vortical, thermal, chemical and acoustic elements. We present a modal linear analysis of a V-shaped flame, as it develops in a lean premixed fuel-air jet exiting from a round nozzle with a central rod. The flame is anchored on the rim of the rod, forming an open cone, as seen from the reaction rate snapshot in Figure 1a. The vorticity of the flow, however, is concentrated in the outer shear layer of the annular jet, as shown in Figure 1b. Reaction and vorticity dynamics therefore are mostly separated, except near the flame tip, where both coalesce.

Axisymmetric simulations in the laminar regime (Reynolds number $Re = 1626$) display limit-cycle oscillations. In our reacting flow equations, the chemistry is accounted for through a simplistic one-step reaction model, which apparently produces the essential elements for such typical V-flame instability, although it is not *a priori* expected to yield reliable quantitative predictions for a given fuel. Linear global eigenmodes of the mean flow in the limit-cycle state are computed, and a family of slightly unstable modes with harmonic eigenfrequencies ("arc branch") is found. Their fundamental frequency is consistent with the periodicity of the limit cycle, and their harmonic character suggests a non-local feedback. A close inspection of the eigenfunctions clearly indicates a dominant role of hydrodynamic instability waves in the outer shear layer that are generated at the nozzle edge, and that generate global pressure fluctuations as they shake the downstream end of the flame. This scenario constitutes a particular case of *intrinsic thermo-acoustic* instability in unconfined flames [1, 2].

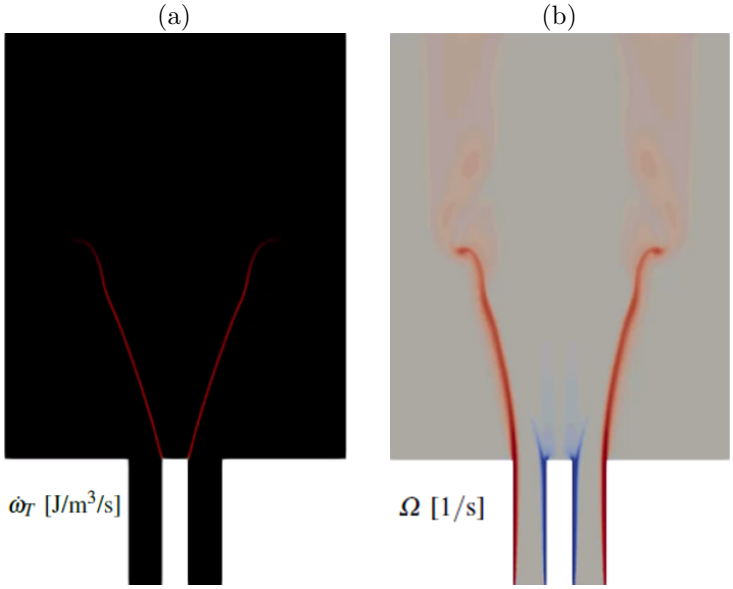

FIGURE 1. *Axisymmetric limit-cycle oscillations in a laminar V-flame: (a) reaction rate; (b) vorticity.*

References

[1] A. Avdonin, M. Meindl and W. Polifke. Thermoacoustic analysis of a laminar premixed flame using a linearized reactive flow solver. *Proc. Combust. Inst.*, 37(4):5307–5314, 2019.
[2] C. Wang, T. Kaiser, M. Meindl, K. Oberleithner, W. Polifke and L. Lesshafft. Linear instability of a premixed slot flame: flame transfer function and resolvent analysis. *Combust. Flame*, 240:112016, 2022.

RESOLVENT ANALYSIS OF A ROUND SWIRLING TURBULENT JET

Quentin Chevalier[1], Lutz Lesshafft[1]
[1] *Laboratoire d'Hydrodynamique, CNRS, Ecole polytechnique, Institut Polytechnique de Paris, 91120 Palaiseau, France*

Observation of streaks in round jets is a relatively recent result [1]. Since these coherent structures were found to play a critical role in the transition to turbulence with flat plates [3], one can wonder what role they could play in jets. Several instability works [2] have led to a better characterisation of the linear behaviour of turbulent round jets, as well as stress several mechanisms that amplify them.

We propose to apply the same analysis to rotating jets, and study them through linear resolvent formalism. This allows us to go from high Reynolds Navier-Stokes to most amplified forcing and response at a given frequency.

In order to obtain a turbulent jet, we use the eddy viscosity model of Spalart-Allmaras as implemented in the OpenFOAM code. Therefore our parameters are : Reynolds number, fixed at $Re = 400000$, Strouhal number St, rotation intensity S and azimuthal decomposition index m.

We'd like to stress a first preliminary result. Looking at figure 1 one can see a clear separatino from positive and negative m in the rotating case as well as a strong amplification of lower frequencies in the case $|m| > 0$.

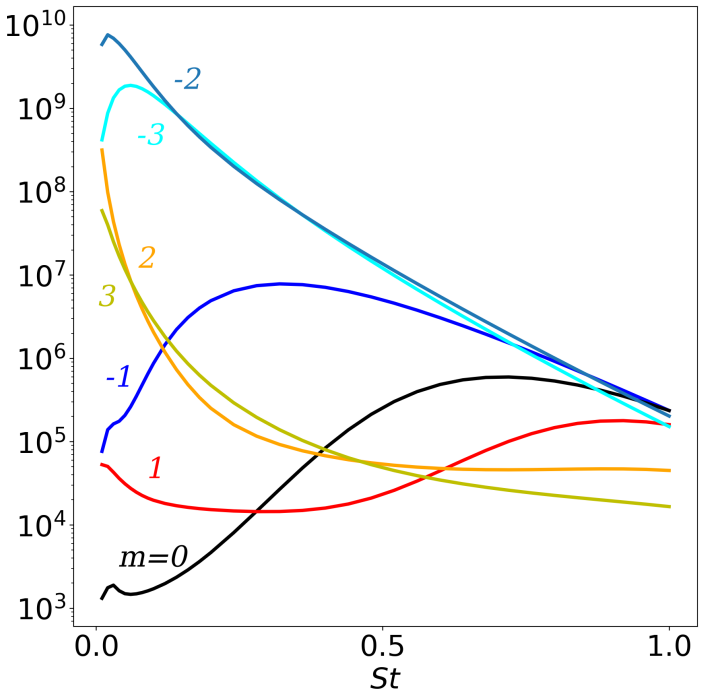

FIGURE 1. *Graphe des gains obtenus* $Re = 400000$ *et* $S = 1$

References

[1] P. A. S. NOGUEIRA, A. V. G. CAVALIERI, P. JORDAN & V. JAUNET, Large-scale streaky structures in turbulent jets, *Journal of Fluid Mechanics*, **873**, 211-237 (2019)
[2] E. PICKERING, G. RIGAS, P. A. S. NOGUEIRA, A. V. G. CAVALIERI, O. T. SCHMIDT & T. COLONIUS, Lift-up, Kelvin-Helmholtz and Orr mechanisms in turbulent jets, *Journal of Fluid Mechanics*, **896**, A2 (2020)
[3] F. WALEFFE, On a self-sustaining process in shear flows, *Physics of Fluids*, **9**, 883–900 (1997)

MEAN RESOLVENT OPERATOR OF A STATISTICALLY STEADY FLOW

Colin Leclercq, Denis Sipp
DAAA, ONERA, Université Paris Saclay, 8 rue des Vertugadins, 92190 Meudon, France

This work addresses the relevance of linear time-invariant (LTI) input-output models of statistically steady flows, in relation to flow control and resolvent/modal analyses about a mean flow. The existence of a transfer function or resolvent operator is indeed inherent to LTI systems, but fully-developed unsteady flows do not fall into that category. However, it is well-known that resolvent analysis about a mean flow often yields insightful results regarding coherent structures and amplification mechanisms producing them [1]. It is also known that small-amplitude harmonic forcings may be used to identify transfer functions from actuators to sensors which are relevant for control purposes [2]. Finally, it is commonly observed that modal analysis about the mean of a periodic flow yields both the fundamental frequency of that flow [3] – a property often termed RZIF [5] – and the associated coherent motion.

To clarify these observations, we lift in [4] the *ad hoc* assumption of linearization about a mean flow and investigate the time-dependent character of the linear response to forcing of the periodic fluidic pinball, by impulsively forcing the time-varying tangent system at different instants. Using the mean impulse response, we compute the corresponding mean frequency response and compare it with the frequency response about the mean flow (see figure 1). Excellent agreement is overall observed, but key differences are also noted.

Using the harmonic balance (HB) framework, we then elucidate the connection between the two transfer functions, which enlightens the aforementioned observations from the literature, in the case of periodic flows. We show that small-amplitude harmonic forcings may be used to identify a unique LTI operator even though the base flow is time-varying. This transfer function is the statistically optimal LTI representation of the input-output behaviour based on the mean resolvent operator $\mathbf{R}_0$. This operator is a frequential representation of the mean Koopman operator, with purely imaginary poles at resonant frequencies of the periodic base flow. The resolvent operator about the mean flow $\mathbf{R}_{\overline{\mathbf{U}}}$ is a reduced-order approximation of $\mathbf{R}_0$, which explains the agreement between the two transfer functions and the RZIF property. Conveniently, $\mathbf{R}_0$ does not suffer from the same ambiguity that $\mathbf{R}_{\overline{\mathbf{U}}}$ recently noted by [6].

The HB theory extends to quasi-periodic flows but does not apply to more complex flows. Yet, it is verified numerically that the mean linear response to forcing approximates the linear response about the mean flow in both the chaotic fluidic pinball and the stochastic flow over a backward-facing step, hinting at a more general connection between $\mathbf{R}_0$ and $\mathbf{R}_{\overline{\mathbf{U}}}$.

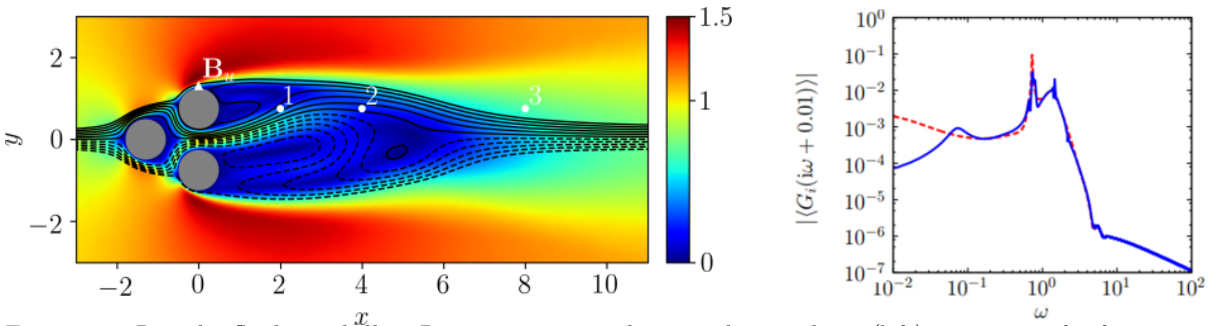

FIGURE 1. *Periodic fluidic pinball at* $Re = 100$*, mean velocity and streamlines (left); mean transfer function in solid blue line versus transfer function about the mean flow in dashed red line (right), from volume force actuator* $\mathbf{B}_u$ *near the top cylinder to vertical velocity probe* 2 *in the wake.*

References

[1] B. J. McKeon and A. S. Sharma, A. S. A critical-layer framework for turbulent pipe flow. *J. Fluid Mech.*, 658, 336-382, 2010.
[2] J. A. Dahan, A. S. Morgans and S. Lardeau. Feedback control for form-drag reduction on a bluff body with a blunt trailing edge. *J. Fluid Mech.*, 704, 360–387, 2012.
[3] B. Pier. On the frequency selection of finite-amplitude vortex shedding in the cylinder wake. *J. Fluid Mech.*, 458, 407–417, 2002.
[4] C. Leclercq, D. Sipp. Mean resolvent operator of a statistically steady flow. https://arxiv.org/pdf/2210.07104.pdf (under review).
[5] S. E. Turton, L.S. Tuckerman and D. Barkley. Prediction of frequencies in thermosolutal convection from mean flows. *Physical Rev. E*, 91(4), 043009, 2015.
[6] U. Karban, B. Bugeat, E. Martini, A. Towne, A. V. G. Cavalieri, L. Lesshafft, A. Agarwal, P. Jordan and T. Colonius. Ambiguity in mean-flow-based linear analysis. *J. Fluid Mech.*, 900, R5, 2020.

RESOLVENT OPTIMISATION VIA NONLINEAR VARIABLE TRANSFORMATION

Ugur Karban[1], André Cavalieri[2], Peter Jordan[3], Tim Colonius[4]
[1] *Aerospace Engineering Department, Middle East Technical University, Ankara, Turkey*
[2] *Instituto Tecnológico de Aeronáutica, São José dos Campos/SP, Brazil*
[3] *Département Fluides, Thermique, Combustion, Institut Pprime, CNRS-University of Poitiers-ENSMA, France*
[4] *Division of Engineering and Applied Science, California Institute of Technology, Pasadena, California 91125, USA,*

In a previous study [1], we showed mean-flow-based linear analysis depends on the choice of dependent variables. It was argued that this ambiguity could be used for optimization of resolvent-based models via specific choice of variables. In this study, we will present a methodology to achieve this goal.
A key parameter to measure the performance of resolvent-based models is the alignment between the response modes of the resolvent operator and the SPOD modes of the flow. SPOD modes correspond to the most-energetic coherent structures that exist in the flow. Similarity between the response modes, which depends only on the mean-flow quantities, and the SPOD modes indicates a potential to predict the dynamic flow structures using RANS-type analyses. There is an ever expanding literature on the investigation of such a similarity in different turbulent flows. In Beneddine *et al.* (2016) [2], the similarity between the optimal response and SPOD modes was related to the high-gain separation observed in the resolvent operator. The underlying idea was that in case of very high-gain separation, the response would be dominated by the optimal response mode regardless of the forcing color. In a later study by Symon *et al.* (2018) [3], the success of the resolvent analysis was shown to depend on the non-normality of the mean-flow-based linear operator. One measure of non-normality involves the distance of the least stable eigenvalue to the imaginary axis. They state that for pseudo-resonant systems, where this distance is small, resolvent analysis is more likely to provide information about the coherent structures of the flow.
We will test in our study if these two criteria can be used for optimization of resolvent analysis via variable transformation, which causes change in the eigenvalues/singular values of the linear/resolvent operator. We will show using a model problem based on Ginzburg-Landau equation that maximization of the gain separation does not necessarily increase the alignment between the optimal response and SPOD modes. The alignment does increase on the other hand, if the least stable eigenvalue is brought closer to the imaginary axis. Figure 1 shows for the model problem the improvement in the alignment between the optimal response and SPOD modes thanks to a nonlinear transformation. In the full paper, we will apply this approach to a turbulent channel to test its applicability in a real flow case.

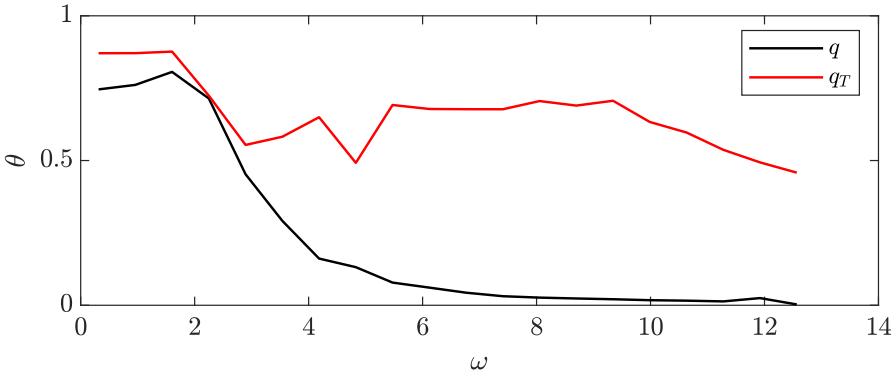

FIGURE 1. *Alignment level, θ, in the original (black) and the transformed systems (red) for a range of frequencies.*

References

[1] U. Karban, B. Bugeat, E. Martini, A. Towne, A. V. G. Cavalieri, L. Lesshafft, A. Agarwal, P. Jordan, and T. Colonius. Ambiguity in mean-flow-based linear analysis. *Journal of Fluid Mechanics*, 900:R5, 2020.
[2] S. Beneddine, D. Sipp, A. Arnault, J. Dandois, and L. Lesshafft. Conditions for validity of mean flow stability analysis. *Journal of Fluid Mechanics*, 798:485–504, 2016.
[3] S. Symon, K. Rosenberg, S. T. M. Dawson, B. J. McKeon. Non-normality and classification of amplification mechanisms in stability and resolvent analysis. *Pyhsical Review Fluids*, 3(5):053902, 2018.

TOWARDS EFFICIENT AND ROBUST OPTIMISATION OF UNSTEADY COMPLEX FLOWS

Taraneh Sayadi
Institut Jean le Rond d'Alembert, Sorbonne Université/CNRS

The past decades have seen remarkable progress in computing capabilities, allowing CFD to become an ever more present tool in describing and predicting unsteady complex flows. However, robust optimisation and control of these flows on the basis of such high-fidelity simulations remains a big challenge. Targeted manipulation of such flows by enhanced designs or active control strategies is indeed crucial for improvements in performance and robustness. It is also necessary for venturing beyond standard operating conditions, and to ultimately meet the ever more stringent regulations on pollutants and emissions. The main bottleneck arises from the large cost associated with performing each function evaluation (a full and potentially unsteady CFD calculation), and suboptimal performance of state-of-the-art optimisation algorithms in the presence of strong nonlinearities and turbulence.

During this talk we will introduce state-of-the-art algorithms optimisation spanning from gradient-based to derivative-free techniques with various degree of complexity, where a multi fidelity approach (resorting to model reduction procedures) is used to reduce the numerical cost of both the function and gradient calculations. We will also explore promising but less conventional techniques which could serve as serious alternatives to these more traditional approaches.

ENERGY GROWTH IN VARIABLE-DENSITY TRAILING VORTICES

J. Sablon[1], J. Fontane[1], G. Nastro[1], L. Joly[1]
[1] *ISAE-SUPAERO, Université de Toulouse, 10 Avenue Édouard Belin, 31055 Toulouse, France*

The stability of trailing vortices has been studied for years and remains an essential research subject nowadays. These vortices generated by the wings (or any finite foil) are an unavoidable by-product of the lift generation. They can be hazardous when aircraft are following each other especially during take-off and landing phases [4]. This leads to substantial security distances between each aircraft in the airports and consequently to higher operating costs. Nowadays, the ecological footprint of the aircraft is a major issue for the civil aviation industry. The reduction of the vortex persistence is likely to reduce the occurrence of contrails in the sky by an increase of the mixing of the different gases. As the contrails have a significant contribution to the aviation-induced radiative forcing [2], their mitigation is expected to a reduce the climate impact of the sector. The study of instabilities which are present on isolated vortices or vortex systems is a necessary first step to better understand the destabilisation mechanisms and stands as a key point for control strategies that could be implemented on aircraft.

More specifically, this study is conducted on an isolated variable-density tridimensional vortex described by an analytical base flow model corresponding to the q-vortex, a parallel version of the Batchelor vortex [1], where the swirl number q measures the ratio between the azimuthal and the axial characteristic velocity scales. A Gaussian density profile is superimposed to the q-vortex to get a plausible variable-density profile. First, proceeding to a modal stability analysis, an exhaustive exploration of the large parameter space has been conducted to consider the influence of the Atwood number At, the Reynolds number Re, the density-to-vorticity radius ratio of the base flow ε, the swirl number q and both the axial k and azimuthal m wavenumbers of the mode [3]. Second, a non-modal stability analysis has been performed using a direct-adjoint optimisation loop to get a better understanding of the destabilisation phenomena and the dynamics of the vortex at finite times. Because the Navier–Stokes operator is non-normal, short term perturbations are observed with significant transient energy growth that may lead to vortex breakdown even if the flow is stable at large times. The axial vorticity field of an optimal perturbation and its response are shown alongside the energy gain evolution on figure 1 for a dense vortex core ($At = 0.5$, $Re = 10^3$, $Sc = 1$, $\varepsilon = 2$, $q = 0.2$, $k = 0.7$ and $m = -1$). The gain supplement represents the extra gain obtained with injection of the optimal excitation (i.e. the adjoint mode) compared to the evolution of the pure modal instability.

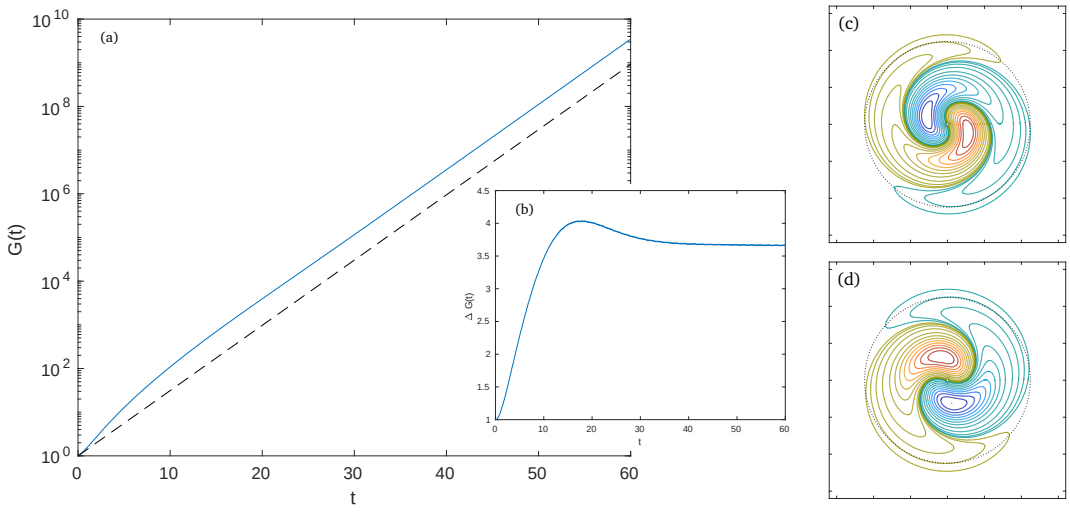

Figure 1: (a) Energy gain evolution over time. (b) Energy gain supplement obtained with the optimal excitation. Axial vorticity field of the optimal excitation (c) and the optimal response (d).

References

[1] G. K. Batchelor Axial flow in trailing line vortices. *Journal of Fluid Mechanics*, 20(4):645–658, 1964.
[2] D. Lee *et al.* The contribution of global aviation to anthropogenic climate forcing for 2000 to 2018. *Atmospheric Environment*, 244:117834, 2021.
[3] J. Sablon, J. Fontane, L. Joly. Stability of high-density trailing vortices. *Theor. Comput. Fluid Dyn.*, 2023.
[4] P. R. Spalart. Airplane trailing vortices. *Annu. Rev. Fluid Mech.*, 30(1):107–138, 1998.

LINEAR PATH INSTABILITY OF BUOYANCY-DRIVEN PERMEABLE DISKS

P.G. Ledda[1], G. Vagnoli[2], G.A. Zampogna[3], S. Camarri[4], F. Gallaire[3]
[1] *DICAAR, Università degli Studi di Cagliari, Cagliari, Italy*
[2] *Gran Sasso Science Institute, L'Aquila, Italy*
[3] *LFMI, Ecole Polytechnique Federale de Lausanne, Lausanne, Switzerland*
[4] *DICI, Università di Pisa, Pisa, Italy*

The prediction of trajectories of buoyancy-driven bodies in a viscous fluid is a problem of interest in many engineering and scientific disciplines (cf. Ern *et al.* [1] for a review). Intriguing falling or rising paths stem from the interaction between the buoyancy-driven object and the surrounding fluid. Simple-shaped objects, such as disks, present a great variety of trajectories, ranging from zig-zag to tumbling and chaotic motions [2]. These trajectories are sensitive to local modifications of the object: the presence of an internal hole alters the wake past the falling disk and stabilizes the falling trajectory [3]. The idea that flow through internal holes may promote the stability of wake flows has been confirmed for both natural and artificial systems, in particular when a diffused permeability is considered [4]. However, systematic studies on the effect of permeability on trajectories of buoyancy-driven objects are lacking, yet. In the impervious case, linear stability analysis revealed itself as a suitable tool to investigate the departure from the vertical trajectory [5]. We perform a linear stability analysis of the steady vertical path of a thin permeable disk, modeled via a stress-jump condition which stems from homogenization theory. The flow relative velocity, in the case of vertical motion, presents a recirculation region detached from the disk. An increase in permeability leads to detachment and shrinking of the recirculation region, until it disappears (see Figure 1(a)). In analogy with the impervious disk case [5], one non-oscillatory and several oscillatory modes destabilize the vertical trajectory. Permeability progressively filters out the wake dynamics from the instability of the steady vertical path, first stabilizing modes dominated by wake oscillations. A further increase in permeability quenches all linear instabilities, as shown in Figure 1(b). For sufficiently large permeabilities, the disk first undergoes a non-oscillatory instability, which is expected to lead to a steady oblique path with a constant disk inclination, in the nonlinear regime (Figure 1(c)). Results are compared against analyses of actual, full-scale, microstructured disks, with a good agreement in terms of flow patterns and instability thresholds.

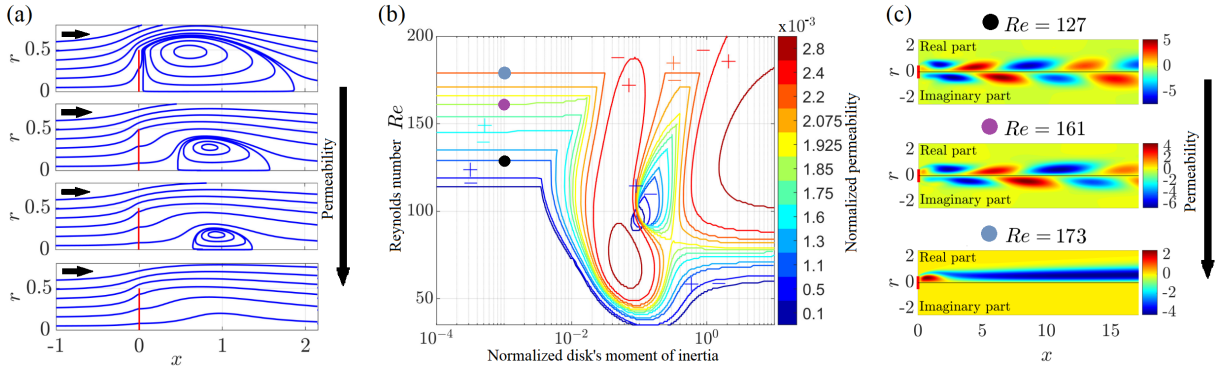

FIGURE 1. *(a) Streamlines of the relative flow velocity of the steady vertical path, for fixed falling Reynolds number* $Re = 85$ *and increasing permeability. (b) Marginal stability curves for the instability of the steady vertical path as functions of the Reynolds number and of the disk's moment of inertia, for increasing values of permeability. The plus and minus sign help in identifying the stable and unstable regions in the parameters' space. (c) Axial velocity mode for increasing permeability and fixed disk's moment of inertia, as reported in panel (b).*

References

[1] Ern, P., Risso, F., Fabre, D., and Magnaudet, J. (2012). Wake-induced oscillatory paths of bodies freely rising or falling in fluids. *Annual Review of Fluid Mechanics*, 44:97–121.
[2] Auguste, F., Magnaudet, J., and Fabre, D. (2013). Falling styles of disks. *Journal of Fluid Mechanics*, 719:388–405.
[3] Vincent, L. and Shambaugh, W. S. and Kanso, E. (2016). Holes stabilize freely falling coins. *Journal of Fluid Mechanics*, 801:250–259.
[4] Ledda, P. G., Siconolfi, L., Viola, F., Gallaire, F., and Camarri, S. (2018). Suppression of von kármán vortex streets past porous rectangular cylinders. *Physical Review Fluids*, 3:103901.
[5] Tchoufag, J., Fabre, D., and Magnaudet, J. (2014). Global linear stability analysis of the wake and path of buoyancy-driven disks and thin cylinders. *Journal of Fluid Mechanics*, 740:278–311.

MECHANISMS FOR THREE-DIMENSIONAL INSTABILITIES IN THE WAKE BEHIND A CYLINDER

Andrey I. Aleksyuk[1], Matthias Heil[1]
[1]*Department of Mathematics, University of Manchester, United Kingdom*

The two-dimensional time-periodic viscous fluid flow (the von Kármán vortex street) behind a circular cylinder is linearly unstable to two modes of three-dimensional perturbations, labelled A and B, at critical Reynolds numbers $\mathrm{Re}_A \approx 190$ and $\mathrm{Re}_B \approx 260$ and critical wavelengths $\lambda_A \approx 4$ and $\lambda_B \approx 0.8$ diameters of the cylinder respectively [1, 2]. Despite previous research narrowing down the source of these instabilities to the vortex formation region [3, 4], identifying the underlying physical mechanisms remains a challenging problem due to the complexity of the non-stationary flow in this region. In this talk, we address this problem by leveraging the fact that the essential mechanisms for modes A and B are preserved in the limits of infinitely large and short wavelengths, respectively, and by exploiting the asymptotic expansion of the solution to simplify the problem.

For mode A, we show that the three-dimensional flow tends to organise such that, in each streamwise slice, it still corresponds to the base-flow two-dimensional solution, but at shifted times [5]; see Figure 1a, b. This suggests an explanation for the observed pattern of the perturbations and provides a possible criterion for the unambiguous classification of three-dimensional instabilities of this kind.

For mode B, we propose a way of justifying the hypothesis [4, 6, 7] that local instability along a closed trajectory (the so-called orbit 3) in the vortex formation region is responsible for the instability [8]; see Figure 1c. This hypothesis was initially built upon a WKBJ-based analysis in the limit of inviscid perturbations with infinite wavenumber. The lack of justification for these assumptions resulted in conflicting views in the literature [6, 7]. Our approach justifies the infinite-wavenumber assumption and shows new evidence that the "inviscid" instability along orbit 3 is, indeed, at the core of the mode B instability.

Finally, we discuss the selection of critical parameters for the instabilities and rationalise the non-trivial dependence of the growth rate on the spanwise wavenumber by identifying the contribution of basic physical mechanisms to flow destabilisation. Our results have broad implications for a general understanding of the underlying mechanisms for large- and short-wavelength three-dimensional instabilities.

This research was supported by the Royal Society Newton International Fellowship (NIF\R1\201343). The authors would like to acknowledge the assistance given by Research IT, and the use of the HPC Pool funded by the Research Lifecycle Programme at the University of Manchester.

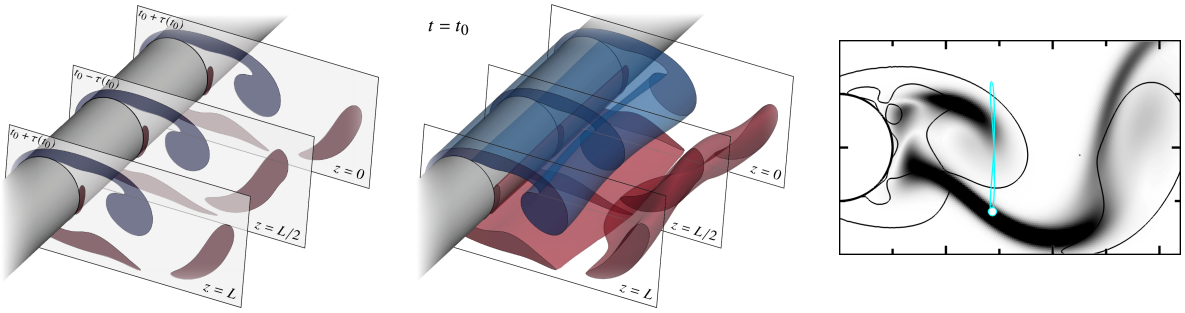

(a) 2D base flow at different times *(b) 3D perturbed flow* *(c) Orbit 3 and mode-B perturbations*

FIGURE 1. *Illustration of the time-shifting pattern of mode A (a,b) and orbit 3 associated with the mode-B instability (c).*

References

[1] Barkley, D., Henderson, R.D. Three-dimensional Floquet stability analysis of the wake of a circular cylinder. *J. Fluid Mech.*, **322**, 215–241 (1996).
[2] Williamson, C.H.K. Three-dimensional wake transition. *J. Fluid Mech.*, **328**, 345–407, (1996).
[3] Barkley, D. Confined three-dimensional stability analysis of the cylinder wake. *Phys. Rev. E*, **71**, 017301 (2005).
[4] Giannetti, F., Camarri, S., Luchini, P. Structural sensitivity of the secondary instability in the wake of a circular cylinder. *J. Fluid Mech.*, **651**, 319–337 (2010).
[5] Aleksyuk, A.I., Heil, M. On the onset of long-wavelength three-dimensional instability in the cylinder wake. *J. Fluid Mech.*, (2023, under review).
[6] Giannetti, F. WKBJ analysis in the periodic wake of a cylinder. *Theor. App. Mech. Lett.*, **5**(3), 107–110 (2015).
[7] Jethani, Y., Kumar, K., Sameen, A., Mathur, M. Local origin of mode-B secondary instability in the flow past a circular cylinder. *Phys. Rev. Fluids*, **3**(10), 103902 (2018).
[8] Aleksyuk, A.I., Heil, M. On the onset of short-wavelength three-dimensional instability in the cylinder wake. *J. Fluid Mech.*, (2023, in preparation).

QUASI-PERIODIC OPTIMAL PERTURBATIONS IN A STREAKY BOUNDARY LAYER

A. Jouin[1,2], S. Cherubini[1] and J.-C. Robinet[2]
[1] *DMMM, Politecnico di Bari, Via Edoardo Orabona, 4, Bari BA, Italy,*
[2] *DynFluid, ENSAM, 151, Bd. de l'Hôpital, 75013 Paris, France*

Subcritical transition to turbulence of a boundary layer is investigated, with a focus on the passage from streaks to turbulent spots. Thus, we consider the flow over a flat plate on which are superimposed linear optimal streaks. Non modal stability analysis of this configuration is performed via the Bloch wave formalism introduced in [1] for n-periodic systems. For moderate amplitude of the streaks, the system exhibits "frustration", defined in [2] as the inability of an ordered system to find a unique ground state due to a competition of wavelengths. In the context of transient growth, this phenomenon appears as a degeneracy of the largest singular value of the linearised Navier-Stokes operator: several optimal perturbations share the same optimal gain and optimal time despite different detuning factors. From there, Wannier functions [3], commonly used in solid state physics, are introduced in the context of transient growth. These functions are obtained from the superposition of Bloch waves with different detuning factors. The resulting perturbation presents some interesting features: it is optimal through linearity and quasi-periodic due to interference between the Bloch waves. As it can be seen in figure 1, these disturbances are characterised by the presence of localised streaky structures that can be arranged in an oblique fashion ($200 \leq z \leq 280$) or form a staggered pattern ($z \approx 400$). Ultimately, this new type of optimal perturbaiton may play a significant role in the formation and development of turbulent bands and spots.

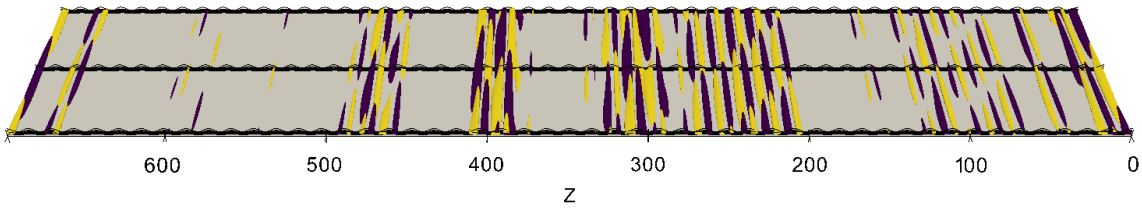

FIGURE 1. *Streamwise velocity component of the optimal quasi-periodic Wannier function at the optimal time* T_{opt}. *The disturbance is obtained for* $Re_\delta = 430$, $\alpha = 0.05$ *and for a system composed of* $n = 50$ *streaks. Black lines denotes isocontours of the base flow.*

References

[1] P. Schmid. Stability analysis for n-periodic arrays of fluid systems. *Phys. Rev. Fluids*, 2, 113902, 2017.
[2] M. Nixon, E. Ronen, A. A. Friesem, N. Davidson. Observing geometric frustration with thousands of coupled lasers. *Phys. Rev. Lett.*, 110(18):184102, 2013.
[3] G. H. Wannier. The Structure of Electronic Excitation Levels in Insulating Crystals. *Phys. Rev.*, 52, 191, 1937.

STABILITY PREDICTION OF MULTIPLE FREELY-OSCILLATING BODIES

Théo Mouyen[1,2], Javier Sierra-Ausín[1,2], Flavio Giannetti[2], David Fabre[1]
[1] *Institut de Mécanique des fluides de Toulouse (IMFT), Toulouse 31400, France*
[2] *Dipartimento di Ingegneria (DIIN),Universitá degli Studi di Salerno,Fisciano 84084, Italy*

Vortex induced vibrations are of great interest to many fields of engineering. One of their latest practical application worth mentioning is the design of submerged moving or deformable structures that are able to convert energy from marine currents and waves.
The VIVACE project [2] proposes, for instance, the extraction of energy from marine currents at low speeds using arrays of spring mounted cylinders. Taking advantage of the fluid-structure instabilities experienced by the array of spring mounted cylinders, one may efficiently harvest mechanical energy from the motion of multiple freely oscillating bodies.
The analysis of Vortex Induce Vibrations (VIV) of a single body has received considerable attention, e.g., the case of a single oscillating cylinder [1]. However, the identification of the physical mechanisms behind the fluid-structure instabilities of multiple interacting bodies remains vastly unexplored. For this purpose, we propose a Linearised Arbitrary Lagrangian Eulerian (L-ALE) method to explore the dynamics of multiple freely-oscillating cylinders. The L-ALE method rationalises the Eulerian motion of the flow with the Lagrangian displacement of the fluid-solid interface. It is practically done by introducing an extension displacement field $\hat{\boldsymbol{\xi}}_e$, which propagates into the fluid the solid deformation ([3]). The motion y_n of each cylinder in the transversal direction is governed by the following equation

$$\ddot{y}_n + \frac{4\pi\gamma_n}{U_n^*}\dot{y}_n + \left(\frac{2\pi}{U_n^*}\right)^2 y_n = \frac{2C_{y_n}(t)}{\pi m_n^*} \text{ for } n = 1, \ldots, N \tag{1}$$

where U_n^* is the reduced velocity, $C_{y_n}(t)$ is the vertical force coefficient and m_n^* the mass ratio between the cylinder and fluid densities. The cylinders having only one degree of freedom, the displacement field is a function of the cylinders' displacement and can be therefore decoupled from the fluids equations.
Our code will be compared both to a single cylinder and a tandem ([4]), see figure 1.
The number, their distance, their mass, and damping ratio, as well as their shape are some of the parameters that influence the stability of the system. We will investigate configurations that produce the greatest amplitudes of motion, and a stability map of the system will be presented. References

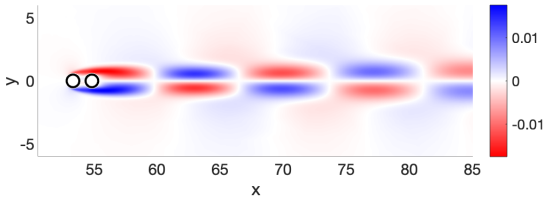

FIGURE 1. *Transversal velocity of the leading eigenmode for the two cylinders configuration ($N = 2$) with a reduced mass $m^* = 2.54$ and reduced velocity $U^* = 15$ at $Re = 100$.*

[1] Charles HK, Williamson and R, Govardhan. *Vortex-induced vibrations. Annual review of fluid mechanics*, 36(1):413–455, 2004.
[2] Michael M, Bernitsas and Kamaldev, Raghavan and Y, Ben-Simon and EMH, Garcia *VIVACE (Vortex Induced Vibration Aquatic Clean Energy): A new concept in generation of clean and renewable energy from fluid flow. Journal of offshore mechanics and Arctic engineering*, 130(4)
[3] JL, Pfister and O, Marquet and M, Carini *Linear stability analysis of strongly coupled fluid–structure problems with the Arbitrary-Lagrangian–Eulerian method. Computer Methods in Applied Mechanics and Engineering*, 355:663–689, 2019.
[4] A, Tirri and A, Nitti and J, Sierra-Ausin and F, Giannetti, Marco D, de Tullio*Linear stability analysis of fluid–structure interaction problems with an immersed boundary method. Computer Methods in Applied Mechanics and Engineering*, 117:103830, 2023.

A REVISED GAP-AVERAGED MODEL FOR FARADAY WAVES IN HELE-SHAW CELLS

Alessandro Bongarzone, François Gallaire

Laboratory of Fluid Mechanics and Instabilities, École Polytechnique Fédérale de Lausanne, Lausanne, CH-1015, Switzerland

Previous theoretical analyses of Faraday waves in Hele-Shaw cells [1] typically rely on the Darcy approximation, which is based on the parabolic flow profile assumption in the narrow direction and that translates in a damping coefficient $\gamma = 12\nu/b^2$, with ν the fluid kinematic viscosity and b the cell's gap-size. However, Darcy's model is known to be inaccurate whenever inertia is not negligible, e.g. in unsteady flows. In this work, we propose a revised gap-averaged linear model that accounts for inertial effects induced by the unsteady terms in the Navier-Stokes equations. Such a scenario corresponds to a pulsatile flow where the fluid's motion reduces to a two-dimensional oscillating Poiseuille flow [2]. This results in a modified damping coefficient, $\gamma = \chi\nu/b^2$, with $\chi = \chi_r + i\chi_i$ complex-valued, which is a function of the ratio between the Stokes boundary layer thickness $\delta = \sqrt{2\nu/\Omega}$ and the cell's gap-size b, and whose value depends on the frequency of the system's response, Ω, specific to each unstable parametric Faraday tongue, i.e. $\Omega = n\omega/2$ $(n = 1, 2, ...)$ with $\omega = 2\pi f$ the driving frequency. We consider the case of Faraday waves in a thin annulus [3] (see Fig.1), for which the system's natural frequencies obey to the non-dimensional dispersion relation $\omega_m^2 = \left(m + m^3/Bo\right)\tanh\left(mh/R\right)$, where Bo is the Bond number and m is an integer representing the azimuthal wavenumber. We show that the Darcy's model typically underestimates the Faraday threshold and overlooks a frequency detuning introduced by χ_i, that appears essential to correctly predict the location of the Faraday tongue in the frequency spectrum (see Fig.1). The latter aspect is confirmed by a full numerical eigenvalue calculation of the actual system's natural frequencies (see Fig. 2), which provides the driving frequencies around which the Faraday tongues are centered, hence proving the predictive power of the present revised gap-averaged model.

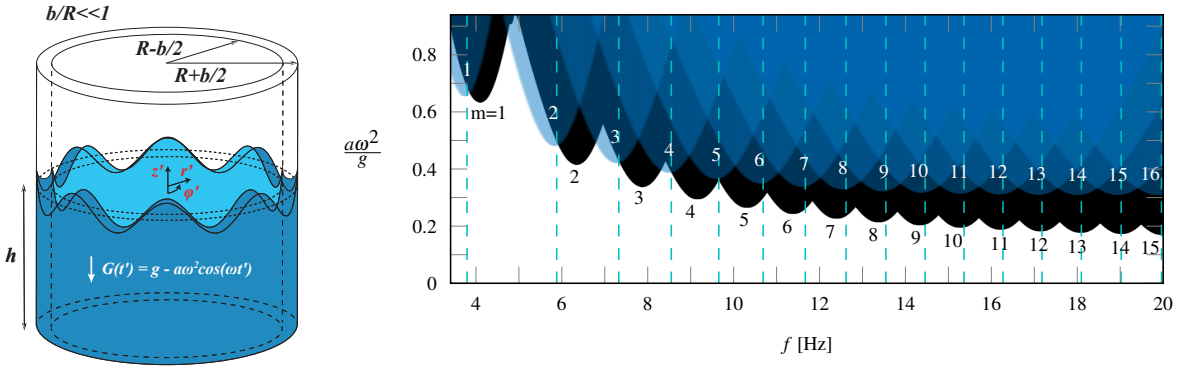

Figure 1: **Left**, sketch of the thin annulus vertically excited at a frequency ω with amplitude a. **Right**, sub-harmonic Faraday tongues for a container with nominal radius $R = 47.7\,\text{mm}$, gap-size $b = 2\,\text{mm}$ and filled to a depth $h = 60\,\text{mm}$ with pure ethanol. Black regions: unstable tongues computed for $\gamma = 12\nu/b^2$. Blue regions: tongues computed with $\gamma = \chi\nu/b^2$. The associated m is indicated by the numbers. Vertical dashed lines gives the locations of the actual system's natural frequencies (twice their values) computed via a full numerical eigenvalue calculation, i.e. by dropping out the Hele-Shaw approximation.

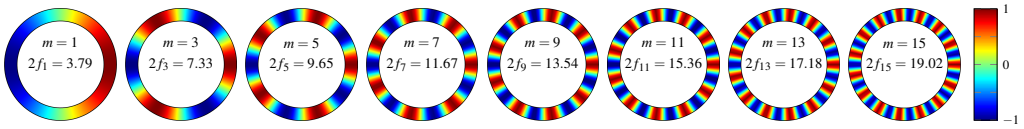

Figure 2: Top view of the free surface deformations numerically computed as eigenmodes of the full system, i.e. without invoking the Hele-Shaw approximation, and for $m = 1, 3, 5, 7, 9, 11, 13$ and 15. The corresponding eigenfrequencies in Hz, $f_m/2$, are also reported. These values are indicated in Fig. 1 as vertical dashed lines. Here $R = 47.7\,\text{mm}$ and $b = 2\,\text{mm}$, but for visualization purposes b/R is not at scale.

References

[1] J. Li, X. Li and S. Liao. Stability and hysteresis of faraday waves in Hele-Shaw cells. *J. Fluid Mech.*, **871**, 2019.
[2] F. Viola, F. Gallaire and B. Dollet. Sloshing in a Hele-Shaw cell: experiments and theory. *J. Fluid Mech.*, **831**, 2017.
[3] S. Douady, S. Fauve and O. Thual. Oscillatory phase modulation of parametrically forced surface waves. *EPL*, **10**, 1989.

ADJOINT-BASED SENSITIVITY OF SHOCK-LADEN FLOWS

Daniel Bodony, Alexandru Fikl and Sandeep Murthy
Department of Aerospace Engineering
University of Illinois at Urbana-Champaign

When seeking to understand or reduce the sound generated by a shock-laden jet using global [1] or resolvent mode descriptions of the jet, the presence of the strong shock waves must be addressed. In prior work [2, 1], weak shocks were present but not given specific treatment. The premise of this presentation is to discuss the interplay between numerics and the need to compute the sensitivity of one or more measures of the flow when shocks are present, using the inviscid limit of Burgers equation, for which analytical results serve as a guide, and the Euler equations as guides.

Consider solving the inviscid Burgers' equation numerically with a shock in the initial condition using numerical methods suitable for approximating discontinuous solutions using WENO, MUSCL, or localized artificial diffusivity (LAD) methods, each of which may be expressed as

$$\frac{\mathrm{d}\vec{u}}{\mathrm{d}t} + \mathsf{D}_1[\vec{u}]\vec{f} = \mathsf{P}^{-1}\tilde{\mathsf{D}}_p^T\Phi[\vec{u}]\tilde{\mathsf{D}}_p\vec{u} + \mathrm{BC}, \tag{1}$$

where $\mathsf{D}_1 = \mathsf{P}^{-1}\mathsf{Q}$ is a first derivative operator dependent on the solution $\vec{u}$ (as in WENO), $\Phi[\vec{u}]$ is an artificial dissipation or upwinding term that is dependent on the solution $\vec{u}$, $\vec{f} = \vec{u}\odot\vec{u}/2$ is the inviscid flux (and $\odot$ denotes the elementwise Hadamard product), and BC represents the boundary conditions. The operator $\mathsf{P}^{-1}\tilde{\mathsf{D}}_p^T(\cdot)\tilde{\mathsf{D}}_p$ represents the narrow stencil form of the $(2p)$th derivative. The matrix $\mathsf{P} = \mathsf{P}^T > 0$ is a norm specification of D_1, $\tilde{\mathsf{D}}_p$, and Φ uniquely defines the numerical method.

We derive the corresponding adjoint method-of-lines equation by defining the P-based inner product $\langle\vec{a},\vec{b}\rangle_\mathsf{P} = \vec{a}^T\mathsf{P}\vec{b}$ and proceed in the usual way. The end result of the algebra is the method-of-lines scheme

$$-\frac{\mathrm{d}\vec{p}}{\mathrm{d}t} - \vec{u}\odot\mathsf{D}_1[\vec{u}]\vec{p} = \mathsf{P}^{-1}\tilde{\mathsf{D}}_p^T\Phi[\vec{u}]\tilde{\mathsf{D}}_p\vec{p} + \mathrm{BC}^\dagger + G'(\vec{u};\vec{u}^*) + \vec{S}[\vec{u}]\vec{p}, \tag{2}$$

where it is understood that $\vec{u}$ satisfies the forward equation (Eq.(1)), $\mathrm{BC}^\dagger$ are the adjoint boundary conditions, and G' is the derivative of the smooth objective function evaluated with target solution $\vec{u}^*$.

The contributions to $\vec{S}$ arise from the nonlinearities in the operators $\mathsf{D}_1[\vec{u}]$ (as in WENO) and from those in $\Phi[\vec{u}]$ for MUSCL and LAD. Important to the adjoint is the fact that the variation of Q is not smooth with respect to $\vec{u}$ because of the stencil-switching functions used to define WENO. Thus the source term $\vec{S}$ is non-zero in the vicinity of the shock and its value does not diminish with increasing grid resolution but, instead, occupies a smaller spatial support.

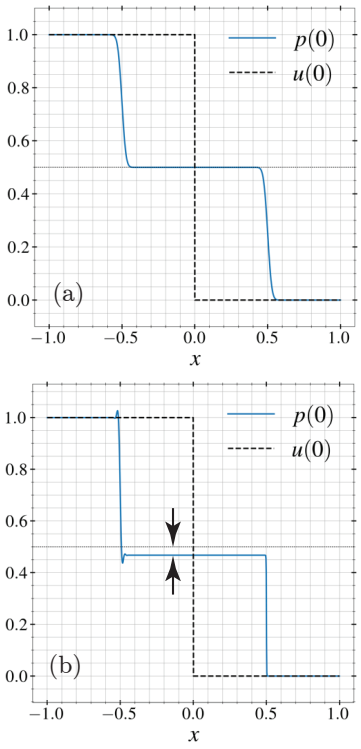

FIGURE 1. *Adjoint solutions $p(x,0)$ for using (a) LAD and (b) WENO.*

For MUSCL and LAD methods, the source term is proportional to the variation of $\Phi[\vec{u}]$. For composite differentiable LAD methods, the variation of Φ with $\vec{u}$ is smooth. For MUSCL schemes, on the other hand, the elements of $\Phi[\vec{u}]$ are computed on the basis of the bounded variation of the solution between adjacent cells using non-differentiable slope-limiters. When the variation of Φ is evaluated, these jumps appear as additional source terms in $\vec{S}$ with magnitudes that do not diminish with increasing grid resolution; instead, they become more spatially compact, as in the case of WENO.

Example numerical solutions at $t = 0$ are given in Fig. 1 to demonstrate. The analytical adjoint solution has value $p(x,0) = 1/2$ for $|x| < 1/2$ and the deviation of the numerical $\vec{p}(0)$ from $1/2$ is due to non-smoothness of the numerical method. Observe that LAD has the proper value while WENO does not.

References

[1] M. Natarajan, J. B. Freund, and D. J. Bodony. Global mode-based control of laminar and turbulent high-speed jets. *Special issue of Comptes Rendus Mé chanique on jet noise*, 346(10):978–996, 2018.
[2] J. Kim, D. J. Bodony, and J. B. Freund. Adjoint-based control of loud events in a turbulent jet. *Journal of Fluid Mechanics*, 741:28–59, 2014.

NONLINEAR DYNAMICS, STABILITY AND SENSITIVITY OF A SIMPLIFIED DRAGONFLY WING IN GLIDING FLIGHT

Gabriele Nastro[1], Maxime Fiore[1], Michael Bauerheim[1]
[1]*ISAE-SUPAERO, Université de Toulouse, France*

Various numerical studies [1, 2] have investigated the aerodynamic performance of a simplified 2D dragonfly wing in gliding flight. This airfoil consists in two corrugations combined with a rear arc (see Figure 1), which provides overall good aerodynamic mean performance at low Reynolds numbers. This configuration also exhibits a complex unsteady behaviour, with various regimes of oscillations and transition to chaos when the angle of attack is changed at a fixed Reynolds number [2]. However, the underlying mechanisms driving those unsteady regimes are not yet fully understood.
Therefore, the main objective of the present study is to combine direct numerical simulations (DNS), global stability analyses and advanced post-processing tools to better characterise and understand the unsteady behaviour of this dragonfly wing. To do so, these numerical tools are applied to three angles of attack at $Re = 6000$, typical of the three regimes already observed: (i) monochromatic oscillations, (ii) oscillations with non-commensurate frequencies, and (iii) chaos.
In addition to global stability analyses combined with DNS, adjoint-based sensitivity analyses are performed in order to identify regions of the flow where generic structural modifications of the linearised Navier-Stokes operator lead to the strongest drift of the leading eigenvalue [3] and also investigate the influence of baseflow modifications and application of external body forces on the stability features [4, 5].
Moreover, the interest of this particular configuration also lies in the presence of different length-scales characteristing the flow recirculation zones which generally drive the self-sustained modes (see the blue line in Figure 1). In this context, taking advantage of the three-dimensional nature of the flow solver, we further explore the effect of an extruded three-dimensional dragonfly wing which leads to an even more complex scenario.

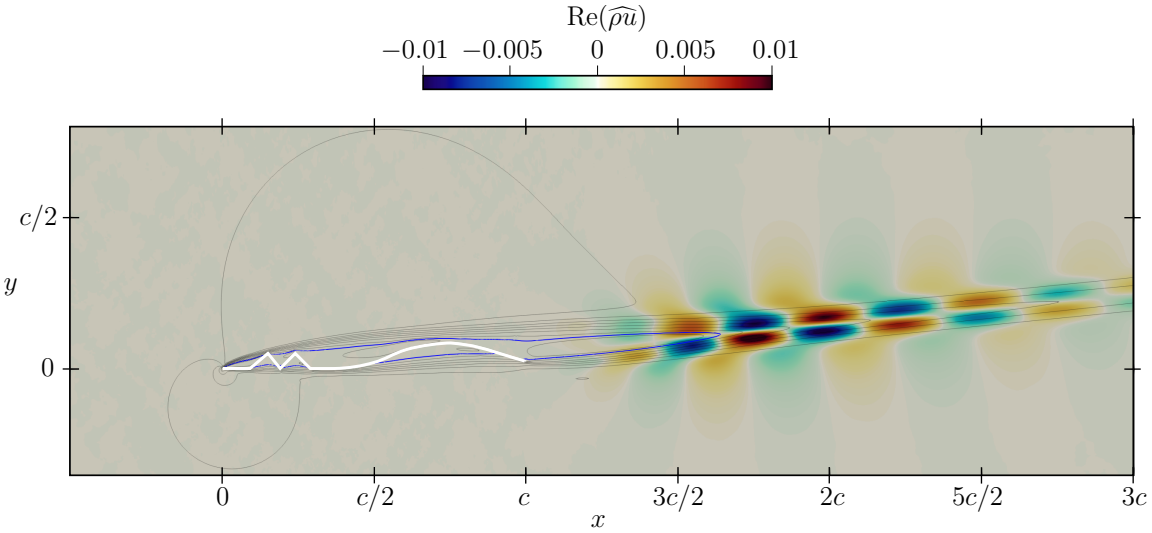

FIGURE 1. Re($\widehat{\rho u}$) *of the eigenfunction corresponding to the most unstable global mode, i.e. the two-dimensional von Kármán mode, for* $\alpha = 7°$, $Re = 6000$ *and* $M = 0.026$. *The solid lines represent the isocontours of the longitudinal velocity* U *of the base flow and the blue line highlights the locus of the points for which* $U = 0$.

References

[1] D-E. Levy, and A. Seifert. Simplified dragonfly airfoil aerodynamics at Reynolds numbers below 8000. *Phys. Fluids*, 21, 071901, 2009.
[2] M. Bauerheim, and V. Chapin. Route to chaos on a dragonfly wing cross section in gliding flight. *Phys. Rev. E*, 102(1): 011102, 2020.
[3] F. Giannetti, and P. Luchini. Structural sensitivity of the first instability of the cylinder wake. *J. Fluid Mech.*, 581 (1): 167–197, 2007.
[4] O. Marquet, D. Sipp, and L. Jacquin. Sensitivity analysis and passive control of cylinder flow. *J. Fluid Mech.*, 615: 221–252, 2008.
[5] G. Nastro, J.-C. Robinet, J.-C. Loiseau, P.-Y. Passaggia, and N. Mazellier. Global stability, sensitivity and passive control of low-Reynolds-number flows around NACA 4412 swept wings. *J. Fluid Mech.*, 957(A5), 2023.

STABILITY ANALYSIS OF A STREAKY BOUNDARY LAYER INDUCED BY MINIATURE VORTEX GENERATORS

András Szabó[1], Péter Tamás Nagy[1], György Paál[1]
[1] *Department of Hydrodynamic Systems, Faculty of Mechanical Engineering, Budapest University of Technology and Economics, H-1111, Budapest, Bertalan Lajos u. 4 - 6*

Miniature Vortex Generators (MVGs) are experimentally confirmed to be able to attenuate the growth of the Tollmien-Schlichting waves [1]. Therefore, their ability to delay laminar-turbulent transition in boundary layers as passive flow control devices has a considerable practical motivation; e.g., there are recent experimental efforts towards applying MVGs on a fuselage of a laminar aircraft [2]. However, their MVG geometry is likely suboptimal since the initial MVG geometries were based on vortex generators used to delay shock-induced separation [3]. In this work, a large parametric study is conducted on rectangular MVG geometries using an efficient modeling framework that combines three-dimensional CFD, Boundary Region Equations, and BiGlobal stability analysis. The base flow calculation is validated with the experiments of [4]; furthermore, stability analysis of the experimental cases is presented. Then, the parametric study varying the spanwise periodicity, the distance of the MVG pairs, and the MVG height is performed on a $(7 \times 5 \times 4)$ grid, in which the stability of 140 configurations is investigated.
Fig. 1 shows the simulations of experiments of [4] and the parametric study. The x axis displays the transition Reynolds number, measuring the stabilization of the TS waves far downstream. The y axis shows the N factor of the secondary instabilities that may arise in the presence of very strong streaks induced just downstream of the MVGs: this measures the potential advancement of transition. It is clear that compared to the best experimental case (red at (1800-4)), the efficiency of the MVGs could be substantially increased, based on which recommendations are given for more detailed future studies.

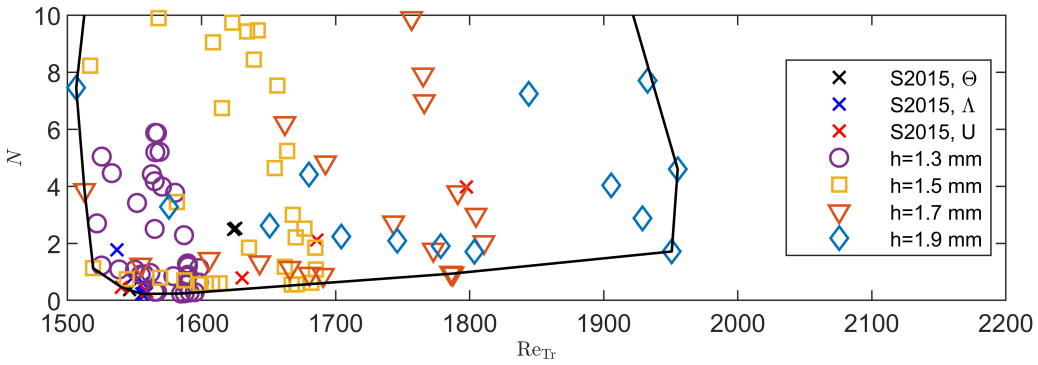

FIGURE 1. *Simulated cases on the transition Reynolds number-secondary instability N factor plane. S2015 denotes the experiments of [4], the rest of the cases are from the parametric study. The black curve denotes the convex hull of the points - the lower right part can be considered as the optimum.*

References

[1] Jens H.M. Fransson. Transition to turbulence delay using a passive flow control strategy. *Procedia IUTAM*, 14:385–393, 2015. IUTAM_ABCM Symposium on Laminar Turbulent Transition.
[2] Andre Weingärtner, Santhosh B. Mamidala, and Jens H. Fransson. Application of miniature vortex generators for boundary layer transition delay. In *AIAA Paper 2023-0097*, 2023.
[3] Jens H M Fransson and Alessandro Talamelli. On the generation of steady streamwise streaks in flat-plate boundary layers. *Journal of Fluid Mechanics*, 698:211–234, 2012.
[4] Sohrab S Sattarzadeh and Jens H M Fransson. On the scaling of streamwise streaks and their efficiency to attenuate tollmien-schlichting waves. *Experiments in Fluids*, 56:58, 3 2015.

ERROR-DRIVEN GLOBAL STABILITY ANALYSIS OF 180°-BEND PIPE TRANSITIONAL FLOW

Valerio Lupi[1], Daniele Massaro[1], Adam Peplinski[1], Philipp Schlatter[1,2]
[1] *SimEx/FLOW, Engineering Mechanics, KTH Royal Institute of Technology, Stockholm, Sweden*
[2] *Institute of Fluid Mechanics, Friedrich-Alexander Universität Erlangen-Nürnberg, Nürnberg, Germany (after 1.4.2023)*

We investigate the global stability of the flow in a 180°-bend pipe with curvature $\delta = 1/3$ (see Fig. 1). Previously, Lupi et al. [1] studied the stability of the 90°-bend pipe flow, observing a Hopf bifurcation at $Re_b = 2531$, with the region located 15° downstream of the bend inlet, on the outer wall, acting as the "wavemaker". Generally, we observe the underlying mechanism which triggers the transition to be extremely sensitive to adequate resolution. Thus, in the current study, we rely on an error-driven approach where the mesh is designed to be optimal for a specific solution. By using the spectral error indicator (SEI) [2] and our adaptive mesh refinement (AMR) implementation in the open-source code Nek5000 [3], we design multiple separate meshes for each solution field, *e.g.* baseflow and perturbation. This method represents a novel approach for the stability analysis of more complicated geometries where the needed resolution is not a priori given.

By means of this methodology, the 180°-bend pipe global instability mechanism is investigated. First, a set of non-linear direct numerical simulations (DNS) is performed to establish the critical Reynolds number. Differently from Hashemi et al. [4], but in agreement with Lupi et al. [1], the flow is found to be unsteady at $Re_b \approx 2550$. The steady baseflow is thus established at such Reynolds number via selective frequency damping (SFD) [5]. Then, the linearised Navier–Stokes equations are solved around the extracted base flow on a different mesh, initialising the simulation with noise uncorrelated in space. We observe a recirculation bubble on the outer wall of the bend, similarly to the case of a 90°-bend pipe [1]. The temporal signals extracted from local velocity probes show the appearance of a limit cycle with period approximately equal to $T = 4.3\,D/U_b$, where D and U_b are the pipe diameter and the bulk velocity, respectively.

The first global instability analysis of the 180°-bend pipe flow is presented, using a novel error-driven approach with the adaptive mesh refinement technique. We detect the leading unstable eigenvalue and discuss the main similarities and differences with other curved pipes, *e.g.* the 90°-bend and the toroidal pipe.

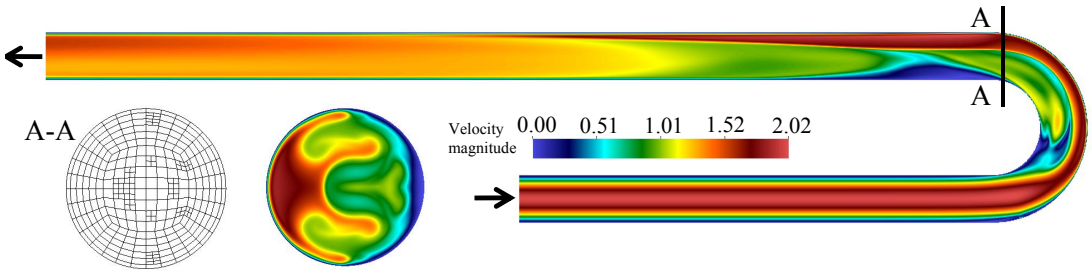

FIGURE 1. *Pseudocolours of the velocity magnitude for the base flow extracted via selective frequency damping with the non-conforming mesh shown at A-A.*

References

[1] V. Lupi, J. Canton, and P. Schlatter. Global stability analysis of a 90°-bend pipe flow. *Int. J. Heat Fluid Flow*, 86:108742, 2020.
[2] C. Mavriplis. *Nonconforming Discretizations and a Posteriori Error Estimators for Adaptive Spectral Element Techniques*. PhD Thesis, MIT, 1989.
[3] N. Offermans, D. Massaro, A. Peplinski, and P. Schlatter. Error-driven adaptive mesh refinement for unsteady turbulent flows in spectral-element simulations. *Comput. Fluids*, 251:105736, 2023.
[4] A. Hashemi, P. F. Fischer, and F. Loth. Direct numerical simulation of transitional flow in a finite length curved pipe. *J. Turbul.*, 19(8):664–682, 2018.
[5] E. Åkervik, L. Brandt, D. S. Henningson, J. Hœpffner, O. Marxen, and P. Schlatter. Steady solutions of the Navier–Stokes equations by selective frequency damping. *Phys. Fluids*, 18(6):068102, 2006.

WEAK NONLINEARITY FOR STRONG NOMNORMALITY

Yves-Marie Ducimetière, Edouard Boujo, François Gallaire

Laboratory of Fluid Mechanics and Instabilities, École Polytechnique Fédérale de Lausanne, Lausanne, CH-1015, Switzerland

We propose a theoretical approach to derive amplitude equations governing the weakly nonlinear evolution of nonnormal dynamical systems when they experience transient growth or respond to harmonic forcing. This approach reconciles the nonmodal nature of these growth mechanisms and the need for a center manifold to project the leading-order dynamics. Under the hypothesis of strong nonnormality, we take advantage of the fact that small operator perturbations suffice to make the inverse resolvent and the inverse propagator singular, which we encompass in a multiple-scale asymptotic expansion. The methodology is outlined for a generic nonlinear dynamical system, and several application cases which highlight common nonnormal mechanisms in hydrodynamics: the streamwise convective nonnormal amplification in the flow past a backward-facing step, and the Orr and lift-up mechanisms in the plane Poiseuille flow. For the two-dimensional flow down a backward-facing step of expansion ratio 2 and Reynolds number Re=500 (Fig. 1a), the linear response $u_o(x,y)$ to harmonic forcing (Fig. 1c) is maximum at a nondimensional frequency of 0.08 (Fig. 1d) for an optimal forcing structure $f_o(x,y)$ given in Fig. 1b, with a gain of approximately $G_{lin}(\omega = 2\pi 0.08) \approx 7.10^3$, as computed in the literature [1, 2]. In order to investigate the effect of nonlinearities under a small forcing $F\epsilon^3 f_o$, we use the following Ansatz for the response $u = \epsilon A(t/\epsilon^2)u_0(x,y)\exp(i\omega t)$, where $\epsilon = G_{lin}^{-2}$ is the small parameter and demonstrate that the amplitude A is governed by the following forced Landau equation

$$\epsilon^2 \frac{dA}{dt} = \gamma F - \eta A - \mu |A|^2 A, \tag{1}$$

where the parameters γ, η and μ are given as closed form expressions involving only the solutions of linear systems. The resulting weakly nonlinear predictions regarding the response saturation in amplitude match direct numerical simulations well at different forcing frequencies (Fig. 1d).

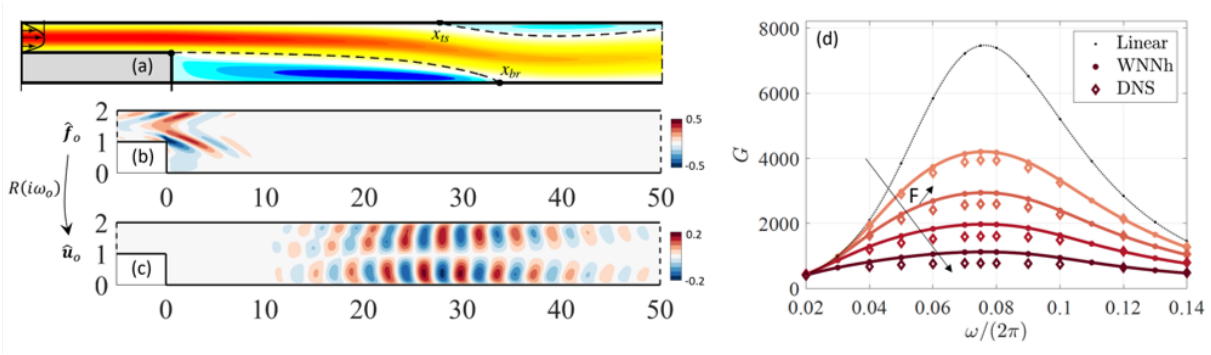

Figure 1: (a) Backward facing step flow at Re=500, (b) optimal forcing at $\omega = 2\pi 0.08$, (c) associated permanent response and (d) gain for different forcing intensities F as obtained from Eq. 1 (WWNh) and from DNS.

References

[1] E. Boujo and F. Gallaire. Sensitivity and open-loop control of stochastic response in a noise amplifier flow: the backward-facing step. *J. Fluid Mech.*, **762**, 2015.

[2] V. Mantic-Lugo and F. Gallaire. Self-consistent model for the saturation mechanism of the response to harmonic forcing in the backward-facing step flow. *J. Fluid Mech.*, **793**, 2016.

NONLINEAR TRANSITION MECHANISMS OF SEPARATION BUBBLES

Flavio Savarino[1], Arthur Poulain[2], Denis Sipp[2], Georgios Rigas[1]
[1]*Department of Aeronautics, Imperial College London, London SW7 2AZ, United Kingdom*
[2]*DAAA, ONERA, Université Paris Saclay, F-92190 Meudon, France*

Flow separation affects the aerodynamic performance of vehicles due to the increased drag and unsteadiness arising from the laminar to turbulence transition of the separated shear layer. At high Mach numbers, the transition results also in significant thermal loading. To date, most numerical techniques to analyse the stability of laminar boundary layers subject to external disturbances are linear (*i.e.* resolvent analysis) and thus fail to describe the non-linear transitional dynamics (amplitude saturation, mean flow modification, energy transfer among mechanisms).

In order to accurately capture the transitional mechanisms, we take into account the nonlinearity by considering a finite number of nonlinearly interacting modes using the Harmonic Balance Method [1]. Non-linear optimisation is employed to calculate the optimal forcing-response mechanisms that maximise the skin friction coefficient, with the latter used as an objective proxy of the transition process. Till now, the method has been applied to zero pressure gradient flat plate boundary layer flows. In this study, we extend and apply the method to wall-bounded flows with localised separation, so-called laminar separation bubbles. Specifically, we consider:

- Incompressible laminar separation bubbles (LSB) due to pressure gradients (see figure 1).
- Compressible laminar separation bubbles due to oblique shock waves (SBLI).

We show that an efficient path to transition is initiated by the Kelvin-Helmholtz (KH) instability which then non-linearly transfers energy to streamwise streaks and KH super-harmonic waves. The interacting multi-modal instabilities cause spanwise deformation of the mean bubble and earlier reattachment of the shear layer. A detailed analysis of the transition mechanisms will be presented.

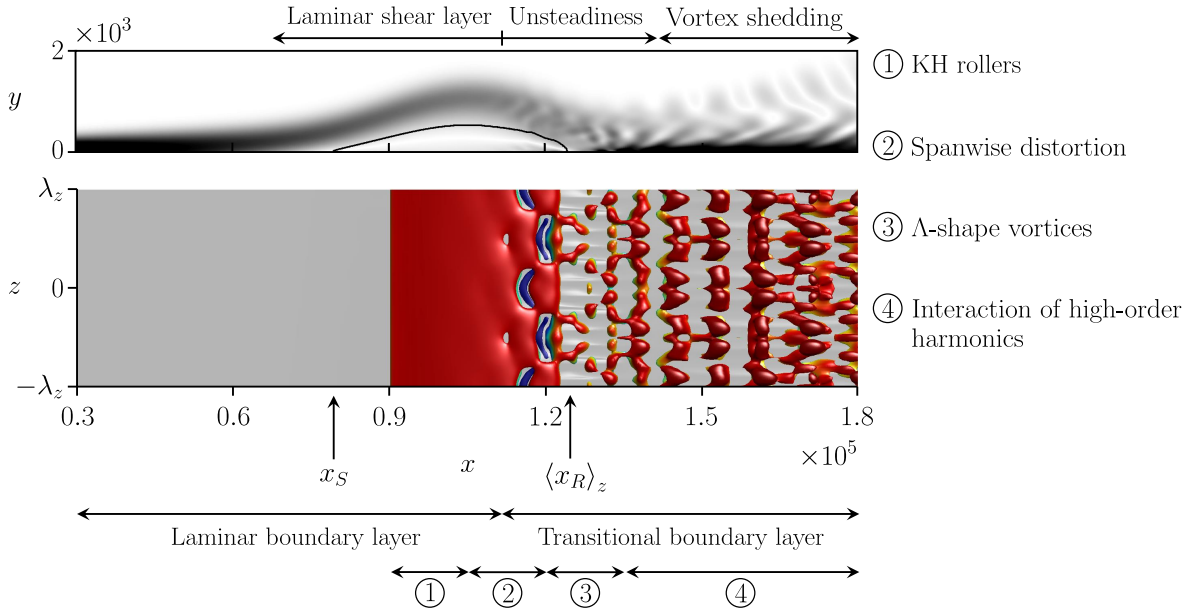

FIGURE 1. *Optimal nonlinear response of LSB using 6 harmonics in span, and 2 frequency harmonics. (Top) Instantaneous spanwise-averaged spanwise vorticity ($\langle\omega_z\rangle_z$) contours and (bottom) Q-criterion isosurfaces coloured with streamwise velocity. The 3D mean-flow is displayed with a grey isosurface where $\langle u\rangle_t = 0$. Separation and spanwise-averaged reattachment locations are indicated with arrows.*

References

[1] G. Rigas, D. Sipp and T. Colonius. *Nonlinear input/output analysis: application to boundary layer transition. J. Fluid Mech*, 911, 2021.

THE IMPACT OF PERIODIC INFLOW FLUCTUATIONS ON THE SIZE AND DYNAMICS OF THE SEPARATED FLOW OVER A BUMP

Himpu Marbona[1,2], Daniel Rodríguez[1], Alejandro Martínez-Cava[1,3], Eusebio Valero[1,2]
[1] *School of Aeronautics (ETSIAE/UPM), Universidad Politécnica de Madrid, Spain*
[2] *Center for Computational Simulation, Universidad Politécnica de Madrid, Spain*
[3] *Instituto Universitario "Ignacio da Riva" (IDR/UPM), Universidad Politécnica de Madrid, Spain*

Laminar flow separation has a detrimental impact of the aerodynamics and performance of low-pressure turbines operating at high altitude, micro aerial vehicles (MAV) and high-altitude unmanned air vehicles (UAV). While separation is caused by local adverse pressure gradients, the dynamics of the separated flow are dominated by flow instability and the size of the separated flow region is governed by the laminar-turbulent transition process. Different scenarios for such transition are well understood for steady inflow conditions. On the other hand, the incoming flow encountered by LPT blades is affected periodically by the passing of wakes from the precedent blade row [1], and flapping MAV and UAV airfoils present laminar flow separation combined with a periodic change of their flow conditions. The dynamics and transition of the separated flow in these cases has received much less attention.

Direct numerical simulations are performed here of the flow over a wall-mounted bump geometry inside of a channel. The bump geometry reproduces similar pressure gradients as those encountered on the suction side of an LPT blade and has been previously investigated both experimentally and numerically [2, 3]. Departing from a steady inflow condition, the total pressure p_t at the inlet section is varied harmonically with a prescribed reduced frequency f^* and amplitude Δp_t. Several combinations of (f^*,Δp_t) are analysed. Triple decomposition is used to extract the flow components that are respectively coherent (i.e. correlated) with the inflow phase and incoherent. This aims to isolate periodic motions of the separated shear layer directly caused by the inflow fluctuation from the stochastic shedding of vortices and their subsequent interactions. Two extreme cases are identified: for low f^* and Δp_t, the transition process is analogous to that of the steady inflow case. For large f^* and Δp_t, the inflow fluctuation gives rise to a large-size coherent cluster of vortices; its advection reduces the separated flow size transiently but also has a remarkable impact in its time average. Intermediate cases illustrate that small amplitude changes can be effective in promoting a fast reattachment if the correct frequencies are excited. These observations are used to guide flow control via periodic suction and blowing for the steady inflow case.

Acknowledgements: This work has received funding from the European Union's Horizon 2020 research and innovation programme under the Marie Skodowska Curie grant agreements No 955923-SSECOID and 101019137-FLOWCID. D.R. also acknowledges funding by the Government of the Community of Madrid within the multi-annual agreement with Universidad Politcnica de Madrid through the Program of Excellence in Faculty (V-PRICIT line 3).

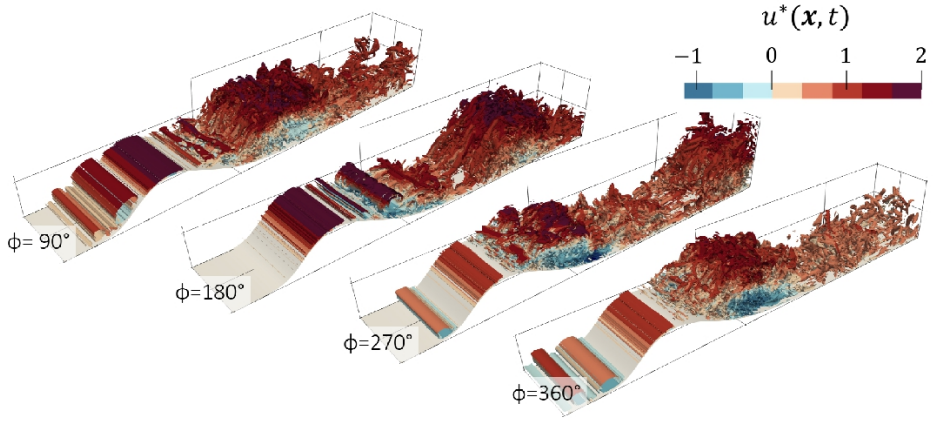

FIGURE 1. *Q-isosurface for* $\Delta p_t = 0.1$ *and* $f^* = 2$ *at different inflow phases.*

References

[1] J. D. Coull and H. P. Hodson. Unsteady boundary-layer transition in low-pressure turbines. *Journal of Fluid Mechanics* 681, 370–410, 2011
[2] J. Saavedra and G. Paniagua. Transient performance of separated flows: characterization and active flow control. *Journal of Engineering for Gas Turbines and Power* 141, 011002, 2018
[3] J. Saavedra and G. Paniagua. Experimental analysis of Reynolds effect on flow detachment and sudden flow release on a wall-mounted hump. *Experimental Thermal and Fluid Science* 126, 110398, 2021

SPANWISE MODULATION AND SECONDARY INSTABILITY OF KELVIN-HELMHOLTZ ROLLS BY CROSSFLOW MODES ON A ROTATING AIRFOIL

Thales Coelho Leite Fava[1], Daniele Massaro[1], Dan Henningson[1], Philipp Schlatter[1], Ardeshir Hanifi[1]
[1] *KTH Royal Institute of Technology, Dept. of Engineering Mechanics, FLOW and SeRC, SE-100 44 Stockholm, Sweden*

This work assesses the role of rotation on the boundary layer stability of a wind turbine blade. To accomplish this, the direct numerical simulation (DNS) of a spanwise section at 68% of the radius of the DTU 10 MW wind turbine was performed, with an angle of attack of 12.8°. The Reynolds and rotation numbers are Re_c=3×10^5 and Ro_c=0.0523 based on the chord (c) and resultant velocity from the wind and rotation (U_∞). A static blade simulation (Ro_c=0, without Coriolis and centrifugal forces) was also carried out. The results indicate a laminar separation bubble (LSB) in the region x=0.025−0.12 (x=x^*/c) in the rotating case and x=0.03−0.115 in the non-rotating one, with a height 34.7% larger in the former. This results from the Coriolis force promoting a streamwise deceleration of the flow. Rotation also generates a spanwise velocity (W=W^*/U_∞) directed towards the blade tip with a maximum of 8.2% inside the LSB, reversing direction after reattachment. W=0 in the non-rotating case. The LSB triggers a Kelvin-Helmholtz (KH) instability forming spanwise rolls, as seen in Fig. 2. Here, two main differences can be noted: i) the inception of the KH rolls and transition occurs earlier in the rotating case; ii) there is a spanwise modulation of the rolls with spanwise wavenumber $\beta \approx 400$ (β=$\beta^* c$) in the rotating case, absent in the non-rotating blade. This can be better observed in a plane at x=0.14, as shown in Figs. 2(a) and 2(b). At x=0.17 (Figs. 2(c) and 2(d)), secondary instability of the rolls occurs in both cases with the formation of hairpin vortices. However, the rotating-case structures differ significantly due to the spanwise modulation promoted by the streamwise vortices. Primary spatial stability analysis of the mean flow indicates that β=0 and β=400 disturbances are more unstable inside the LSB in the rotating case, explaining i) and ii). Moreover, they show that β=400 modes are nearly aligned with x (propagation angle of up to 82°), as noted in the DNS. Secondary stability analyses of the flow will be presented.

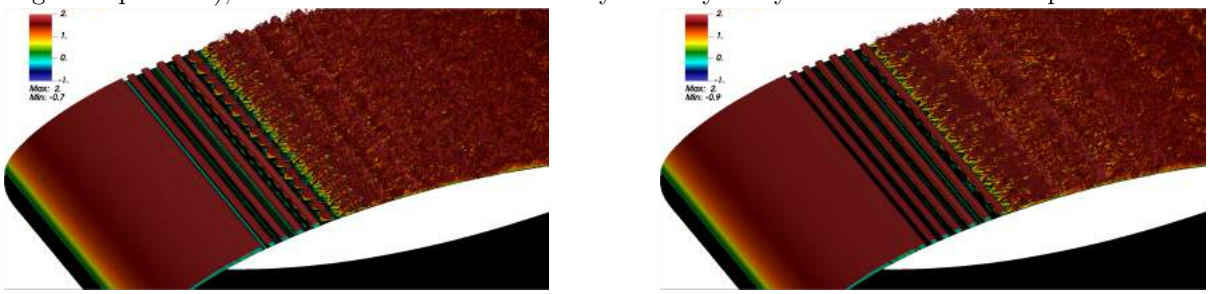

(a) Rotating. (b) Non-rotating.

FIGURE 1. $\lambda_2 = -0.1$ *iso-surfaces colored by streamwise velocity on the airfoil suction side.*

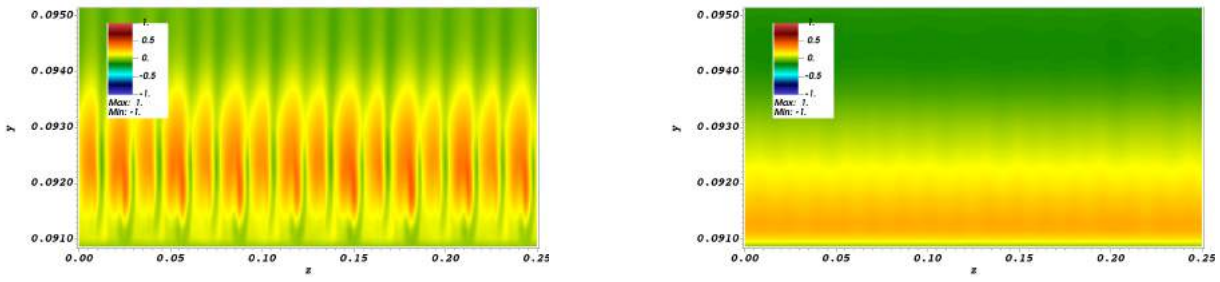

(a) Rotating, $x = 0.14$. (b) Non-rotating, $x = 0.14$.

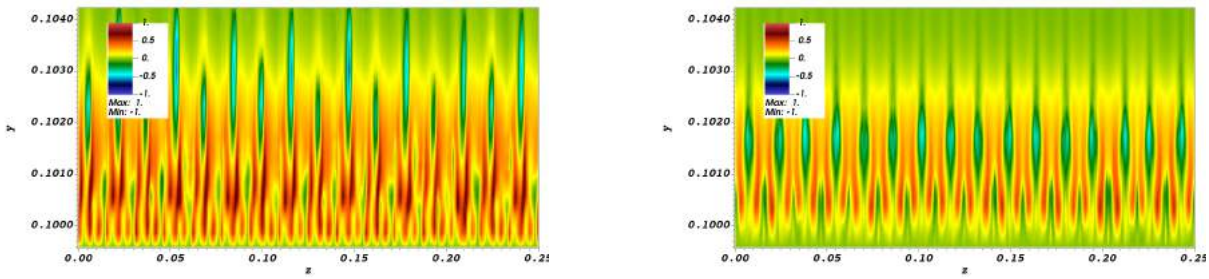

(c) Rotating, $x = 0.17$. (d) Non-rotating, $x = 0.17$.

FIGURE 2. *Contours of streamwise velocity perturbation ($u' = u - \langle u \rangle_{z,t}$) in cross-sectional planes.*

DELAY OF SEPARATION AND TRANSITION FOR A LAMINAR AIRFOIL USING ACTIVE FLOW CONTROL

Hermann F. Fasel, Shirzad Hosseinverdi
Department of Aerospace and Mechanical Engineering, University of Arizona, Tucson, AZ 85721, USA,

Despite many years of research dating back to the seminal work of Gaster [1], the intricate interaction of boundary layer separation and transition in laminar separation bubbles remains a highly relevant and challenging problem in fluid dynamics. The objective of this research is to answer the question whether the surprising effectiveness of selected 2-D harmonic forcing that can lead to relaminarization and transition delay reported for the canonical separation bubbles in the model geometry (i.e., flat-plate) [2] could also be realized for the flow over wings with a laminar airfoil where the boundary-layer can separate on both the suction and pressure sides. Toward this end, high-fidelity direct numerical simulations (DNS) are employed to investigate both the uncontrolled and controlled flow for a wing section with a modified NACA $64_3 - 618$ airfoil at a chord Reynolds number of $Re = 200,000$ and zero degrees angle of attack. For the uncontrolled flow plotted in Figure 1(a), the separated shear layer at both the suction and pressure sides 'rolls up' and "rollers" grow in intensity due to the Kelvin-Helmholtz instability, followed by the shedding of strong spanwise coherent vortices, which finally leads to turbulent reattachment upstream of the trailing edge.

When the separation bubble on the suction surface was forced by 2-D disturbances that are introduced upstream of the separation location at $x_f/c = 0.34$ with a non-dimensional forcing frequency of $St_f = 10$ and forcing amplitude of $A_v = 0.1\%$, the flow topology shown in Figure 1(b) reveals that the flow is "locking on" to the forcing, as it is now shedding spanwise "rollers" at the forcing frequency. In particular, transition is significantly delayed on the suction side and the flow remains virtually 2-D and laminar. It can be conjectured that the 2-D forcing with a large enough amplitude is suppressing the temporally growing 3-D disturbances due to the fact that the secondary absolute instability is prevented. For this active flow control, the forcing frequency was much smaller than the dominant shedding frequency of the underlying uncontrolled flow, i.e., $St \approx 15$. Therefore, additional DNS was performed to investigate the response of the separation bubble to an active flow control strategy using $St_f = 15$. Instantaneous flow visualization of the established controlled flow provided in Figure 1(c) exhibits a striking contrast to the previous case, in that transition sets in immediately after the mean reattachment location. The rapid breakdown of the flow towards turbulence with $St_f = 15$ could be explained by the fact that the controlled flow becomes secondarily unstable with respect to 3-D disturbances that can grow in time due to the absolute secondary instability mechanism. This highlights the importance of properly chosen forcing frequencies when the active control of transition is desired.

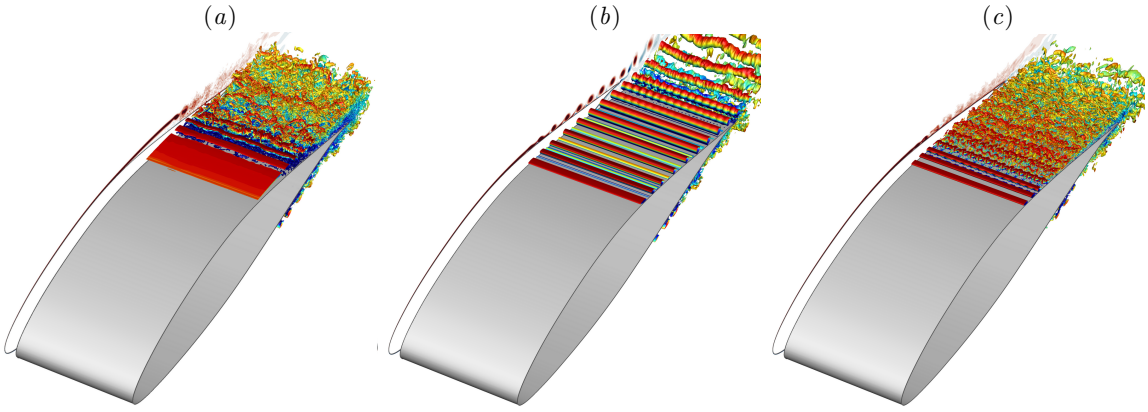

FIGURE 1. *Instantaneous flow visualization of flow past NACA* $64_3 - 618$ *airfoil: Uncontrolled flow (a), controlled flow on the suction side with* $St_f = 10$ *(b), and with* $St_f = 15$ *(c). Plotted are iso-surfaces of* $\lambda_2 = -85$ *colored by* $u-$*velocity in perspective view together with the contours of* ω_z-*vorticity in the* $x - y$ *plane.*

References

[1] M. Gaster. The structure and behaviour of laminar separation bubbles. *In ARC, Reports and Memoranda, No. 3595*, Aeronautical Research Council, 1976.
[2] M. Embacher, and H. F. Fasel. Direct numerical simulations of laminar separation bubbles: investigation of absolute instability and active flow control of transition to turbulence. *J. Fluid Mech.*, 747, 141–185, 2014.

PASSIVE CONTROL OF CROSSFLOW INSTABILITY AND TRANSITION DELAY USING A SMOOTH SURFACE PROTUBERANCE

A.F. Rius-Vidales[1], S. Westerbeek[1], L.M.G.F. Morais[1], M. Soyler[1], M. Kotsonis[1]
[1]*Flow Physics and Technology, Aerodynamic Section, Delft University of Technology, The Netherlands*

Creative solutions to reduce the total drag of high-subsonic transport aircraft are required to limit the environmental impact of the expanding commercial aviation industry. From the perspective of aerodynamics, reducing the skin friction drag through laminar flow control techniques is an active area of investigation. A limitation in the practical application of LFC techniques is the challenging operational environment, where control devices (passive or active) need to comply with strict robustness, reliability and manufacturing constraints . In contrast to common wisdom, recent experiments by [1] and [2] have identified that two-dimensional irregularities can in-fact delay laminar-turbulent transition under certain conditions. In addition, [3] numerically assessed the stability of a swept wing boundary layer featuring a shallow smooth wall protuberance (i.e., a hump) using a Harmonic Navier-Stokes (HNS) approach. The results show the stabilization of the primary CF instability mode for most studied configurations. Henceforth, the present work investigates the influence of a newly designed smooth, symmetrical surface hump (SH), a protuberance on the wing surface, on the development of the well-known stationary crossflow (CF) instability and its effect on boundary layer transition. Towards this end, wind tunnel experiments are conducted at a chord Reynolds number of 2.3 million on a 45° swept wing model. Infrared (IR) thermography is used to evaluate the laminar-turbulent transition behaviour. Detailed Particle Image Velocimetry (PIV) measurements and HNS simulations are used to determine the effect of the SH on the stability of incoming CF vortices. The results presented at the workshop reveal a strong dependence of stabilisation on the initial amplitude of the incoming CF disturbances. At a high amplitude (i.e. non-linear regime), the addition of a symmetrical hump to the surface leads to a strong amplification of the primary CF instability via interaction with higher harmonics, resulting in an abrupt upstream displacement of laminar-to-turbulent transition to the vicinity of the surface protuberance. In stark contrast, at a lower amplitude of the incoming CF vortices (i.e. linear regime), a strong stabilization of the primary CFI mode and a significant transition delay is observed when comparing with the baseline configuration (i.e. without hump), as shown in figures 1 (IIa-IIb). To the authors' knowledge, this is the first experimental/numerical work that uses a hump as a successful passive laminar flow control device in a swept wing configuration.

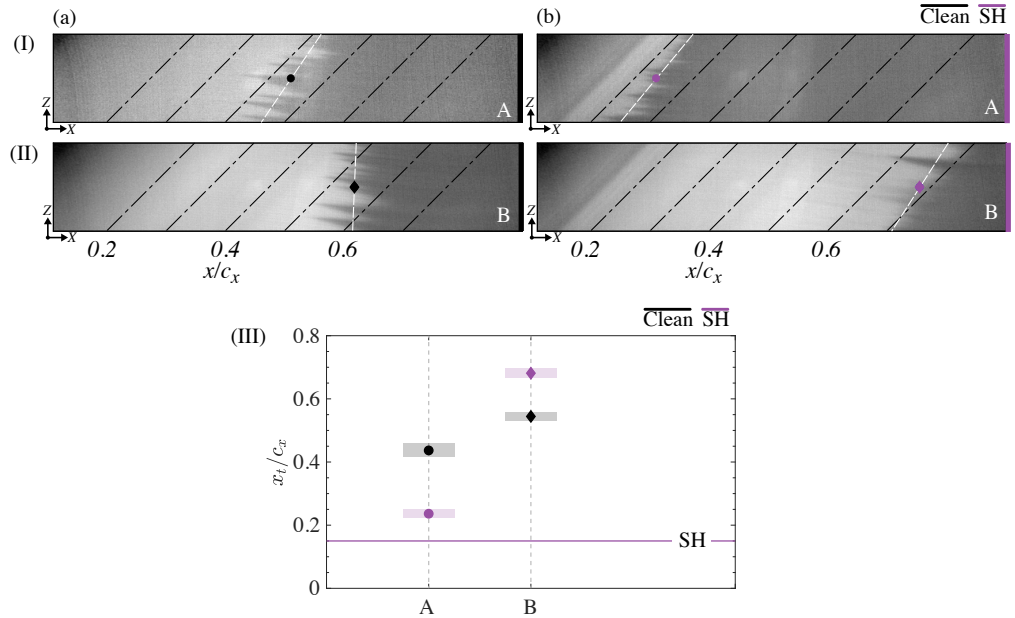

FIGURE 1. *(I,II) Thermal maps from infrared camera (flow from left to right, light and dark areas show the laminar and turbulent flow regions) at* $Re_{c_X} = 2.3 \times 10^6$ *and* $\alpha = 3°$ *for the Clean (a) and symmetrical hump (SH) configurations at high (A) and lower (B) amplitude of the CF vortices. (III) Transition location identification for each of the cases.*

References

[1] Ivanov,A. V. and Mischenko,D. A. *Delay of laminar-turbulent transition on swept-wing with help of sweeping surface relief.* AIP Conference Proceedings, 2125 1, 2019.
[2] A.F. Rius-Vidales and M. Kotsonis *Impact of a forward-facing step on the development of crossflow instability.* Journal of Fluid Mechanics,924 A34, 2021.
[3] S. Westerbeek, J.A. Franco Sumariva, T. Michelis, S. Hein and M. Kotsonis *Linear and Nonlinear Stability Analysis of a Three-Dimensional Boundary Layer over a Hump.* AIAA Scitech Forum,AIAA 2023-0678, 2023.

ESTABLISHMENT OF EXTRACTION METHOD USING LINEAR RESPONSE TO ARTIFICIAL DISTURBANCE FOR BOUNDARY LAYER TRANSITION PROCESS INDUCED BY FREE STREAM TURBULENCE

A. Yoshida[1], K. Matsui[1], K. Kato[1] and M. Matsubara[1]
[1] *Department of Mechanical Systems Engineering, Shinshu University, 4-17-1, Wakasato, Nagano, 380-8553, Japan*
Email: 22w4077d@shinshu-u.ac.jp

Free Stream Turbulence (FST) is one of the main causes in boundary layer transition. Norimatsu et al.[1] studied the energy growth rate of disturbance in the boundary layer on a flat plate with FST, and suggested nonlinearity of the disturbance receptivity around the leading edge. On the other hand, Matsubara et al.[2] developed a linear response extraction method that extracts the disturbance structure in the turbulent boundary layer by introducing artificial periodic disturbances to the turbulent boundary layer, which is a strong nonlinearity, and ensemble-averaging the measured velocity fluctuation according to the disturbance. In order to elucidate the receptivity of FST, we apply this method to the boundary layer transition caused by FST and attempt to extract the disturbance structure in the boundary layer.

In this experiment, disturbance caused by amplitude controlled by the speaker was introduced upstream of leading edge of a flat plate in a wind tunnel. We measured velocity fluctuations in the boundary layer by a hot wire anemometer. The coordinate system (x, y, z) is defined in the streamwise, wall-normal and spanwise direction with the origin at the leading edge. From the measured velocity u, we obtained the ensemble average $\langle u \rangle$ according to the artificial disturbance. Subtracting the time-averaged velocity $\bar{u}$, we calculated the periodic component $\tilde{u} = \langle u \rangle - \bar{u}$ and the non-periodic component $\hat{u} = u - \bar{u} - \tilde{u}$. Figure 1. shows the distribution of periodic fluctuation component $\widetilde{u}$ of the boundary layer at $x = 50$ mm with the periodic disturbance at 500 Hz with (a) and without (b) FST caused by a turbulent grid upstream of the leading edge, which generates FST. The vertical axis y/δ^* is the wall-normal position normalized by the displacement thickness δ^*, and the horizontal axis ϕ is the phase time of the artificial disturbance, which can be interpreted as the streamwise position using Taylor's frozen flow hypothesis, in which the positive ϕ corresponds to upstream. Figure 1.(a) shows that the disturbance extends in the streamwise in $y/\delta^* < 3$, and (b) shows the same shape as in (a), indicating that the same structure exists in the boundary layer with FST. The long extension in the streamwise is considered to be caused by the lower advection velocity near the wall. Figure 2. shows the relationship between rms of the periodic fluctuation component $\widetilde{u}_{rms}$ and Reynolds stress due to the non-periodic fluctuation component $\widetilde{\hat{u}\hat{u}}_{rms}$ with different amplitude of the artificial disturbance. It can be confirmed that there is linearity between the voltage amplitude of the speaker E and $\widetilde{u}_{rms}$, $\widetilde{\hat{u}\hat{u}}_{rms}$ in the boundary layer in both cases with and without FST. From the above, it can be considered that the linear response in the boundary layer to the artificial disturbance generated in the free stream can be extracted, and the extraction method can be considered to have been established as an experiment on the boundary layer transition due to FST.

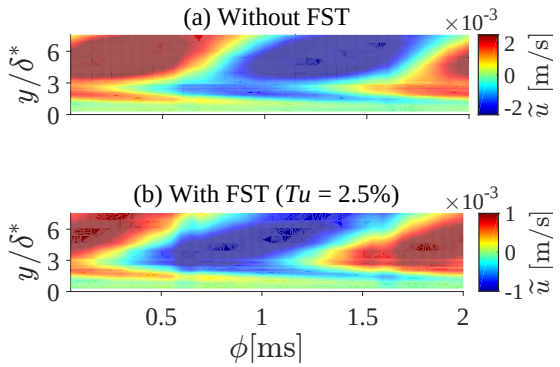

FIGURE 1. *Contour maps of $\widetilde{u}$ in the boundary layer at $x = 50$ mm, $E = 0.2$ V.*

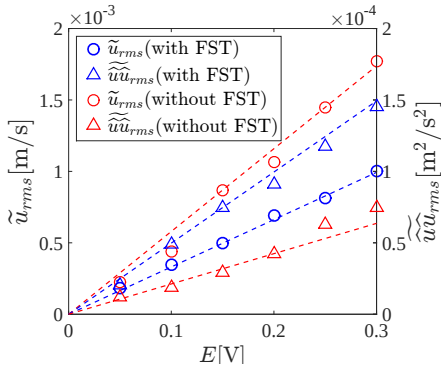

FIGURE 2. *Amplitudes E vs $\widetilde{u}_{rms}$ and $\widetilde{\hat{u}\hat{u}}_{rms}$ at $x = 50$ mm, $y = 2.3\delta^*$.*

References

[1] R. Norimatsu, S. Takai, and M. Matsubara. Relation between disturbance of boundary layer and free stream turbulence component. *Proceedings of the ASME-JSME-KSME 2011 Joint Fluids Engineering Conference*, 1:2987–2992, 2011.
[2] M. Matsubara, M. Nagasaki, T. Matsumoto, and T. Mishiba. Linear-disturbance structure in a turbulent boundary layer. *Proc. the 4th Int. Conf. Jets, Waeks and Separated Flows*, ICJWSF2013-1211, 2013.

TRANSIENT GROWTH IN FLAT-PLATE BOUNDARY LAYERS WITH A HIGHLY NON-IDEAL FLUID

Pietro Carlo Boldini[1], Benjamin Bugeat[1], Rene Pecnik[1]
[1]*Process & Energy Department, Delft University of Technology, Leeghwaterstraat 39, 2628 CB Delft, The Netherlands*

Hydrodynamic instabilities in flat-plate boundary layers for fluids working in a thermodynamic region close to the vapour–liquid critical point have recently attracted considerable attention [1]. Studies of Ren et al. [2] and Bugeat et al. [3] have revealed the existence of an additional, unstable and inviscid linear mode (see figure 1), when the temperature distribution crosses the pseudoboiling temperature, T_{pb} (transcritical case). Nevertheless, it is still unclear whether transient-growth mechanisms can similarly lead to large transient amplification of disturbances when the fluid is not assumed to be an ideal gas.

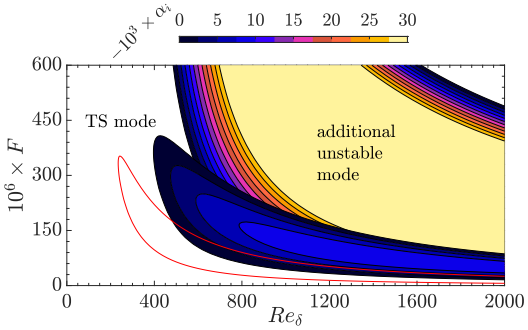

Figure 1: LST of the transcritical regime: modal stability diagram at $M_\infty = 0.001$. Neutral stability for IG (——).

In the present work, we carry out a non-modal stability analysis on flat-plate boundary layers with carbon dioxide at a supercritical pressure of 80 bar. We employ the NIST REFPROP database to generate look-up tables, accounting for the highly non-ideal equation of state and transport properties. Unlike Ren et al., we consider an isothermal wall at T_w combined with a low Mach number ($M_\infty = 0.001$) to minimise the effect of viscous heating. Optimal disturbances are calculated in the spatial framework [4] using an eigenvector decomposition of the locally-parallel, linearised Navier-Stokes equations for the liquid-like (subcritical), gas-like (supercritical) and transcritical (RG) regimes. Optimal energy growths, based on the perturbation kinetic energy, are compared to the ideal-gas model (IG). In the transcritical regime, non-ideal gas effects enhance the algebraic growth, most prominently when the fluid is cooled over the pseudoboiling line (figure 2). Streamwise vortices and velocity streaks are recovered in the optimal perturbations and corresponding outputs, respectively, for both wall heating and cooling (figure 3). Thermal streaks (ρ' and T') also become very significant, especially when $T_w < T_{pb}, T_\infty > T_{pb}$ (cooling case) in figure 3(b). Interestingly, a large second peak of streamwise velocity above the pseudoboiling line was observed when $T_w > T_{pb}, T_\infty < T_{pb}$ (heating case). Overall, this study shows for the first time the strong level of transient growth caused by wall cooling over the pseudoboiling line. Influence of wall temperature and Mach number on the transient growth in supercritical carbon dioxide and other highly non-ideal fluids will follow.

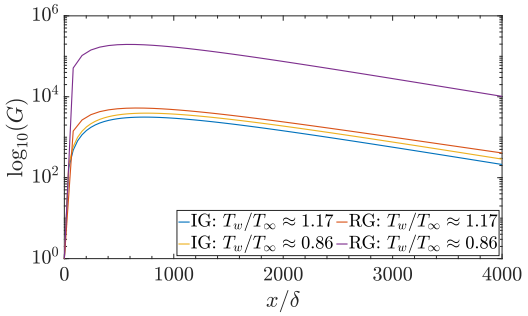

Figure 2: Maximum transient energy amplification G over streamwise distance x/δ: IG vs. RG (transcritical) for wall-heating and -cooling cases.

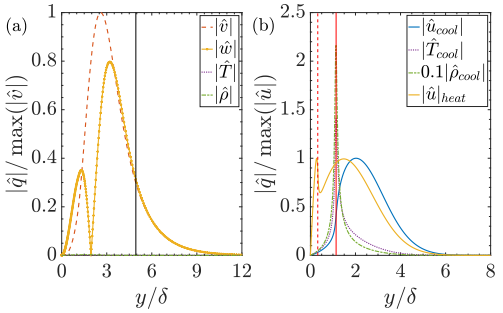

Figure 3: RG: optimal perturbations (a) and the corresponding output (b) for wall-cooling case ($M_\infty = 0.001$, $T_\infty/T_{pb} = 1.10$ and $T_w/T_{pb} = 0.95$). Streamwise velocity perturbation $|\hat{u}|$ for heating case in (—). Boundary-layer thickness (—) and pseudoboiling point for cooling (—) and heating (- -).

References

[1] J.-C. Robinet, and X. Gloerfelt. Instabilities in non-ideal fluids. *J. Fluid Mech.*, 880, 1–4, 2019.
[2] J. Ren, O. Marxen, and R. Pecnik. Boundary-layer stability of supercritical fluids in the vicinity of the Widom line. *J. Fluid Mech.*, 871, 831–864, 2019.
[3] B. Bugeat, P. C. Boldini, and R. Pecnik. On the new unstable mode in the boundary layer flow of supercritical fluids. *Proceedings of the 12th International Symposium on Turbulence and Shear Flow Phenomena (TSFP-12)*, 2022.
[4] A. Tumin, and E. Reshotko. Spatial Theory of Optimal Disturbances in Boundary Layers. *Phys. Fluids*, 13 (7), 2097–2104, 2001.

EFFECT OF EDDY VISCOSITY ON THE RESOLVENT ANALYSIS OF COHERENT STRUCTURES IN THE NEAR-FIELD OF A NACA0012 AIRFOIL

Demange, S.[1], von Saldern, J. G. R.[1], Yuan, Z.[2], Hanifi, A.[2], Cavalieri, A.[3], Kaiser, T. L.[1], Oberleithner, K.[1]

[1] *Laboratory for Flow Instabilities and Dynamics, Technische Universität Berlin*
[2] *FLOW, Department of Engineering Mechanics, KTH Royal Institute of Technology*
[3] *Divisao de Engenharia Aeronáutica, Instituto Tecnológico de Aeronáutica.*

We investigate the coherent structures in the turbulent flow around a NACA0012 airfoil at 3° angle of attack by performing global resolvent analyses of the spanwise-time-averaged fields from compressible large eddy simulations (LES). Previous studies [1, 2] have shown significant correlations between spanwise-coherent structures and the trailing edge noise generated by airfoils, making their modelling and quantitative prediction valuable for noise emission reduction. Recently, modelling of these structures with global resolvent analyses[3, 4] about the turbulent mean flow has shown good qualitative agreement with nonlinear numerical simulations in the near-field of airfoils.

The present work aims to further improve the quantitative comparison between coherent structures obtained by resolvent analyses and by data-driven methods, by modelling the dissipative part of the nonlinear forcing in the resolvent method with an eddy viscosity field, similarly to Kuhn *et al.* [5] for the wavepackets of turbulent jets. To the authors' knowledge, this has not yet been done for the flow around airfoils. The eddy viscosity field is obtained by assimilating the LES mean flow with a physics-informed neural network (PINN) [6] based on the RANS equations, and its effect on resolvent modes is evaluated for two cases displaying respectively oscillator- and amplifier-types of dynamics are investigated: (i) the transitional flow near a smooth airfoil at low Reynolds number ($Re = 5\times10^4$), yielding *tonal* trailing-edge noise through a feedback loop [4]; (ii) the fully turbulent flow at $Re = 2 \times 10^5$ obtained by tripping the boundary layer, which results in *broadband* trailing-edge noise.

The accuracy of the model is evaluated in terms of the projection of the optimal resolvent mode onto the most energetic structure in the flow obtained with spectral proper orthogonal decomposition (SPOD). Preliminary results for the low Reynolds case are displayed in figure 1, and show a good agreement between SPOD and resolvent modes at the main tone frequency.

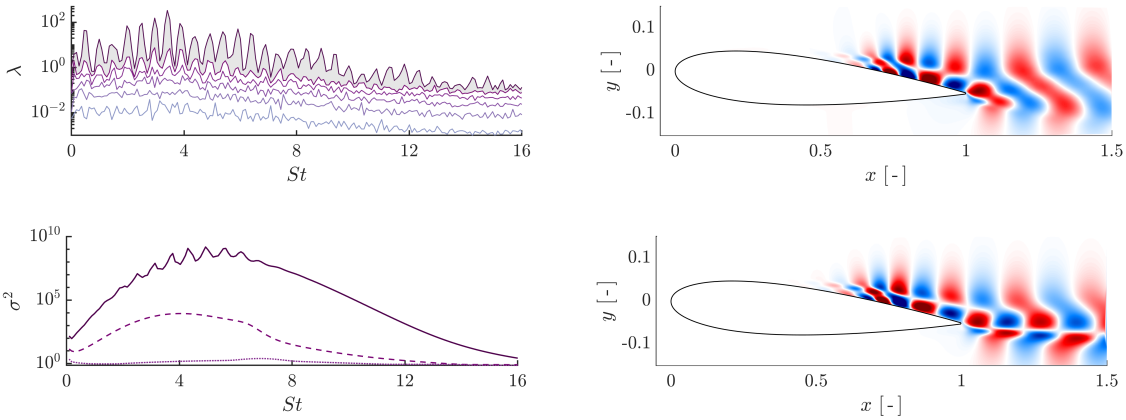

Figure 1: Results from the SPOD (top) and resolvent (bottom) analyses for the transitional flow ($Re = 5 \times 10^4$) around the smooth NACA0012 airfoil: the SPOD spectrum and resolvent gains are shown on the left, and the leading mode shapes at Strouhal $St = 3.4$ on the right.

References

[1] J. Ribeiro, W. Wolf. Identification of coherent structures in the flow past a NACA0012 airfoil via proper orthogonal decomposition. *Phys. Fluids*, 29, 085104, (2017), https://doi.org/10.1063/1.4997202.
[2] A. Sano, L. Abreu, A. Cavalieri, W. Wolf. Trailing-edge noise from the scattering of spanwise-coherent structures. *Phys. Rev. Fluids*, 4, 094602, (2019), https://doi.org/10.1103/PhysRevFluids.4.094602.
[3] L. Abreu, A. Tanarro, A. Cavalieri, P. Schlatter, R. Vinuesa, A. Hanifi, D. Henningson. Spanwise-coherent hydrodynamic waves around flat plates and airfoils. *J. Fluid Mech.*, 927, A1, (2021), https://doi.org/10.1017/jfm.2021.718.
[4] T. Ricciardi, W. Wolf, K. Taira. Transition, intermittency and phase interference effects in airfoil secondary tones and acoustic feedback loop. *J. Fluid Mech.*, 937, A23, (2022), https://doi.org/10.1017/jfm.2022.129.
[5] P. Kuhn, J. Soria, K. Oberleithner. Linear modelling of self-similar jet turbulence. *J. Fluid Mech.*, 919, A7, (2021), https://doi.org/10.1017/jfm.2021.292.
[6] J.G.R. von Saldern, J.M. Reumschüssel, T.L. Kaiser, M. Sieber, K. Oberleithner. Mean flow data assimilation based on physics-informed neural networks. *Phys. Fluids*, 34, 115129, (2022), https://doi.org/10.1063/5.0116218.

STABILITY AND TRANSITION OF SWEPT BOUNDARY LAYERS IN COOLED WALL CONDITIONS: COMMISSIONING OF EXPERIMENTS AND INITIAL RESULTS

M. Barahona[1], A. F. Rius-Vidales[1], W. J. Baars[1], M. Kotsonis[1]
[1] *Section of Aerodynamics, Delft University of Technology, Delft, The Netherlands.*

Recent developments on the use of liquid hydrogen (LH2) in aviation have again steered the interest towards an old idea to reduce skin-friction drag: wall-cooling. The on-board cryogenic fuel presents a significant source of cooling power that, if used to lower the temperature of the aircraft's skin (e.g., at the wings, nacelles and fuselage), could extend the laminar flow region and significantly reduce the skin-friction drag [1].

Wall-cooling lowers the fluid's near-wall viscosity, thereby reducing the deficiency of momentum in the flow. This leads to fuller velocity profiles, where the amplification of instabilities is notably deterred. Several authors have previously demonstrated through experiments [2] and linear stability theory [3] that, given their viscous nature, Tollmien-Schlichting (TS) waves are greatly stabilized using this flow control strategy. However, the effectiveness of wall-cooling in stabilizing the crossflow instability (CFI) remains a point of debate. The stability of swept wings subject to wall cooling was studied in [4] using compressible local stability theory. The author's findings suggest that CFI is mildly stabilized compared to the stabilization achieved on TS waves. Nevertheless, to the best of the authors' knowledge, no experimental investigations are available to confirm this conclusion. The lack of experimental and numerical studies examining the full development of CF vortices (linear and non-linear regime) in the presence of wall-cooling hinders the validation of these propositions and challenges the problem understanding.

The present work aims to experimentally study the effects of wall-cooling on the laminar-to-turbulent transition of stationary CF vortices. With this objective, the surface temperature of a swept flat plate is lowered using a liquid cold plate integrated on the back-side of the flow-exposed surface, see Figure 1. A first set of experiments is performed in the A-tunnel, a low-turbulence (Tu = 0.07%) and humidity-controlled wind tunnel at the Delft University of Technology. During the experiments, a dehumidifier reduces the fluid's dew point to avoid the onset of condensation on the cold surface. Temperature and velocity yz-planes at different x-coordinates are measured using Cold- and Hot-Wire Anemometry, respectively. Additionally, Infrared Thermography is used to characterize the transition location under different temperature ratios, T_w/T_a. The amplification of the CF vortices is retrieved from experiments and compared with predictions from Compressible Linear Stability Theory under equivalent wall temperature and freestream conditions.

This work aims to openly examine a thermal flow control strategy for transition delay, tailored to the current global scenario of LH2-fueled aviation. The methodology, challenges, and initial findings during the commissioning of the experiments will be presented in the workshop.

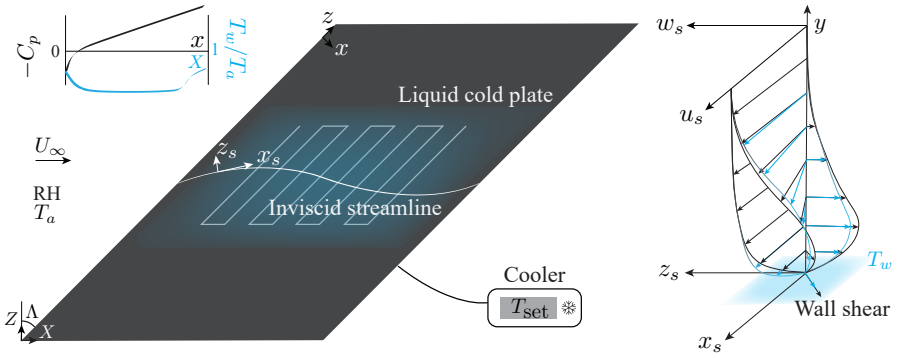

FIGURE 1. *Schematic of the experimental set-up and the wall-cooled three-dimensional boundary layer.*

References

[1] E. Reshotko. *Drag reduction by cooling in hydrogen-fueled aircraft. Journal of Aircraft* 16.9: 584–590, 1979.
[2] Y. S. Kachanov, V. V. Koslov and V. Ya. Levchenko. *Experimental Study of the Influence of Cooling on the Stability of Laminar Boundary Layers. Izvestia Sibirskiogo Otdielenia Ak. Nauk SSSR, Seria Technicheskikh Nauk,* No. 8–2, pp. 75-79, 1974.
[3] L. I. Boehman and M. G. Mariscalco. *Stability of highly-cooled compressible laminar boundary layers. AFFDL-TR-76-148,* 1976.
[4] S. G. Lekoudis *Stability of the Boundary Layer on a Swept Wing with Wall Cooling. AIAA Journal* 18.9: 1029–1035, 1980.

EFFECTS OF A HIGHLY-NON-IDEAL FLUID FOR THE INSTABILITY OF A THREE-DIMENSIONAL BOUNDARY-LAYER FLOW

Jie Ren, Markus Kloker
Institute of Aerodynamics and Gas Dynamics, University of Stuttgart, Germany

Hydrodynamic instability paved the way to understand the initial phases of laminar- turbulent transition and shape the design of aerodynamic devices with lowered drag. While for hypersonic flow it is clear that thermodynamic/-chemical effects need be accounted for due to the high temperatures occurring, the present work underpins that also for low-speed flow at ambient temperatures non-ideal, i.e. real-gas effects can play a strong role. For the considered Newtonian fluids the viscosity does not depend on the shear in the flow, but on temperature – like for ideal compressible fluids – and density or pressure of the fluid, a consequence of intermolecular forces when the pressure is large. But not only the viscosity is concerned, all transport and thermodynamic properties behave non-ideally. Fluids at these large pressures gain in attention in industrial processes, last but not least in energy conversion machines. It has been shown that a supercritical fluid like CO2 at 80 bar pressure may give rise to an otherwise absent inviscid instability in the canonical zero-pressure-gradient flat- plate boundary-layer in the transcritical (pseudoboiling) regime. The present work investigates 3D boundary layers with favorable pressure gradient (FPG) in thermo- dynamically non-ideal regimes. The flow set-up is matched to the redesigned DLR (German Aerospace Center) experiment on cross-flow instability in air flow, with identical pressure-coefficient distribution, sweep angle and Reynolds number, at a low Mach number. The flow temperature relative to the Widom line – also known as the pseudocritical line – thus characterizes the non-ideality of the flow. We consider supercritical (gas-like), subcritical (liquid-like) and transcritical regimes, where the flow temperature remains above, below or crosses the Widom line. The stability analyses of the parabolized Navier-Stokes baseflows indicate that wall heating destabilizes the flow in the supercritical regime while wall cooling stabilizes, both effects similar to the ideal-fluid situation but being stronger. On the contrary, wall heating/cooling exhibits reversed effects in the subcritical regime, like for an ideal liquid. In the transcritical regime, with its sharp gradients of the thermodynamic and transport properties, wall heating stabilizes the flow. Most substantially, however, wall cooling provokes a changeover of the leading instability mechanism: The streamwise flow with its FPG attains inflectional wall-normal profiles, and the invoked inviscid Tollmien–Schlichting instability prevails with growth rates up to one order of magnitude larger than those of the cross-flow mode. The streamwise perturbation patterns of the flows in their linear instability regime are shown by mimicking wave trains emanating from virtual point-disturbance sources. If a laminar flow state is sought, the transcritical thermodynamic state with a cooling wall must be avoided. A sensitivity study unveils that it is not sufficient to analyze the altered baseflows with an ideal-fluid instability solver, but both the base- and the disturbance-flow solver need to account for the non-ideality.

THREE-DIMENSIONAL INSTABILITIES

Elliot Badcock[1], Shahid Mughal[2]
Imperial College London; Department of Mathematics, South Kensington Campus, London SW7 2AZ.
[1] *ejb321@ic.ac.uk;* [2] *s.mughal@imperial.ac.uk*

Modelling the evolution of fully three-dimensional boundary layer instabilities can be most naturally achieved using a three-dimensional version of the parabolised stability equations (PSE3D). We will discuss some recent advancements to the PSE3D methodology when applied to non-orthogonal boundary layer flows using a local point to point surface marching procedure (PPM-PSE3D). When contrasted against the conventional bi-global PSE3D formulation, which is limited by the computational demands of inverting very large matrices in the LU factorisation step in the primary marching-plane direction, PPM-PSE3D is a very efficient numerical approach when used to model flow disturbance evolution over a complete aircraft wings which exhibit true three-dimensionality in the boundary layer development in the wing span.

In the PPM-PSE3D method the spanwise wavenumber is an additional unknown quantity which must be solved for during the spatial marching procedure. To therefore complete the equation set, an additional constraint must be employed alongside the dispersion relation. This has usually been achieved by discretising the irrotationality condition (1; 2),

$$\frac{\partial \alpha}{\partial z} = \frac{\partial \beta}{\partial x}, \tag{1}$$

where α and β are the wavenumbers in the streamwise (x) and spanwise (z) directions respectively. Previous works (2) have discretised this quantity in the spanwise direction based on the direction of the inviscid freestream, and then obtained β via a streamwise integration. This supposes that a disturbance wave travels in the direction of the freestream. We will compare this technique against use of the group velocity as the direction of propagation of the disturbance in the spanwise discretisation. Additionally, we will compare the subsequent streamwise integration of (1) to calculate β, with the use ray-tracing techniques.

The second aspect we will address in the workshop is how one computes the N-factor, or kinetic energy growth, of disturbances which exhibit spanwise variations in the growth rates. N-factors are used in the laminar-turbulent transition criterion and as switches in RANS solvers. For two dimensional or infinitely swept flows, we calculate the N-factor by simply integrating along the streamwise or line-of-flight direction. Whereas, for truly three-dimensional flows there exists an ambiguity to the direction of propagation of the disturbances, or put mathematically; what path should we integrate along? As well as the line-of-flight, we will compare two additional integration paths for the N-factor: the inviscid freestream, and the group velocity. Example N-factors using the line-of-flight, inviscid freestream and group velocity as integration directions are given in figure 1.

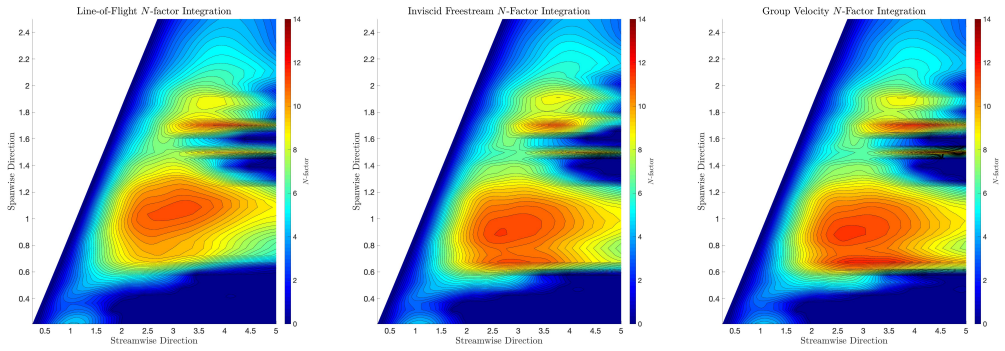

FIGURE 1. *Example N-factors for a flow over the AFRL 1303 UCAV concept UAV (2). (a) Line of flight; (b) Inviscid Streamline; (c) Group Velocity.*

References

[1] Moyes, A., Beyak, E., Travis, T. S. and Reed, H. L. Accurate and Efficient Modeling of Boundary-Layer Instabilities. *AIAA 2019-1907*, 2019.

[2] Arthur, M., Horton, H. P. and Mughal, M. S. Modeling of Natural Transition in Properly Three-Dimensional Flows *AIAA 2009-3556*, 2009.

GLOBAL INSTABILITY PRODUCED BY INFINITESIMAL ROUGHNESS

Jonathan J Healey[1]
[1] *Department of Mathematics, Keele University, Keele, ST5 5BG, UK* *j.j.healey@keele.ac.uk*

The propagation properties of unstable waves can be as important as the instability itself. When the parallel flow approximation is made, disturbances localized in space and time can be represented by Fourier-Laplace integrals of normal modes, and at large times the solution is dominated by a saddle, called the pinch-point, in the complex wavenumber plane. The dispersion relation at the pinch-point predicts whether the parallel flow is absolutely unstable, i.e. whether there is long-term growth in the rest-frame, see [1]. Of course, physical flows always vary to some extent in the flow direction. [2] used WKB theory to show how a further saddle condition in the complex x plane, where x is the streamwise coordinate, can be used to construct global modes that determine the global instability of the inhomogeneous flow, i.e. whether there is long-term growth in the rest-frame.

Global instability theories can also be developed using Floquet theory when the flow is spatially periodic. [3] showed that in this case a pinch-point condition for the Floquet exponent plays a similar role to the wavenumber pinch-point condition that controls absolute instability in parallel flows.

We show that including spatial periodicity of arbitrarily small amplitude can create pinch-points in the Floquet exponent that have no relation to those of the homogeneous version of the problem, and these Floquet global modes (FGM) can have global instability that differs strongly from that of the local absolute instability of the homogenous problem. Furthermore, because the spatially periodic amplitudes are small, a small random spatially inhomogeneous term, modelling random roughness at a boundary, generates a superposition of FGMs associated with each spatial Fourier component of the random roughness, which is ultimately dominated by the wavenumber component with the strongest FGM growth rate.

The key results can be illustrated using a linear amplitude equation in the form

$$\frac{\partial A}{\partial t} + u\frac{\partial A}{\partial x} = [\mu_0 + \epsilon f(x)]A + \gamma_2\frac{\partial^2 A}{\partial x^2} + \gamma_4\frac{\partial^4 A}{\partial x^4} + \gamma_6\frac{\partial^6 A}{\partial x^6}, \tag{1}$$

where u, μ_0, ϵ, γ_2, γ_4 and γ_6 are real or complex constants (to be given in the presentation). The spatially homogeneous case is recovered when $\epsilon = 0$, and then (1) is absolutely stable, but convectively unstable. When $\epsilon \neq 0$ and $f(x) = \cos kx$, (1) is a Floquet problem, and for a certain range of k we show that there is Floquet global instability for arbitrarily small ϵ. In Figure 1 we present numerical solutions to (1) for two values of ϵ, for the case when $f(x)$ is a random function with a broad wavenumber spectrum, which models a random roughness term, for a spatially localized initial condition.

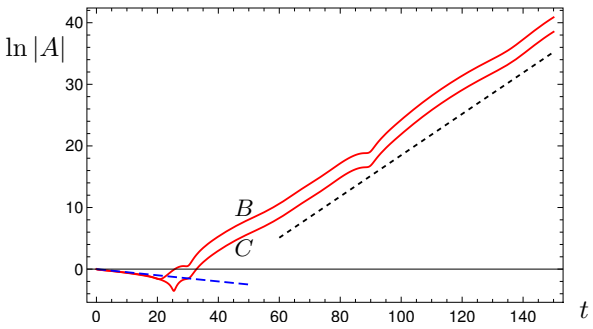

FIGURE 1. *Time dependence of numerical solutions to (1) at $x = 0$. Red line B is for $\epsilon = 0.01$, red line C is for $\epsilon = 0.001$, dashed lines are asymptotic predictions for growth/decay rates, see text for details.*

At early times solutions follow the decay rate of the absolute frequency from $\epsilon = 0$ theory (blue longer dashed line), then growth appears and follows the Floquet global theory (black shorter dashed line) for the value of k that produces the strongest Floquet global instability. Reducing ϵ simply delays the onset of the Floquet global instability, but does not affect the Floquet global instability growth rate.

In the presentation we will show that confined mixing layers can show the same behaviour.

References

[1] R. J. Briggs. *Electron-stream interaction with plasmas*. MIT, 1964.
[2] P. Huerre, and P. A. Monkewitz. Local and global instabilities in spatially developing flows. *Ann. Rev. Fluid Mech.*, 22:473–537, 1990.
[3] L. Brevdo, and T. J. Bridges. Absolute and convective instabilities of spatially periodic flows. *Phil. Trans. R. Soc. Lond. A*, 354:1027–1064, 1996.

TOPOLOGY OPTIMIZATION OF ROUGHNESS ELEMENTS TO DELAY MODAL TRANSITION IN BOUNDARY LAYERS

Harrison Nobis[1], Philipp Schlatter[1], Eddie Wadbro[2], Martin Berggren[3], Dan Henningson[1]
[1]*FLOW Centre and Swedish e-Science Research Centre (SeRC), KTH Mechanics, Royal Institute of Technology, Stockholm, Sweden*
[2] *Department of Mathematics and Computer Science, Karlstad University, Karlstad, Sweden*
[3]*Department of Computing Science, Umeå University, Umeå, Sweden,*

It is well understood from classical instability theory that stable spanwise streaks in boundary layer flows can dampen the growth of Tollmien-Schlichting (TS) waves [1], suggesting an appealing mechanism to be exploited for passive flow control. In practice, boundary layer modulation of this kind has been generated with spanwise arrays of geometric elements, notably, cylindrical elements and Miniature Vortex Generators (MVGs)[2]. The consensus of these studies indicates that the shape of these devices significantly impacts both the capability of the device to damp TS waves as well as the stability characteristics of the streaky flow they induce.

In this paper, density-based topology optimization is used to design such a passive flow control device on a flat plate configured with the TS waves emanating upstream of the device. Direct Numerical Simulation (DNS) is performed to establish a baseflow, utilizing a Brinkman penalization method to describe the geometry; followed by a subsequent DNS of the linearized Navier-Stokes equations to asses the interaction of the TS wave with the device as well as the stability of the streaky baseflow. The gradient-based optimization algorithm relies on the adjoint-variable method and seeks to minimize the downstream growth of the TS wave while limiting the growth of small perturbations in the wake of the device.

Due to the highly non-linear and non-convex nature of this optimization problem, we apply the optimization procedure to various initial material distributions. The novel designs obtained through this procedure, one of which is presented in figure 1 (left), exhibit features topologically different to either cylinders or MVGs, revealing the capabilities of topology optimization over more conventional design approaches, such as shape optimization. These designs successfully damp the downstream growth of the TS wave in the domain size considered, as seen in figure 1 (right), however, they all utilize a similar mechanism, that of stable streaks. A bi-global stability analysis is used to compare the stability of the streaky baseflow induced by the optimized designs with that of a more conventional MVG.

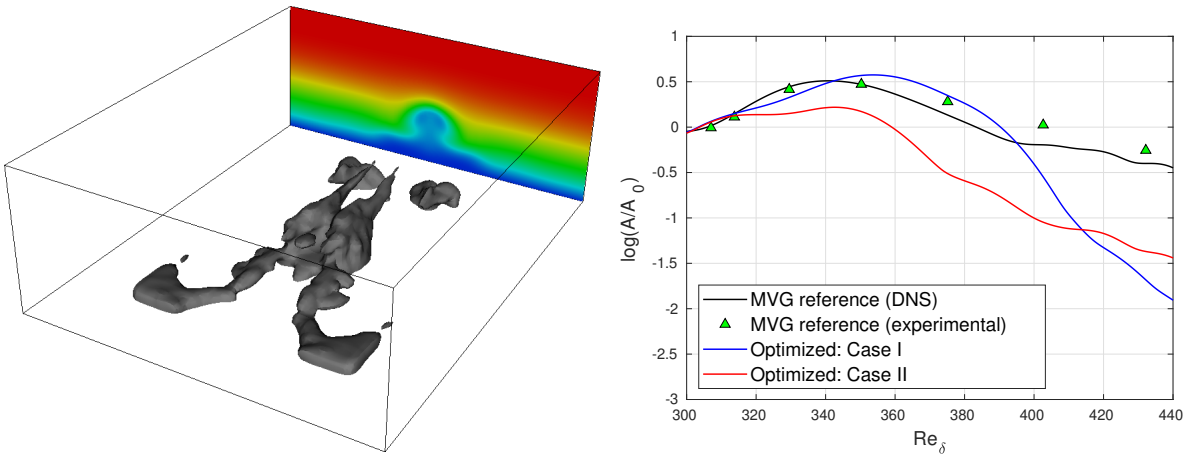

FIGURE 1. *(left) Optimized roughness element (Case I). A plane showing streamwise velocity indicates the streaky baseflow induced immediately behind the device. (Right) Spatial growth of the TS wave amplitude comparing two optimized cases with the experimental MVG data obtained by Shahinfar* et al. *[2].*

References

[1] P. J. Schmid, and D. S. Henningson. *Stability and Transition in Shear Flows*. Springer, Berlin, 2001.
[2] Shahinfar, S. and Fransson, J. H. M. and Sattarzadeh, S. S. and Talamelli, A. Scaling of streamwise boundary layer streaks and their ability to reduce skin-friction drag. *Journal of Fluid Mechanics*, 733:1–32, 2013.

INFLUENCE OF SURFACE IMPERFECTIONS WITH SLIGHTLY ROUNDED CORNERS ON THE EXPECTED LAMINAR-TURBULENCE TRANSITION LOCATION

Juan Alberto Franco[1,2], John Paul Panuthara[1,3], Yannik Heinritz[1,4], Stefan Hein[1]
[1] *German Aerospace Center, Institute of Aerodynamics and Flow Technology, Göttingen, 37073, Germany*
[2] *School of Aeronautics, Universidad Politécnica Madrid, Madrid, 28040, Spain*
[3] *Technical University of Munich, Munich, 85748, Germany*
[4] *University of Applied Science Aachen, Aachen, 52066, Germany*

The presence of surface imperfections on aerodynamics devices, such as steps or gaps of height/depth h comparable with the local boundary-layer displacement thickness δ^*, might alter the spatial development of linear mechanisms that trigger the laminar-turbulent transition process, such as Tollmien-Schlichting (TS) waves or Crossflow Instabilities (CFI). Traditionally, the numerical studies for such configurations assumed that the geometry of the surface imperfections is rectangular at the corners. However, an initial work by Zahn and Rist [1] showed the tremendous impact on the computed N-factor envelope curves if the edge of the corner is slightly distorted. Despite this, no parametric studies have been conducted in order to better quantify the impact of such modelling of the step geometry.

A recent investigation using the AHLNS methodology [2] has shown (see Figure 1) that, in the case of forward-facing steps (FFS), a significant reduction in N-factor (compared with the rectangular step) is found if the upper corner of the step is rounded with a radius r about ten times smaller than the step height h. Interestingly, modelling the step corner geometry with higher curvature radius has no effect of the N-factor envelope curves. On the other hand, an identical approach applied on backward-facing steps (BFS) reveals that N-factor envelope curves are insensitive to such small variations on the step geometry.

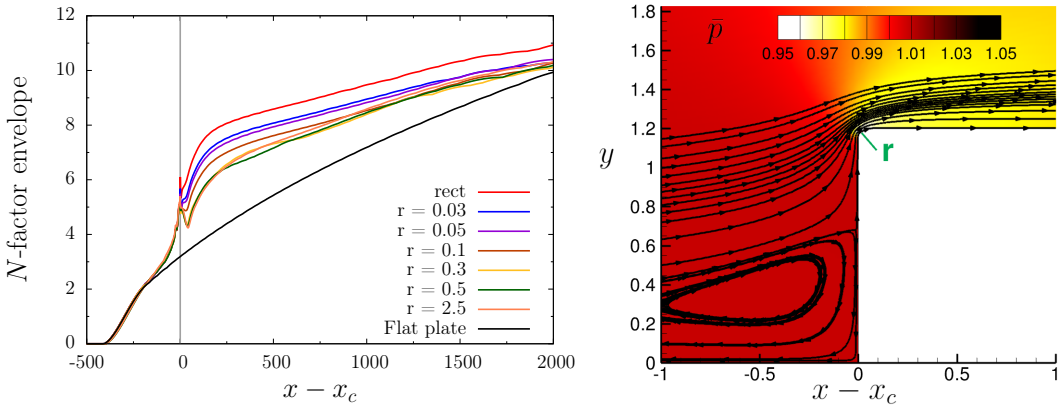

FIGURE 1. *N-factor envelope curves computed with AHLNS for FFS of height h=1.2 and several corner radii r (left). Non-dimensional base flow pressure contours $\bar{p}$ and streamlines for the FFS case with height h=1.2 and corner radius r=0.1 (right). All dimensional lengths are made non-dimensional with δ^*.*

The work is extended to other surface imperfections such as gaps. Moreover, the influence of other parameters will be discussed. The importance of the corner geometry for certain surface imperfections will be highlighted, which might be of relevance for comparisons with experimental results.

References

[1] J. Zahn, and U. Rist. *Active and Natural Suction at Forward-Facing Steps for Delaying Laminar-Turbulent Transition. AIAA J.*, 55:4, 1343-1354, 2017.
[2] J. A. Franco, and S. Hein. *Adaptive Harmonic Linearized Navier-Stokes equations used for boundary layer instability analysis in the presence of large streamwise gradients. AIAA Aerospace Sciences Meeting*, 2018-1548, 2018.

DELAY OF LAMINAR–TURBULENT TRANSITION BY ROTATING CYLINDRICAL ROUGHNESS ELEMENTS IN A LAMINAR WATER CHANNEL

Tristan M. Römer[1], Christoph Wenzel[1], Ulrich Rist[1]
[1] *University of Stuttgart, Pfaffenwaldring 21, D-70569 Stuttgart, Germany, roemer@iag.uni-stuttgart.de / wenzel@iag.uni-stuttgart.de / rist@iag.uni-stuttgart.de*

Delaying laminar–turbulent transition in boundary layers is of great interest and practical importance, as it can reduce surface friction by up to an order of magnitude. It has been the prevailing opinion for years that three–dimensional (3D) surface roughness elements can solely promote the transition process in Blasius boundary layers. Fransson et al. [1] showed, however, that boundary layer streaks induced by cylindrical roughness elements are able to control the Tollmien–Schlichting (TS) instabilities up to a complete transition delay, indeed. In a numerical investigation from Wu et al. [4], it has been further observed that also counter rotating cylindrical roughness element are capable to control the TS instabilities. However, the inviscid inflectional mode caused by the distortion of the cylinder in the boundary layer at medium rotation speed can premature transition. In this talk, it is shown by experimental investigations that by actively rotating a cylinder pair, the boundary layer primary instability can be stabilized and the laminar–turbulent transition can be delayed in a realistic flow configuration [2].

The experimental setup is given in the top figure, highlighting the flow field around the pair of rotating cylinders via a dye visualization. For the rotating cylinders, the streak amplitude A_{st} increases, see Figure 1 (left). A_{st} is defined as in Shahinfar et al. [3]: $A_{\mathrm{st}}(y_k) = (\max_z(\bar{u}) - \min_z(\bar{u}))/(2U_e)$; U_e is the free–stream velocity and the maximum/minimum of $\bar{u}$ is calculated at constant $z_k = 0$ position. According to the hypothesis of Fransson et al. [1], a higher streak amplitude is destined to stabilize the boundary layer. Figure 1 (right) shows the evaluated intermittency factor γ at different streamwise positions x_k downstream of the rotating cylinders; if $\gamma = 0$, the flow is laminar, $\gamma = 1$ indicates a fully turbulent flow. Compared to a TS wave disturbed boundary layer (black line), the intermittency function indicates a transition delay up to a rotation speed of $\Omega_u = 0.343$. The mechanism for the transition delay is in the amplified streaks induced by the rotating cylinders, which are able to attenuate the TS–like mode [4].

The advantage of this active transition delay mechanism lies in the controllability of the laminar–turbulent transition that can be adjusted by the rotation speed of the cylinders.

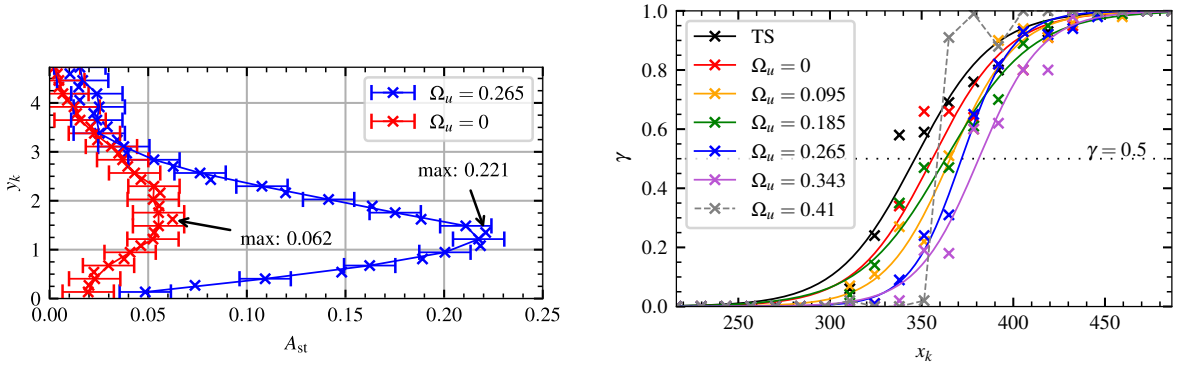

FIGURE 1. *Left: Streak amplitude A_{st} at $x_k = 216.2$. Right: Intermittency function downstream of the cylinders. Measurements were carried out using a hot-film probe.*

References

[1] J. H. M. Fransson, A. Talamelli, B. Luca and C. Cossu. Delaying transition to turbulence by a passive mechanism. *Phys Rev Lett*, 96(6):064501, 2006.
[2] T. M. Römer, K. A. Schulz, Y. Wu, C. Wenzel, and U. Rist. Delay of laminar–turbulent transition by counter–rotating cylindrical roughness elements in a laminar flat plate boundary layer. *Exp in Fluids*, 64(42), 2023.
[3] S. Shahinfar, S. S. Sattarzadeh, J. H. M. Fransson and A. Talamelli. Revival of Classical Vortex Generators Now for Transition Delay *Phys Rev Lett*, 109(7):074501, 2012.
[4] Y. Wu, A. G. Axtmann and U. Rist. Linear stability analysis of a boundary layer with rotating wall–normal cylindrical roughness elements. *J Fluid Mech*, 915:A132, 2021.

NUMERICAL AND EXPERIMENTAL STUDY OF THE GAP-INDUCED BOUNDARY LAYER TRANSITION

Felipe O. Aguirre[1], Victor B. Victorino[1], Marcello A. F. Medeiros[1]
[1] *São Carlos School of Engineering, University of São Paulo Author*

The studies from [1] and [2] have shown that, depending on the gap geometry and flow conditions, a mechanism which bypasses the growth of Tollmien- Schlichting (T-S) waves, can cause the transition in boundary layers. Therefore, this study aims at investigate numerically and experimentally the boundary layer transition induced by a gap. We conducted direct numerical simulation (DNS) of the compressible Navier-Stokes equations and linear stability analysis using a time-stepping method. The experiments were carried out at the Low Acoustic Noise and Turbulence (LANT) wind tunnel [3]. The linear stability analysis results showed two- and three-dimensional unstable modes, Rossiter and centrifugal, respectively, in runs corresponding to the bypass transition. This analysis supported the selection of parameters for a 3D simulation run. The λ_2 iso-surfaces in Fig. 1 show two-dimensional Kenvin-Helmholtz vortices being convected from the cavity, while three-dimensional structures develop far downstream. The Rossiter mode appears to have a greater influence on the transition than the centrifugal mode. However, the centrifugal mode is also essential for causing the bypass transition. Furthermore, the experiments indicated the presence of Rossiter modes in the bypass transition. Figure 2 (left) compares hot-wire signals from conditions corresponding to natural and bypass transition caused by a gap, respectively. Regarding the smooth flat plate, the transition is dominated by T-S waves, as indicated by a shaded area in Fig. 2 (right), with a spike around one second indicating the onset of turbulent bursts in Fig. 2 (left). Conversely, the bypass transition run displays a flatter spectrum up to 1 kHz and a higher-frequency tonal (black dashed line), as well as the first harmonic (magenta dashed line). These sharp peaks are attributed to the Rossiter modes.

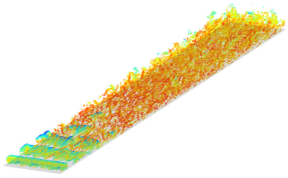

FIGURE 1. *Vortices visualized using the λ_2 method downstream of the gap*

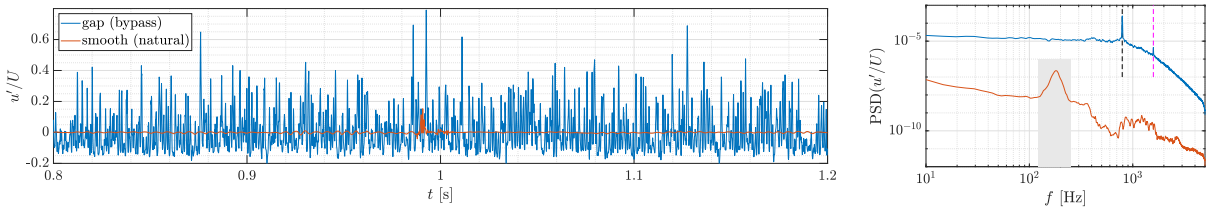

FIGURE 2. *(left) Velocity fluctuation records from the natural transition over the smooth plate and the transition bypassed by a gap with a depth of $D/\delta^* \approx 2$; (right) Power spectra from the time series exhibited in the left.*

References

[1] J. D. Crouch, and V. S. Kosorygin, and M. I. Sutanto. Modeling Gap Effects on Transition Dominated by Tollmien-Schlichting Instability. *AIAA AVIATION Forum* June 15-19, 2020.
[2] S. Beguet et al. Modeling of transverse gaps effects on boundary-layer transition. *Journal of Aircraft*, v. 54, n. 2, p. 794–801, 2017. ISSN 00218669.
[3] F. R. Amaral et al. The low acoustic noise and turbulence wind tunnel of the University of Sao Paulo. *Aeronautical Journal*, p. 1–33, 2021. ISSN 00019240.

TRANSONIC BOUNDARY LAYER NATURAL TRANSITION ANALYSIS OVER A GAPPED WING SECTION

Ganlin Lyu[1], Chao Chen[2], Shahid Mughal[1], Xi Du[2], Spencer J. Sherwin[1]
[1]*Imperial College London, United Kingdom*
[2]*Beijing Aircraft Technology Research Institute of COMAC, Beijing, 102211, China,*

Laminar boundary layer natural transition analysis over wings is of particular interest in the civil aviation industry, where a real wing experiences transonic flow at a high Reynolds number, while the surface geometry can contain irregularities in the form of steps and gaps. The sizes of these surface irregularities are typically comparable with (or larger than) the local boundary layer thickness and therefore have considerable influence on the growth of disturbances inside the laminar boundary layer. In the current study we focus on transition analysis over gap-type irregularities on a wing section taken out of the well-known CRM-NLF model. This study utilizes the high-order solvers in the spectral/hp element framework Nektar++ [1] and adopts the embedded DG simulation strategy, where high-fidelity simulations are carried out in a near-wall, reduced domain while a low-fidelity RANS fields over the full CRM-NLF model is first obtained to provide boundary data distributions [2]. This embedded simulation strategy balances the fidelity and computational cost, and guarantees the simulation to be performed under a real pressure distribution through a specifically designed pressure compatible Riemann boundary condition [3]. We present analysis in both two-dimensional (2D) and three-dimensional (3D) conditions. In the 2D study, a gap of 2mm x 8mm (depth x length) is scaled to the CRM-NLF model and is then introduced to the wall near the leading edge. The density, velocity, and pressure distributions at the inflow boundary are the same as outer RANS fields only except that the crossflow velocity component is removed. Figure 1(a) provides the n-factor curves, whose disturbance frequencies are 60k, 50k, 40k, and 30k Hz, over the wing section for both clean and gapped cases. It shows that the influence of the gap is localized. The n-factor curves of the gapped case first jump at the gap but then tend to converge back to the respective n-factor curves of the clean case. As for the 3D study, the same clean and gapped geometries are considered and quasi-3D simulations are performed, which makes all of the distributions at the inflow boundary the same as the outer RANS fields. In Figure 1(b) we present that inside the gap exists a self-sustained oscillation and it sheds disturbances to the downstream region. The frequency properties of the oscillation and shaded disturbances are further discussed.

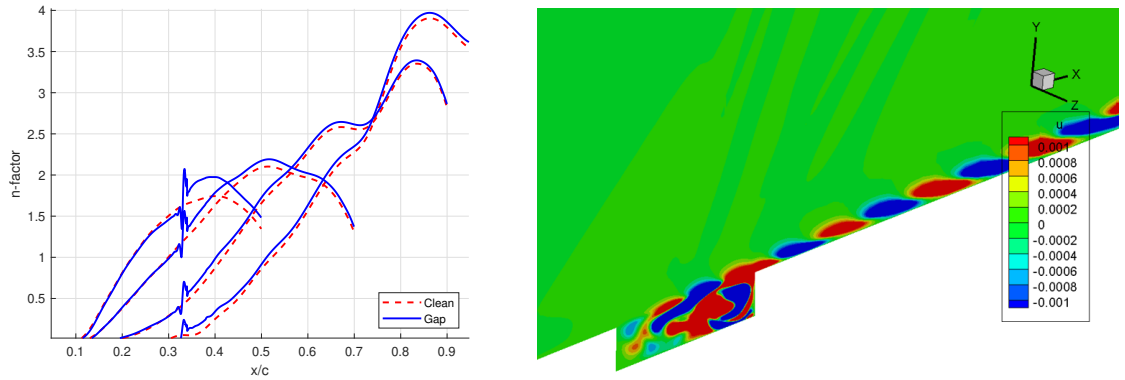

(a) N-factor comparisons in the 2D study. Disturbance frequencies are 60k, 50k, 40k, and 30k Hz from left to right

(b) Self-sustained oscillation in the 3D gap

FIGURE 1. *N-factors in 2D study and oscillations inside the 3D gap.*

References

[1] C.D. Cantwell, D. Moxey, A. Comerford, et al. Nektar++: An Open-source Spectral/hp Element Famework. *Comp. Phys. Comm.*, 192:205–219, 2015.
[2] G. Lyu, C. Chen, X. Du, M.S. Mughal, and S.J. Sherwin. Open-source framework for transonic boundary layer natural transition analysis over complex geometries in Nektar++. *AIAA Paper*, 2022-4032, 2022.
[3] G. Lyu, C. Chen, X. Du, and S.J. Sherwin. Stable, entropy-pressure compatible subsonic Riemann boundary condition for embedded DG compressible flow simulations. *J. Comp. Phys.*, 476:111896, 2023.

Author Index

ERCOFTAC SIG 33 MAP

1 Conference Room - Complesso Monumentale San Francesco

2 Lunch breaks - Piazza Pasqual Gal

3 Welcome Aperitif - Aquatica Restaurant